COMPARATIVE TRANSCRIPTIONAL PROFILING OF THE UTERUS ACCORDING TO STAGE OF THE ESTROUS CYCLE AND PREGNANCY STATUS IN GILTS

A Thesis

presented to

the Faculty of the Graduate School

University of Missouri-Columbia

In Partial Fulfillment

of the Requirements for the Degree

Master of Science

By

JIN-GEOL KIM

Dr. Jonathan A. Green, Thesis Supervisor

Dr. Randall S. Prather, Thesis Supervisor

May 2007

The undersigned, appointed by the dean of the Graduate School, have examined the thesis entitled

COMPARATIVE TRANSCRIPTIONAL PROFILING OF THE UTERUS ACCORDING TO THE ESTROUS CYCLE AND PREGNANCY STATUS IN GILTS

presented by Jin-Geol Kim,

a candidate for the degree of Master of Science,

and hereby certify that, in their opinion, it is worthy of acceptance.

_____

Professor Jonathan A. Green

_____

Professor Randall S. Prather

_____

Professor Yuksel Agca

_____

Professor Peter Sutovsky

_____

Professor Michael F. Smith

ACKNOWLEDGEMENTS

There are several people who must be thanked for helping me successfully complete this Master degree. First and foremost I have to thank my Lord and Savior, Jesus Christ. It was only His strength and wisdom that allowed me to finish; apart from Him I can not do anything.

The next most important two people I have to thank are Drs. Jonathan Green and Randall Prather. They saw in me potential and took the chance of having me as your student. The past years have been an incredible leering experience for me under your guide and support. I will always be grateful for the opportunity in Animal Sciences, University of Missouri-Columbia. I would also like to thank the members on my committee: Dr. Yuksel Agca, thank you for your delicate attention and always opened your office for me. Dr. Peter Sutovsky, thank you for being my greatest encourager, helping me think about ubiquitination during the endometrial growth and the implantation. Dr. Michael Smith, thank you for teaching the helpful class of reproductive physiology.

The data presented in this thesis required many hours of labor intensive work that I could not have done by myself. Especially, Kristin Whitworth, thank you for helping and assisting many experimental techniques. Cansu Agca, August Rieke, Melissa Samuel, David Wax, Bhanu Telugu Prakash, Tina Parks, and Dr. Clifton Murphy thank you for assisting and handling with animal trials and surgeries. Drs. Jaehwan Kim and Kwangwook Park thank you for introducing to Dr. Prather and helping to adapt myself to new circumstances.

TABLE OF CONTENTS

LIST OF ILLUSTRATIONS

LIST OF TABLES

Table **Page**

COMPARATIVE TRANSCRIPTIONAL PROFILING OF THE UTERUS ACCORDING TO STAGE OF THE ESTROUS CYCLE AND PREGNANCY STATUS IN GILTS

Jin-Geol Kim

Dr. Jonathan A. Green, Thesis Supervisor

Dr. Randall S. Prather, Thesis Supervisor

ABSTRACT

In most mammals, female reproductive organs including the ovary, oviduct and uterus undergo extensive tissue remodeling throughout the estrous cycle and during pregnancy. These changes, which are reflective of temporal and spatial specific gene expression, are required to promote successful embryonic development and fetal growth, particularly during the early pregnancy where early embryonic loss during the first 30 days of gestation is approximately 20 to 30%. The uterine endometrium nourishes the embryo by providing an environment conducive to gamete maturation, fertilization, placental attachment and the continued growth of the conceptus. A better understanding of these developmental events arbitrating conceptus-endometrial interactions will have important applications for understanding prenatal loss and improving domestic animal productivity.

This study has investigated the expression patterns of genes during the estrous cycle and pregnancy, and led to the identification of numerous differentially transcribed transcripts by using cDNA microarray and qRT-PCR. Not unexpectedly, many of these

genes are estrogen- and/or progesterone-responsive and, presumably, play key roles in establishing and maintaining the pregnancy. Moreover, a number of uterus-specific transcripts analyzed and identified in this study are very helpful for a thorough understanding of uterine physiology throughout how such transcripts change during the estrous cycle and pregnancy.

CHAPTER I

INTRODUCTION

The mammalian ovary, oviduct and uterus undergo many striking physiological changes during the estrous cycle and pregnancy that arise in response to an array of endocrine, paracrine, and autocrine signals. These changes help create the microenvironment required for movement of gametes, capacitation of sperm, fertilization, successful embryonic development and subsequent fetal growth. Most of the overt changes in the reproductive tract are a reflection of temporal- and spatial-specific gene expression in the oviduct and uterus.

In swine, prenatal mortality can reach 30 to 50 % of potential embryos at term due to embryonic/fetal mortality during the course of gestation. A disproportionate number of embryonic losses occur during the first 30 days of gestation – ranging from 20 to 30% (Hanly, 1961; Perry and Rowlands, 1962; Pope, 1994). More specifically, the majority of early embryonic loss occurs during the period of conceptus apposition and attachment between days 13 to 20.

Porcine embryos undergo dramatic elongation through rapid cellular restructuring at the same time that they are signaling their presence to the mother (Geisert et al., 1982a) During this time, the uterine endometrium secretes copious amounts of histotroph, a complex mixture of nutritive and growth promoting substances for the embryo. These secretions are products of endometrial luminal and glandular epithelial cells, and they

include transport proteins, protease inhibitors, cytokines, lymphokines, growth factors, ions, and other molecules (Roberts and Bazer, 1988; Kane et al., 1997; Gray et al., 2004).

This period of conceptus elongation and maternal histotroph production is of particular interest to researchers. Clearly there is a complex interplay between the conceptus and the mother during this time – which also happens to be the time of greatest embryonic loss. A number of hypotheses have been formulated to explain these losses, most of which assume a breakdown in the 'communication' between the mother and her offspring. For example, porcine embryos do not develop synchronously between days 10 and 12 (Perry and Rowlands, 1962; Geisert et al., 1982a). During this time, porcine conceptuses undergo dramatic elongation of the trophectoderm; however, there are differences in morphological development between them: for example, long filamentous, tubular and spherical embryos having various diameters are present within the same uterus (Pope, 1988). The presence of a range of developmental stages is at least partially due to different times of ovulation among follicles in the same ovary (Grant et al., 1989). The different conceptuses exhibit a range of steroid synthesis capacity as well. It has been suggested that conceptuses that are more developmentally advanced relative to their litter mates are better able to grow in the histotroph-rich/estrogen-stimulated uterus. The less developed conceptuses are compromised in that environment and die off. Additionally, a portion of fetal loss may be due to the limited space for embryos in the uterus and possibly the limited capacity of the uterus to provide for nutrient exchange. When attempting to increase the number of conceptuses in the uterus of pigs (Day et al., 1967; Bazer et al., 1969; Vallet, 2000), further losses occurred during later gestation, primarily due to limitations in uterine capacity.

A better understanding of the mechanisms of conceptus - endometrial interactions is required if animal scientists are going to be in a position to increase survival of offspring and thereby increase reproductive efficiency. The goal of this thesis is to gain a better understanding of uterine gene transcriptional changes before, during and after the time of maternal recognition of pregnancy.

CHAPTER II

LITERATURE REVIEW

PORCINE UTERINE PHYSIOLOGY

Just as the oviduct influences the behavior of gametes and the early embryo through the oviductal luminal microenvironment, the primary function of the mammalian uterus is to provide an environment where the conceptus can be nurtured from the blastocyst stage until birth. The mammalian embryos enter the uterus approximately 2.5 – 6 days after conception, depending on the species. Rodent and primate embryos implant at the blastocyst stage soon after hatching from the zona pellucida. In contrast, ungulate embryos remain free-floating in the uterine luminal fluid for a relatively long period, until implantation (Perry and Rowlands, 1962; Stroband et al., 1985). Upon entering the uterus, the embryos undergo cleavage, morulation and blastulation and then hatching from the zona pellucida (Geisert et al., 1982b). In swine, a period of high embryonic mortality occurs between days 10 to 20 of gestation. Embryonic losses by Day 12 are estimated to be 5-10%, whereas embryo losses are around 30% by Days 25 to 30 (Pope, 1994). Blastocyst elongation and attachment take place during this time-frame (Perry and Rowlands, 1962; Dantzer, 1985), and endocrinological cross-talk (via steroids and protein factors) between the endometrium and the conceptus has a pronounced influence on conceptus development.

The uterus undergoes cyclical secretory and development changes throughout the estrous cycle and pregnancy; many of these changes are synchronized to correspond to blastocyst development. Temporal changes in uterine secretory proteins have been characterized in non-pregnant (NP) gilts (Murray, 1972; Squires 1972) and between pregnant and non-pregnant individuals (Roberts, 1988).

Embryo-derived estrogen induces changes in uterine gene expression on days 11 and 12. It also plays a major role in maternal recognition of pregnancy, embryonic migration and spacing, and advancing uterine secretions prior to the time at which they would normally occur in the nonpregnant uterus (Pope, 1994). Therefore, elucidating the mechanisms regulating sequential changes in uterine development, particularly blastocyst-endometrial interactions during early pregnancy, will lend insight into the processes of embryogenesis. The more information that is known about these processes, the more opportunities there will be for animal scientists to understand the mechanisms and causes of embryo mortality. Having such information has the potential to permit the systematic and focused manipulation of gene expression in pregnant swine to improve the reproductive efficiency of this species.

Porcine Uterine Histo-Architecture and Function

In all mammals, the uterus is derived from a specialization of the paramesonephric or Mullerian ducts, which develop into the oviduct, uterus, cervix, and anterior vagina. Morphogenetic events of uterine development commonly include differentiation and growth of the myometrium; differentiation and morphogenesis of the endometrial glands; and organization and stratification of the endometrial stroma (Bartol et al., 1993 and 1999; Gray et al., 2001a; Spencer and Bazer, 2004). Although uterine development is initiated in the fetus, it is completed postnatally with differentiation and development of the endometrial glands (Gray et al., 2001; Spencer and Bazer, 2004).

In pigs, the uterus is connected directly to the isthmus of the oviduct at the uterotubal junction (UTJ). Constriction of the uterotubal junction serves as a major barrier to sperm transport and prevents excessive numbers of spermatozoa from reaching the ampulla, possibly helping to decrease polyspermy in swine. Anatomically, the porcine uterus is a bicornuate type, which is characterized by having two long uterine horns and a small uterine body. It is comprised of the **perimetrium** (a thin serosal layer), the **myometrium** (the outer longitudinal and inner circular smooth muscle layers), and the **endometrium** (the inner portion of the uterus composed of the mucosa and submucosa).

The myometrium exhibits increased contractility in the presence of estrogen (E2) and diminished contractility under progesterone (P4) stimulation. The latter condition is important for successful attachment of the conceptus, transport of sperm and mucus-like material, and the decline in P4 at the end of pregnancy is a major factor in regaining uterine contractility to facilitate the expulsion of the fetus and fetal membranes during parturition.

The endometrium histologically consists of **luminal epithelium** (LE), **glandular epithelium** (GE), **uterine stroma** (S, including two stratified stromal compartments: the **stratum compactum**, a densely organized stromal zone; and the **stratum spongiosum**, a more loosely organized stromal zone), blood vessels, and immune cells (Hafez and Ludwig, 1977; Stroband et al., 1986; Gray et al., 2001). The endometrium secretes materials into the uterine lumen when under the influence of P4; these secretions are also important for the establishment and promotion of embryo development, even prior to implantation (Bazer, 1993; Roberts and Bazer, 1988). In addition, the simple columnar epithelium in the uterine endometrium is comprised of two functionally different cell populations: the luminal (LE) and glandular epithelial (GE) cells (Stroband et al., 1986). These epithelia are composed of ciliated and non-ciliated secretory cells (predominant cells). Ciliated cells are relatively abundant in the LE during all stages of the estrous cycle or early pregnancy (Stroband et al., 1986). Apical microvilli are found on the surface ultrastructure of both LE and GE secretory cells, and there are no differences in the morphology between non-pregnant and early pregnant pigs from estrus up to day 10 (Hafez and Ludwig, 1977; Stroband et al., 1986). Low circulating estrogen concentrations in blood leads to deciliation (Stroband et al., 1986; Krzymowski and Stefanczyk-Krzymowska, 2004). In addition, uterine blood supply is significantly changed during the estrous cycle in all domestic animals (Ford and Christenson, 1979), and flow through the uterine artery is mostly regulated by the estrogen/progesterone ratio in arterial blood (Reynolds and Ford, 1984). The uterine blood supply is maximal during estrus and ovulation in domestic animals, but it is lowest in pigs on days 10 to 12 of the estrous cycle (Ford and Christenson, 1979) and in sheep on days 12 to 13 (Roman-Ponce

et al., 1983). Specially, the volume of uterine blood flow falls by 30 - 40% on day 12 of the porcine estrous cycle compared to the period of around estrus (Ford and Christenson, 1979). The uterine endometrium initiates regressive changes after this period of diminished circulatory flow (Ford and Christenson, 1979; Krzymowski and Stefanczyk-Krzymowska, 2004). Moreover, a rupture of the apical surface of the endometrial cells occurs during the late luteal phase following the release of large amounts of prostaglandin into the surrounding tissues (Hafez and Ludwig, 1977). The endometrial cells then undergo both necrosis and apoptosis (Rotello et al., 1989; Harada et al., 1996; McCormack et al., 1998; Krzymowski and Stefanczyk-Krzymowska, 2004). Endometrial cell death via apoptosis is rapidly increased in the follicular phase when compared to the luteal phase in pigs (Wasowska et al., 2001). The number of apoptotic cells in both the LE and GE of the endometrium is low during the luteal phase (not significant between days 9 and 13); however, the number of apoptotic cells is increased at day 15, with the greatest numbers of apoptotic cells in the luminal epithelium (LE) being on days 17-19 of the estrous cycle (Wasowska et al., 2001; Krzymowski and Stefanczyk-Krzymowska, 2004). Apoptotic cell death in the LE and GE is associated with endometrial remodeling. The removal of fragmented endometrial cellular debris is accompanied by an increased inflow of phagocytes (Hunt et al., 1985; Krzymowski and Stefanczyk-Krzymowska, 2004).

Porcine Uterine Endometrial Glands

Uterine endometrial glands transcytose, synthesize and secrete large amounts of proteins, carbohydrates and lipids, which are particularly important for conceptus survival and development in domestic animals including sheep, cattle, pigs, and horses. Endometrial glands develop after birth in the mouse (Ogasawara et al., 1983; Bigsby and Cunha, 1985), sheep (Bartol et al., 1988; Bartol et al., 1988; Spencer and Bazer 2004) and pig (Spencer et al., 1993; Tarleton et al., 1998; Tarleton et al., 1999). In humans, the initial events of gland formation occur in utero and are completed in the postnatal period. In other words, endometrial glands are absent at birth and begin to develop during the first weeks of neonatal life. In pigs, uterine growth and endometrial development is ovary independent until postnatal day (PND) 60, because the endometrium continues to develop normally up until this time even if ovariectomy is performed at birth (Figure 1) (Bartol et al., 1993; Tarleton et al., 1998 and 1999).

Although absent at birth, endometrial glands of swine begin by bud formation in the luminal epithelium, followed by tubulogenesis. Coiling and branching of epithelial tubes extend radially from the luminal surface through the endometrial stroma to the myometrium by approximately PND 30. Glandular folds of endometrium are intensely apparent by PND 60, and a functionally mature uterus is observed by PND 120 when pigs are capable of supporting a pregnancy (Bartol et al., 1993; Bal and Getty, 1970; Spencer et al., 1993; Tarleton et al., 1998, 1999). The developmental patterns of uterine glands in the neonatal pig are locally regulated in regard to both cell proliferation and differentiation (Bartol et al., 1993; Tarleton et al., 1998).

9

Endometrial gland development has been categorized into two periods: 1) the *infantile* period is the onset of endometrial gland development between birth (PND 0) and PND 7; and 2) the *proliferative* period between PNDs 7 and 14, the time at which DNA synthesis in newly formed GE is maximal based on a BrdU-labeling index (Spencer et al., 1993; Tarleton et al., 1999 and 2001). Active glandular morphogenesis within the stromal matrix is associated with increased DNA synthesis and GE proliferation between PNDs 7 and 14.

In addition to the proliferative period of endometrial development, GE differentiates from LE during the first week of the postnatal period (Tarleton, et al., 1998), and uterine glands rapidly proliferate between birth (PND 0) and PND 14 (Tarleton et al., 1999 and 2001). Estrogen functions in a uterotropic role in the neonatal pig (Spencer, et al., 1993). Wu and Dziuk (1988) and Tarleton et al. (1998) reported that uterine growth and endometrial development in ovariectomized neonatal pigs are an ovary-independent phenomena between PND 0 and 60. Moreover, the beginning of porcine endometrial gland formation is coordinated with changes in gene expression of the estrogen receptor (ER) in stromal cells (S) and nascent GE (Tarleton et al., 1998, 1999 and 2001). Tarleton et al., (1998, 1999 and 2001) reported that the ER is abundant in endometrial GE and weak in S on PND 15. In the LE, ER is effectively absent at this stage. Such observations indicate that the relationships between estrogen (E2) and ER are important for postnatal uterine growth and endometrial development. Homozygous ERα-null mice have hypoplastic uteri that contain all the characteristic cell types within the uterus, but uterine gland numbers are reduced (Lubahn et al., 1993; Curtis et al., 1999).
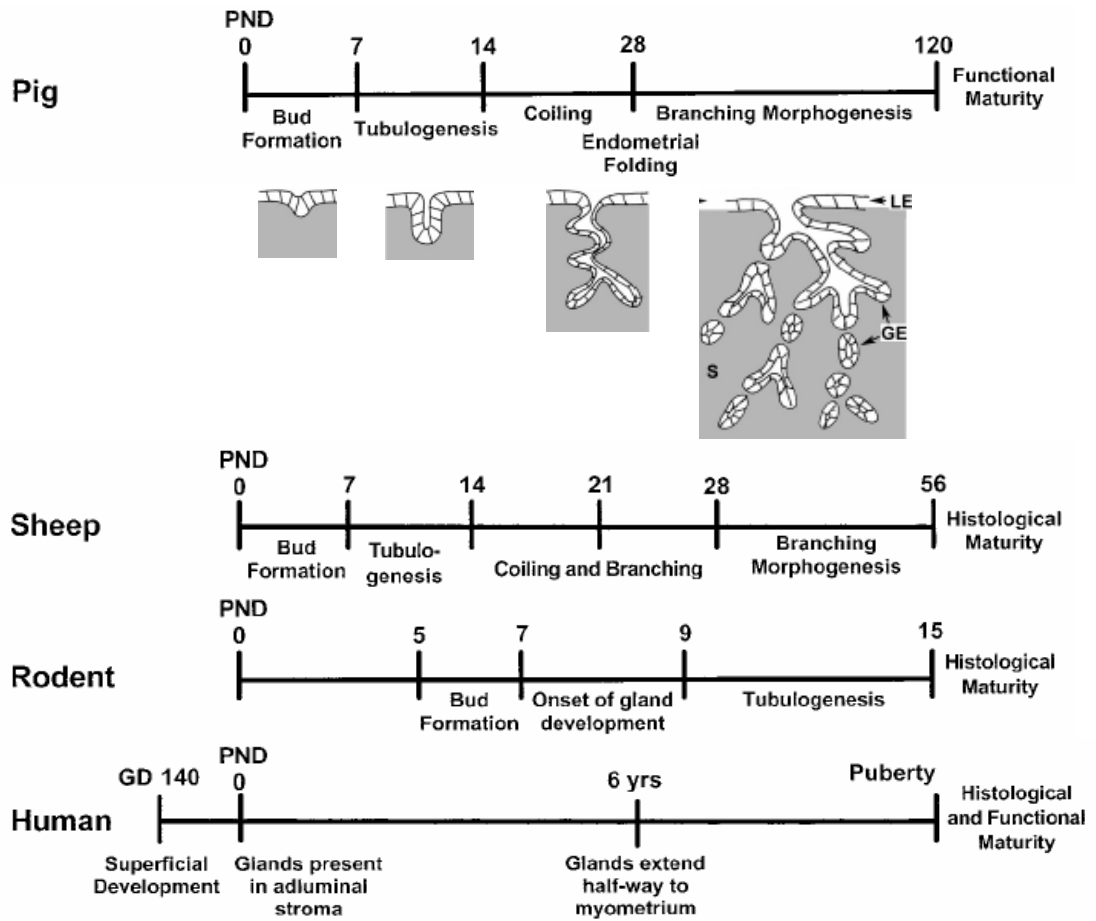
Figure 1. Comparative seminal events of uterine gland morphogenesis in the pig, sheep, rodent, and human. Postnatal day (PND) 0 is the day of birth. GD, gestational day. The figure is modified from Spencer and Bazer (J. Anim. Sci. 2004. 82: E4-E13) and Gray et al. (Bio Repro. 2001. 65: 1311-1323).

Furthermore, estradiol-17β valerate (EV) can alter normal endometrial development. When administered postnatally, EV can induce a general uterine hyperplasia, GE proliferation, and precocious development of endometrial folds in neonatal gilts (Bartol et al., 1993; Spencer et al., 1993; Tarleton et al., 1999 and 2003). Conversely, in the neonatal pig, administration of the antiestrogen, ICI 182,780, from birth can inhibit endometrial maturation and adenogenesis at PND 14, producing glands that are markedly retarded (Tarleton et al., 1999 and 2003). Likewise, endometrial gland development in sheep could also be prevented by strategic endocrine disruption of early postnatal uterine developmental events, thus leading to the creation of the ovine uterine gland knockout model (UGKO) (Spencer et al., 1999). Indeed, the UGKO ewe model provided the first direct evidence that endometrial glands can directly affect conceptus survival and growth in the adult uterus. (Gray et al., 2001 and 2002). In summary, endometrial gland products (histotroph) are critical for embryonic survival and development in mammals (Lessey et al., 1992; Lacroix et al., 1996; Dockery et al., 1996; Tarleton et al., 1999; Gray et al., 2001).

Porcine Uterine Secretions

The uterine endometrium synthesizes and secretes large amounts of protein in response to progesterone (particularly if it is first 'primed' by estrogen exposure). Uterine secretions (histotroph) from the uterine endometrial glands and luminal epithelia serve to nourish the developing conceptus. In ruminants and pigs, areolae are unique placental structures that develop over the mouth of each uterine gland for absorption and transport of uterine histotroph at the maternal-fetal interface (Spencer and Bazer, 2004). A variety of evidence on endometrial secretions has accumulated to illustrate a number of roles for histotroph. For example, uterine secretions are important regulators of conceptus survival and development and implantation/placentation in mammals (Gray, 2001a; Spencer and Bazer, 2004).

Pigs possess a non-invasive diffuse type of epitheliochorial placentation, making these conceptuses entirely dependant on uterine secretions for all but the most easily diffusible molecules. Moreover, the porcine uterus synthesizes different classes of protease inhibitors during early pregnancy. Protease inhibitors probably represent a major defense mechanism through inhibiting proteases of trophoblast origin and from infiltrating neutrophils and mast cells that accompany implantation events (Strickland, 1976; Bischof, 1995; Badinga, 1999).

Most uterine factors, including histo-hematotrophic nutrition, protease inhibitors and related substances, are controlled in an auto-, para-, and endocrine manner in the uterus to maximize production of histotroph. The amount of material flushed from the porcine uterus changes during the estrous cycle and pregnancy. For example, the amount of total protein is typically less than 8 mg per uterine horn between days 2 and 8;

however, up to 50 mg are present at day 15 (Roberts and Bazer, 1988). The amount and composition of protein in uterine flushings does not differ significantly between pregnant and non-pregnant (NP) animals until about day 11 (Geisert et al., 1982a). At that time, glandular epithelial cells are triggered to induce exocytosis of secretory vesicles in response to estrogen production by the conceptuses. NP pigs secrete material into the uterus more gradually but the total amount of protein is about the same as in pregnancy until about day 15. After this point, the amount of protein from the NP endometrium is decreased as progesterone production by the corpora lutea (CL) declines. In contrast, secretory activity of the pregnant endometrium is maintained beyond day 15 (Geisert et al., 1982a and 1982b; Zavy et al., 1984; Roberts and Bazer, 1988).

Among the proteins synthesized by the porcine uterus are large amounts of uteroferrin (Uf), retinol-binding proteins (RBP), serine protease inhibitors, glycoproteins belonging to the serpin superfamily of proteins, and various growth factors. These synthesized and secreted proteins are believed to be important for conceptus growth and development in most mammals, including pigs.

Uteroferrin (Uf; also known as ACP5 and TRAP)

Uteroferrin, also known as purple acid phosphatase, is a basic glycoprotein that is the best characterized component of the uterine progesterone-dependent histotroph (Roberts and Bazer, 1988; Naseri et al., 2004). Uf is a di-iron-containing purple acid phosphatase. A charge-transfer transition between the ferric ion and a tyrosine residue provides the distinctive purple coloration (Lauffer et al., 1983). Uf has a molecular weight of 35 kDa that is identical to an intracellular tartrate-resistant acid phosphatase

normally sequestered in lysosomes (Ling and Roberts, 1993). Uf is also known as TRAP due to its resistance to L(+)-tartrate inhibition (Naseri et al., 2004). Uf is highly abundant and represents as much as 15% of the recovered total protein in uterine flushings from NP and P gilts between days 12 and 16 (Bazer et al., 1975; Roberts and Bazer, 1980 and 1988).

Although the physiological function of Uf is poorly understood, it has been proposed to be a transplacental iron transporter in mammals with epitheliochorial placentation (Renegar et al., 1982; Roberts et al., 1986) and as a mediator in bone resorption by osteoclasts (Moonga et al., 1990; Bull et al., 2002). In vitro studies have shown that TRAP can act by catalyzing the release of phosphate groups from phosphoprotein (Halleen et al., 1998). This reaction modifies both the structure and function of the substrates, including bone matrix phosphoproteins (such as, osteopontin, bone sialoprotein, and osteonectin) (Ek-Rylander B et al., 1994; Bull et al., 2002).

Uf gene transcription is governed by progesterone, and Uf is secreted into the porcine uterine lumen from the deeper uterine glandular epithelia during pregnancy - especially after Day 11 when the embryos elongate (Roberts et al., 1986; Roberts and Bazer, 1988; Geisert et al., 1982a, 1982b). Uf, absorbed directly by the placenta through specialized cells in the areolae, enters the fetal circulation, where it is distributed to sites (such as the liver) of iron metabolism for fetal hematopoiesis or cleared through the fetal kidneys and stored in the allantoic fluid (Buhi et al., 1982; Bazer et al., 1991; Renegar et al., 1982). The residual iron binds to uteroferrin and is carried to the allantoic sac, where it is stored or recycled by transferrin.

From analysis of protein secretion from tissue explants, Uf is synthesized and secreted throughout gestation until late pregnancy, although protein levels decline during the later part of gestation. However, mRNA concentrations reach maximal levels during mid-gestation and remain high until close to the time of parturition (Simmen et al., 1988). Although the synthesis and secretion of Uf are dependent on progesterone, the role of steroid hormones in the regulation of Uf is complex. Progesterone administration into ovariectomized gilts causes an increase in mRNA levels and protein secretion into the uterine lumen; however, estrogen administration decreases mRNA levels but can stimulate Uf secretion (Simmen et al., 1988 and 1989).

Retinol-binding Protein (RBP)

Retinol-binding protein (RBP) is a major secretory protein of the liver as well as a major component of uterine histotroph and peri-implantation conceptuses of sheep, cattle and pigs (Harney et al., 1990 and 1993). RBP is a transport protein (Adams et al., 1981; Clawitter et al., 1990) that delivers vitamin A to the conceptuses. Normally, RBP is secreted by the liver to transport the alcohol form of vitamin A (retinol) through the bloodstream (Clawitter et al., 1990). Porcine uterine RBPs are identical to serum RBP (Stallings-Mann et al., 1993). Clawitter et al. (1990) reported that there were differences in the isoelectric points of uterine RBPs at different stages of pregnancy but these differences appeared to be the result of posttranslational modifications (Stallings-Mann et al., 1993).

RBP is synthesized in the uterine endometrial epithelium and glands (Harney et al., 1994) and represents less than 5% of the recovered total protein in uterine flushings

16

(Adams et al., 1981). The RBP mRNA expression is not significant until at least day 12 and increases significantly at approximately day 15 during the estrous cycle in gilts (Harney et al., 1993), when plasma progesterone levels peak. The RBP mRNA expression is elevated and reaches a maximum at day 30, with a second peak occurring at about day 90 of pregnancy (Harney et al., 1994). The concentration of RBP secreted on day 12 of pregnancy is seven to eight fold higher than that from NP cycling gilts (Trout et al., 1992). Moreover, Trout et al. (1992) reported that the concentration of retinol in uterine flushings at this time is 100 to 1000 times greater than those found in the blood. The presence of RBPs in the uterine flushings of ovariectomized gilts was detected when treated with progesterone only, and progesterone plus estrogen, from days 4 to 15 (Adams et al., 1981; Trout et al., 1991; Groothuis et al., 1997), whereas no detectable protein was recovered from gilts treated with estrogen or vehicle alone (Adams et al., 1981). However, administration of exogenous estrogen on day 11 to NP gilts increased luminal RBP 12 to 24 h later (Trout et al., 1992). More recently, Groothuis et al. (2002) reported that cultured luminal epithelial cells (LE) from postpubertal females treated with progesterone responded to retinol with increased RBP and RBP mRNA, but estrogen decreased RBP and RBP mRNA. Therefore, one must keep in mind that any useful model for studying uterine development and uterine secretion must take into account the cell types involved (i.e., luminal/glandular epithelial cells or stroma) and puberty status of the animals studied (i.e., neonatal, prepubertal, or postpubertal gilts).

Uterine Plasmin/Trypsin Inhibitor (UPTI)

Uterine plasmin/trypsin inhibitors (UPTI) represent a group of related basic, low molecular weight proteinase inhibitors (ranging from 10 to 20 kDa) that are secreted under the influence of progesterone. These inhibitors are relatively specific for plasmin and trypsin, but have a weak affinity for chymotrypsin (Mullins et al., 1980; Stallings-Mann et al, 1994). Its molecular weight was reported to be 15 kDa when first characterized (Mullins et al., 1980); however, Stallings-Mann and colleagues (1994) reported that this proteinase-inhibitor had a slightly lower molecular mass of 14 kDa. This family is comprised of a group of at least four distinct isoforms which constitute as much as 15% of the total protein recovered from uterine flushings of pregnant pigs (Fazleasbas et al., 1982).

UPTI was shown to be present during the luteal phase of the porcine estrous cycle (Mullins et al., 1980) and during pseudopregnancy (Fazleabas et al., 1982) when levels of progesterone were high. It is synthesized predominantly by the surface epithelium of the uterus and not by the deeper glandular epithelium. It is believed to play a role in restricting the invasiveness of the pig conceptuses.

The porcine placenta is of the noninvasive epitheliochorial types in which the microvilli on the surface of the trophoblast interdigitate with the epithelial cells lining on the uterine endometrium. However, the porcine conceptus at day 12 does secrete large amounts of plasminogen activator (Mullins et al., 1980), which can generate the broadly specific proteinase, plasmin, from its precursor plasminogen. Not surprisingly then, the porcine conceptus is capable of tissue invasion when it is transplanted to an ectopic site, such as the kidney capsule or oviduct (Samuel CA, 1971; Samuel and Perry, 1972).

18

Indeed, the extent of trophoblast invasiveness is at least partially dependent upon the relative levels and types of proteinases and proteinase-inhibitors that are present (Fazleabas, 1982; Roberts and Bazer, 1988). Therefore, the maternal uterus must secrete proteinase inhibitors, such as UPTI, to thwart this invasive capability of the porcine conceptus. Although UPTI secretions are correlated with circulating progesterone concentrations, its initial secretion appears to be augmented by the release of estrogen from the elongating conceptuses between days 11 and 13 of pregnancy (Fazleabas et al., 1983; Stallings-Mann et al., 1994). Indeed, a single injection of estradiol valerate at day 11 of the estrous cycle significantly increases the inhibitory activity detected in uterine flushings when compared to pigs receiving only corn oil (Fazleabas et al., 1983).

Other Uterine Secretory Products

Consistent with the observations above, mammalian uteri express a number of common classes of proteinase inhibitors (e.g., tissue inhibitors of metalloproteinases, TIMPs) as well as many species-specific ones (e.g., secretory leukocyte proteinase inhibitor, SLPI; and UPTI) (Fazleabas, 1982; Farmer, 1990; Salamonsen, 1995). Embryos, regardless of the placenta form they eventually develop, exhibit invasive activity when placed into ectopic sites where proteinase inhibitors may not be locally produced (Samuel, 1971). Proteinases including plasminogen activator (PA) have been associated with implantation and outgrowth of embryos between Days 11 and 14 (Fazleabas, 1983; Denker, 1980; Kubo, 1981).

A more complex interaction involves the uterine matrix metalloproteinase (MMP) system of the extracellular matrix (ECM), which is comprised of the proteolytic enzymes

(MMPs) and their tissue inhibitors (TIMPs). This system is essential in a variety of cellular processes such as the dynamic tissue remodeling of the connective tissue framework during uterine growth (e.g., cell proliferation, migration, adhesion and differentiation). It is tightly regulated throughout the estrous cycle as well as during pregnancy, parturition and during postpartum uterine involution (Curry and Osteen, 2003; Zhang and Nothnick, 2005). The MMP system is regulated by changes in the levels of ovarian steroids and their receptors, gonadotropin-releasing hormone (GnRH), growth factors, cytokines and chemokines (e.g., tumor necrosis factors alpha, TNF-alpha; interleukin-1-beta, IL1-beta; IL1-alpha; IL-6; epidermal growth factor, EGF; fibroblast growth factor, FGF; nitric oxide, NO). Specially, MMP-2 (gelatinase A) and MMP-9 (gelatinase B) of the MMP subclass mediate degradation of the basement membrane as an early event in the process of cellular invasion and tissue expansion; therefore, the degradation is important for reproductive tissue growth and remodeling (Cross et al., 1994; Lenhart et al., 2001).

Osteopontin (OPN; secreted phosphoprotein 1, SPP1; bone sialoprotein 1; early T-lymphocyte activation 1) is an extracellular matrix protein that binds integrins to stimulate cell-cell attachment and communication as an integrin-binding ligand that contains an Arg-Gly-Asp (RGD) binding site (Fisher and Fedarko, 2003). OPN has potential to influence a variety of physiological processes including bone mineralization, cancer metastasis, cell-mediated immune responses, inflammation, and angiogenesis (Johnson et al., 2003b). OPN as a highly phosphorylated acidic glycoprotein has also influence tissue remodeling at the conceptus-maternal interface by affecting cell-cell and cell-extracellular matrix (ECM) communication, increasing cell proliferation, migration

20

and survival, and regulating local cytokine networks (Johnson et al., 2003b; White et al., 2005). Uterine, placental, and/or conceptus expression of OPN has been demonstrated in humans (Young et al., 1990; Omigbodun et al., 1997; Lessey BA, 2002), baboons (Fazleabas et al., 1997), mice (Nomura et al., 1988; White et al., 2006), sheep (Johnson et al., 1999 and 2001), and pigs (Garlow et al., 2002; White et al., 2005). In humans, OPN protein is highly expressed in the uterine glands and on the apical surface of the LE during the midsecretory phase, in decidualizing stroma, and on invading cytotrophoblast (Young et al., 1990; Omigbodun et al., 1997; Lessey BA, 2002). In pregnant ewes, OPN increases in uterine flushings between days 11 and 17, and OPN mRNA is up-regulated by progesterone in the endometrial GE; however, the protein itself is localized at the apical endometrial LE, GE, and conceptus trophectoderm (Johnson et al., 1999 and 2001). Through in situ hybridization of pregnant pig uterus, OPN mRNA is highly expressed in only LE contiguous with apposing conceptus trophectoderm on day 15; however, an i.m. injection of estrogen indicated that SPP1 mRNA was present within the entire LE at day 15 and was maintained in the LE and GE through day 90 of PP gilts (White et al., 2005). These studies strongly suggest that OPN is a critical component of pregnancy. Moreover, the estrogen secreted from elongating conceptuses induces OPN mRNA synthesis in endometrial LE during the peri-implantation period. The protein itself accumulates at the conceptus-maternal interface and its presence is maintained throughout pregnancy (White et al., 2005).

Finally, porcine uterine secretions and endometrial expression are also a result of immune system mediators, particularly those involved in feto-maternal communication. Endometrial IL-6, TGF-beta2, interferon (IFN)-gamma and PGE_2 concentrations in

uterine fluid all increase during the time of attachment of porcine embryos. These immune factors have been implicated in the induction of uterine secretions observed in Day 15 pregnant gilts, compared to Day 10 pregnant and cyclic gilts (Robertson 1994; Kauma, 2000; Chabot, 2004).

Implantation and Placentation

Recent advances in transcriptional profiling techniques have identified numerous gene products involved in implantation. The mechanisms for maternal recognition of pregnancy, implantation and placentation in mammals are very complicated, as are the coordinated interactions between the cell surface components of embryonic trophectoderm and uterine cells. Large scale expression analyses using genomic and proteomic technologies have identified a myriad of genes and their products that change during implantation and placentation (Tanaka et al., 2002; Kao et al., 2002; Ushizawa et al., 2004). This section will briefly summarize some current information regarding porcine implantation and placentation.

After fertilization of an oocyte and spermatozoon in the oviduct, the zygote develops into a blastocyst possessing an inner cell mass (ICM) and an outer trophectoderm layer. The implantation of porcine embryos is a superficial and noninvasive process that involves the apposition, attachment and adhesion of the trophectoderm to the uterine luminal/glandular epithelia layers during the time of uterine receptivity (defined as a restricted period when a uterus supports conceptus attachment). In swine and other species within the *Artiodactyla* order little, if any, erosion of the uterine epithelium occurs (Wooding and Flint, 1994; Paria et al., 2002). The apposition and attachment starts to occur as early as day 13, and then is generally completed between days 18-24 of pregnancy (Perry, 1981). However, approximately 25-35% of porcine embryos are lost during this time-frame.

Distinct spatiotemporal expression of many genes occurs in the conceptus and endometrium during the time of apposition and attachment. For instance, carbohydrate

bearing molecules (i.e. peptidoglycans) at the embryonic and uterine cell surfaces play diverse roles during implantation (Carson, 2002). The initial adhesion of trophoblast cells to the uterine epithelium is facilitated by the glycocalyx on the trophoblast and endometrium (Dantzer, 1985; King, 1993). During this time, conceptus microvilli begin to interdigitate with similar protrusions on the apical surface of the uterine epithelium at days 15-16, and then merge together to facilitate the successful attachment of the conceptus (Dantzer, 1985; King, 1993). The adhesion of trophoblast to the uterine epithelium generally begins adjacent to the embryonic disk region and the extent of interdigitation intensifies as development proceeds (Dantzer, 1985; King, 1993).

As the placenta forms, uterine histotroph (nutrient-rich secretions from uterine glands) is absorbed through dome-shaped formations over the openings of uterine glands, known as areolae (Friess et al., 1981; Raub et al., 1985). The stimulation of uterine secretions and their absorption are a synchronized process that takes place between the conceptuses and the uterine endometrium. The protein uptake of conceptuses increases between days 12-18 (Anderson, 1978), which corresponds to the timing at which conceptus estrogen production is elevated (Robertson et al., 1978). The estrogen release influences the uterine environment by increasing endometrial protein synthesis and secretions, the accumulation of glycogen, the thickening of the glycocalyx and reducing cellular degeneration in the luminal epithelium (Geisert et al., 1982a; Roberts and Bazer, 1988; Keys and King, 1992).

After attachment is completed, the placenta proper begins to form with the appearance of the allantois, which arises as a projection from the hindgut of the embryo. The allantois begins to associate with the chorion (trophoblast and its underlying

mesodermal layer) to form the complex chorio-allantoic membrane. As the allantois begins to adhere to the chorion, the yolk sac rapidly regresses, and the exchange of oxygen and nutrients, and the removal of carbon dioxide and metabolic waste, is shifted to the vascularized chorioallantoic membrane (Tiedemann and Minuth, 1980; Dantzer, 1985). Thereafter, the fused membranes begin to form sinuses and channels that eventually unite to form blood vessels that will connect to the developing embryo through the umbilical cord (King, 1993; Carter and Enders, 2004). Placental capillaries expand over the entire surface of the placenta in close contact with the chorionic epithelium, except for the ends, which are nonvascular and form a band of necrotic tissue tips (Ford et al., 2002). Placenta formation is essentially complete by about day 30, and consists of amniotic, allantoic and chorionic membranes. In other words, there are two fluid-filled sacs in which the fetus resides; these are the allantois and amnion (King, 1993).

The porcine placenta is classified as epitheliochorial – having extensive interdigitation of microvilli on the surface of the placenta and uterine luminal epithelium with no erosion of the uterine epithelium (King, 1993; Roberts and Bazer, 1988). It is also considered a diffuse type because attachment extends over the entire chorioallantoic surface (except for the extremities) and throughout the openings of the endometrial glands (Perry, 1981). This diffuse, non-deciduate and epitheliochorial placentation is also found in camels, horses, and hippopotamuses (King, 1993).

The purpose of the chorionic villi is to greatly increase the surface area of contact between the trophoblast and uterine endometrium. These are highly vascularized for the exchange of nutrients and oxygen between the maternal and fetal circulations. In addition

to exhibiting modifications in hemotrophic nutrition, the epitheliochorial placenta of the pig relies extensively on uterine secretions (histotrophe) for nourishment of the developing conceptuses (Roberts and Bazer, 1988). This is achieved via very specialized structures called areolae, which comprise active phagocytic trophoblast cells overlying the mouths of uterine glands (Friess, 1981). Preliminary indications that these regions were critical for the transport of metals and other micronutrients arose from the observation that appreciable concentrations of iron/calcium and acid phosphatase activity have been detected in the cells of the uterine glands, in the gland secretions and the cells of the areolae (Wislocki and Dempsey, 1946). In addition, the numbers of placental areolae are directly related to birth weight in the pig (Knight et al., 1977; van Rens and van der Lende, 2002). When isotopically labeled iron was introduced into the bloodstream of pregnant gilts, a protein-bound form became associated specifically with the uterine glandular epithelium, the uterine secretions, and the areolae (Palludan et al., 1970; King, 1985). Gaseous exchange occurs within the regions of interdigitation where fetal and maternal capillaries are very close, but not in regions of the areolae (Perry, 1981).

Maternal Recognition of Pregnancy

Approximately 30% of embryo loss occurs within the first 30 days of pregnancy, with most of the loss occurring during the second week of gestation (Pope, 1994). Porcine conceptuses undergo dramatic elongation of the trophectoderm between days 10 and 12 through morphological and functional restructuring (Perry and Rowlands, 1962; Geisert et al., 1982; Pope, 1994). The secretion of histotroph is enhanced in response to the presence of conceptuses in the tract beginning on day 10 of gestation, reaching a maximum on day 12 during the time of trophoblast elongation. Secretion tapers off after day 14 once the conceptuses have acquired a thread-like shape (Perry et al., 1973; Geisert et al., 1982a). The maternal recognition of pregnancy signal is believed to be estrogen secreted by the trophoblast during elongation. The conceptuses' secretion of estrogen redirects endometrial prostaglandin $F_{2\alpha}$ ($PGF_{2\alpha}$, acts locally as a luteolysin on the CL to terminate the production of progesterone) secretion toward the uterine lumen where $PGF_{2\alpha}$ is sequestered and metabolized to prevent luteolysis (Bazer and Thatcher, 1977; Bazer et al., 1982). Although conceptus-derived estrogen helps establish the porcine pregnancy, the cellular and molecular mechanisms that are involved are exceedingly complicated and remain relatively undefined.

The mechanisms of maternal recognition of pregnancy vary according to species. For example, conceptuses of domestic ruminants secrete interferon-τ, which interferes indirectly with the pulsatile release of $PGF_{2\alpha}$ from the endometrium and thereby extends the CL lifespan (Roberts et al., 1992b). In humans, maternal recognition of pregnancy is accomplished by conceptus production of chorionic gonadotrophin (CG) as a luteotrophin which maintains the CL by stimulating through LH receptors (Hearn, 1986). Interestingly,

in the mouse semicircadian surges of prolactin (PRL) are induced by copulation and/or by cervical stimuli. These surges are likely responsible for the conversion of the corpus luteum of pregnancy (CLP) from the CL of the estrous cycle. Indeed, if a female mouse is mated to a vasectomized male the resulting PRL pulses are sufficient to prevent a return to estrus because the CLP secretes progesterone sufficient for maintaining a pseudopregnant state of 9-10 days in duration (Gunnet and Freeman, 1984).

In the pig, most of the molecular and cellular events taking place during the estrous cycle and the earliest stages of pregnancy are nearly identical. Following ovulation of the ovarian Graafian follicles, the developing corpora lutea (CL) begin the synthesis and release of progesterone, which is the principal driver of endometrial secretion and receptivity for early embryonic development and implantation (Geisert and Yelich, 1997). In the absence of conceptuses, the synthesis and pulsatile release of $PGF_{2\alpha}$ occurs in the uterine vasculature beginning after day 12 of the estrous cycle. These pulses of $PGF_{2\alpha}$ induce CL regression (luteolysis) on days 15-16 and the animal returns to estrus between days 19-22. In order for a pregnancy to be established, luteolysis of the CL must be prevented to allow progesterone secretion to be maintained. Geisert et al. (1982a, b and c) reported that the CLs are maintained after day 12, following the rapid elongation and development of conceptuses in the uterus. In swine, conceptus-derived estrogen redirects endometrial $PGF_{2\alpha}$ secretion from the uterine venous drainage to the uterine lumen where $PGF_{2\alpha}$ is sequestered and metabolized, thereby preventing luteolysis (Bazer and Thatcher, 1977; Bazer et al., 1982). In support of this model, utero-ovarian vein plasma concentrations of $PGF_{2\alpha}$ are elevated during the period of luteolysis in

nonpregnant (NP) pigs; however, they are not elevated in either pregnant (P) or pseudopregnant (PsP) pigs (Bazer et al., 1982).

In addition, it is also thought that conceptuses can inhibit luteolysis by changing the ratio of PGE_2 to $PGF_{2\alpha}$. PGE_2 has been implicated as both a luteotrophic and antiluteolytic compound (Akinlosotu et al., 1988; Christenson et al., 1990; Waclawik et al., 2006). The porcine embryo releases steroids, regulatory substances and prostaglandins (PGs) (Davis et al., 1983), and predominantly PGE_2 (Stone et al., 1986). The $PGE_2/PGF_{2\alpha}$ ratio affects the regulation of the lifespan of the CL, the growth and differentiation of endometrial cells, uterine blood flow, vascular permeability, embryo migration, and implantation (Davis and Blair, 1993; Stefanczyk-Krzymowska et al., 2005). The $PGE_2/PGF_{2\alpha}$ ratio reaches 1:3 in the NP utero-ovarian vein during the period of luteolysis on days 15-16 (Christenson et al., 1990). However, the $PGE_2/PGF_{2\alpha}$ ratio in the uterus and uterine vein increases over 1:1 during maternal recognition of pregnancy on days 11-14 (Giesert et al., 1982; Davis and Blair, 1993; Christenson et al., 1994). This suggests that PGE_2 can overcome the luteolytic action of $PGF_{2\alpha}$ thereby preventing CL regression. In other words, the PGE_2 secreted by the embryos and its increased synthesis by endometrial cells of early pregnant gilts suggested an important role for PGE_2 in the ovary and uterus at the time of maternal recognition of pregnancy. Therefore, one important prediction about maternal recognition of pregnancy is that conceptuses influence the endometrial activity of enzymes involved in prostaglandin (PG) synthesis.

PGs are synthesized from arachidonic acid, which is further metabolized to an unstable PGH_2 by the cyclooxygenases (COX) enzymes, COX-1 and COX-2. PGH_2 is converted to various PGs (PGE_2, $PGF_{2\alpha}$, PGD_2, PGI_2, and TxA_2) by specific terminal PG

synthases or reductases (Smith et al., 1996; Smith and DeWitt, 1996). PGE_2 is converted into $PGF_{2\alpha}$ by PGF synthase (PGFS), whose activity has recently been identified in bovine endometrium and is down-regulated in bovine endometrial cells by interferon-τ (Xiao et al., 1999; Madore et al., 2003). A recent study by Waclawik et al. (2006) reported that the spatiotemporal expression of PGFS during the porcine estrous cycle is involved in regulating luteolysis and that both PGFS and microsomal PGE synthase-1 (mPGES-1) were suggestive of a supportive role in determining the increase of uterine $PGE_2/PGF_{2\alpha}$ ratio during maternal recognition of pregnancy. Specifically, myometrial PGES and PGFS expression between days 14-16 of the estrous cycle and pregnancy is altered which allows a shift in the uterine PGE_2 to $PGF_{2\alpha}$ ratio after maternal recognition of pregnancy (Franczak et al., 2004; Przala et al., 2006). Moreover, the COX enzymes are the rate-limiting enzymes in the biosynthesis of PGs. Endometrial COX-1 gene and protein expression are slightly increased after day 12 of both the estrous cycle and pregnancy; however, COX-2 gene and protein expression are dramatically increased up to 80- and 10-fold individually during the same period (Geisert et al., 2006). Likewise, in mice Lim et al., (1997) reported that the expression of COX-2 in the receptive uterus requires the presence of mouse blastocysts in the tract. The COX-2 gene contains a κB site that is transcriptionally regulated by the nuclear transcription factor kappa B (NF-κB), which is involved in cellular responses to stimuli such as stress, cytokines (interleukin-1β, IL-1β; tumor necrosis factor-α, TNF-α), free radicals (superoxide, nitric oxide) and bacterial or viral antigens. In humans (King et al., 2001; Page et al., 2002) and mice (Nakamura et al., 2004), endometrial NF-κB activation is likely involved in implantation. Geisert and Yelich (1997) reported that the porcine endometrium secretes a number of

NF-$_k$B-regulated cytokines (IL-6 and LIF) and growth factors (keratinocyte growth factor, KGF) between days 12-15 of pregnancy when conceptuses are undergoing rapid growth and development.

Furthermore, porcine conceptus synthesis of IL-1β, which is a cytokine activator of NF-κB and an important mediator of the inflammatory response, induces endometrial NF-κB activation during the establishment of pregnancy (Tuo et al., 1996; Ross et al., 2003). The expression and release of conceptus-derived IL-1β into the uterine lumen is spatiotemporally associated with rapid trophoblast elongation and with an increase in endometrial IL-1 receptor type 1 gene expression (Ross et al., 2003). Interestingly in mice, both IL-1 receptor types I and II are molecular markers for uterine receptivity (Reese et al., 2001). As an inducer of phospholipase A2, IL-1β regulates the release of arachidonic acid from the phospholipid bilayer of cells (Kol et al., 2002). In other words, tissue remodeling through increased membrane fluidity by IL-1β occurs during rapid elongation of the conceptus and PGs secretion affects placental attachment during the establishment of pregnancy (Kraeling et al., 1985; Gupta et al., 1989; Wellstead et al., 1989). Elongating porcine conceptuses on day 12 highly express COX-2 mRNA (Wilson et al., 2002). Therefore, IL-1β, NF-κB, and COX-2 expressions are spatiotemporally associated during the establishment of pregnancy, because increased COX-2 gene expression on day 12 is consistent with conceptus secretion of IL-1β and activation of endometrial NF-κB during the period of maternal recognition of pregnancy (Geisert et al., 2006).

In summary, estrogens - the putative conceptus signal for maternal recognition of pregnancy - play a major role in preventing luteolysis and inducing uterine changes in

secretion and morphology for attachment in the pig. NF-κB activation by estrogen action and also the function of several other genes (i.e. IL-1β and COX-2 activation) are known to change. However, the molecular bases of the road map connecting the complex processes of maternal recognition of pregnancy are not yet fully understood. Therefore, many more aspects of pregnancy establishment in mammals remain to be identified.

GENE EXPRESSION PROFILING BY USING cDNA MICROARRAYS

Recently, a versatile genomic technology (microarrays) has been developed that takes full advantage of the large scale and rapidly increasing body of genome sequence information. DNA microarrays, using cDNA or gene-specific oligonucleotides, are comprised of orderly arrangements of nucleic acid probes spotted at a high-density on a solid substrate such as a microscopic slide (Quackenbush, 2001 and 2006; Stears et al., 2003). In the mid 1970s it was reported that labeled nucleic acids could be used to monitor the presence of complementary nucleic acid molecules attached to a solid support (Southern et al., 1975; Kafatos et al., 1979; Lennon and Lehrach, 1991; Burgess, 2001). Microarrays are the culmination of these earlier studies and they permit investigators to determine the relative abundance of RNA transcripts in many experimental systems (e.g. transcriptional changes taking place during development, between treatments groups, between tissues within the same organism, etc.) (Kohane et al., 2003). Different spatiotemporal gene expression patterns relate directly to developmental control, morphogenesis, cell proliferation-differentiation, tissue specificity, hormonal communication or cellular stress responses. The area of transcriptomics allows for the examination of whole transcriptome changes across a variety of biological conditions, instead of being limited to the analysis of only a small number of genes (Brady et al., 2006). Therefore, global gene expression measuring mRNA abundance can be simultaneously monitored by using DNA microarrays containing thousands of different RNA molecules at a given point in the life of an organism, tissues, or cells.

Complementary DNA (cDNA) Microarray Experiment

A variety of methods are used to identify transcribed genes; these include expressed sequence tags (ESTs) that represent sequence reads of at least 150 nucleotides, the 15-nucleotide tags used in serial analysis of gene expression (SAGE), and the 17- to 20-nucleotide tags used in massively parallel signature sequencing (MPSS) (Brady et al., 2006). These quantitative experiments that measure transcript abundance have been used to generate expression data across tissue types or developmental stages in biological samples. Moreover, alternative methods of gene expression profiling now include microarrays, and there are two basic approaches to generating gene expressional data by using them. For example, a single-color array performed with the GeneChip (Affymetrix) hybridizes labeled RNA from each biological sample to a single array (Quackenbush, 2006). After removing nonhybridized material by washing, the expression level of each gene is reported as a single fluorescent intensity that represents an estimated level of gene expression (Quackenbush, 2006). In contrast, a two-color array uses two different RNA samples; each is labeled with a different dye and then simultaneously hybridized to a microarray. We are focusing on two-color microarrays in this section.

Microarrays are created with cDNA samples on a solid substrate in a high-density pattern by using a spotting XYZ arrayer having special pins that produce spots that range between 80 and 150 μm in diameter (see the website of Patrick Brown's laboratory at http://cmgm.stanford.edu/pbrown/mguide/tips.html). Also, nucleotide arrays can be produced on a nylon membrane with spots of larger size in a lower-density pattern (Duggan et al., 1999; Southern et al., 1999). Most arrays contain 10,000 to 20,000 spots

on a standard glass microscope slide; however, they can contain up to 80,000 spots (Burgess, 2001). Complementary DNA arrays are typically use cDNAs amplified by the polymerase chain reaction (PCR) to produce a 0.5-2 kb product from a cDNA clone set or a cDNA library, both of which contain sequence-verified genes having a known function/identity or expressed sequence tags (ESTs). The ESTs are segments of genes in which only single-pass sequence information is available.

A typical microarray experiment often involves two populations (e.g. a control and a sample group) of cells or tissues that are identical except for the treatment, developmental stage or disease state of interest. Ribonucleic acid (RNA) is isolated from the cells of each population and then reverse transcribed into cDNA. Each sample is labeled with a different fluorescent dye (e.g. cyanin 3, **Cy3** for green color with a wavelength 532nm and cyanin 5, **Cy5** for red color with a wavelength 635nm). Samples are pooled and hybridized to the same array, the unbound cDNAs are washed away and the different fluorescent images are acquired by using a laser scanner. The intensity values for each probe are analyzed by an image analysis software (e.g., GenePix Pro 6.0 by Molecular Devices at http://www.moleculardevices.com/pages/software/gn_genepix_pro.html), which is used to calculate a quantitative ratio of the level of gene expression between the two samples being compared.

After acquiring fluorescence signals representing the relative amount of hybridization signal at each spot, the signals are analyzed with a background subtraction method representing a number of local and global methods, and/or corrected with the signals arising from the negative controls. The data are normalized by using one of several available software packages to account for differences in the labeling efficiencies

35

with the two fluorescent dyes and for any background signal before the intensity ratios are calculated. There are many different methods for normalization, including locally weighted linear regression (LOWESS) and intensity-dependent normalization (Quackenbush, 2001, 2002 and 2006; Yang et al., 2002). The normalized data is then used to calculate intensity ratios which provide an indication of the relative amounts of any given RNA species in the two samples applied to the microarray. Therefore, biologists can determine expression changes of up- or down-regulated genes which are physiologically relevant in the experiments being studied.

Experimental Design for cDNA Microarrays

Up to now, most microarray experiments have been used with single- or two-color arrays. Recently three- and four-color microarrays have become available. Three- and four-color microarrays can increase design efficiency and power to detect differential expression with additional samples. However, these arrays come with a high cost and the experimental design and analysis remains complex (Forster et al., 2004; Woo et al., 2005). Two-color experimental design for cDNA microarrays remains the most widely accepted and has being applied to many different purposes.

There are also many sources of variation in two-color microarray experimental procedures including biological, technical, and measurement variation. Firstly, biological variation is fundamental to all organisms, and it may be influenced by genetic or environmental factors, as well as by whether the samples are pooled or individual. Second, technical variation can be introduced during the RNA extraction, cDNA synthesis, fluorescent dye labeling, and hybridization conditions of samples. Finally,

36

measurement error is associated with reading the fluorescent signals affected by dust on the array and altering the wavelength for the best image balance (Churchill, 2002; Wei, 2004). Therefore, experiments with two-color spotted cDNA microarrays must be designed in such a way to produce data that are amenable to statistical analysis of both biological and technical replicates. Also, after analysis of the experimental results, an independent verification method should be considered, such as northern or western blot analyses, RT-PCR (or quantitative RT-PCR) or *in situ* hybridization.

Currently, these experimental designs involve the use of dye-swap, loop designs, and reference designs. Dye-swap experiments are used to protect against the possibility of a well-documented phenomenon, which is a labeling effect arising from differences in hybridization efficiency between the two dyes (Jin et al., 2001). Dye swap replications are a highly recommended procedure for cDNA microarray experiments (Churchill, 2002), because it is a simple and effective design for the direct comparison of two samples (Kerr and Churchill, 2001) and it is useful for reducing systematic bias (Jin et al., 2001; Yang et al., 2002; Yang and Speed, 2002). This design is used in two arrays to compare two samples: for example, the control sample is labeled with the red dye (Cy5) and the treatment sample is labeled with the green dye (Cy3) on the first array. Then, the dye labeling is reversed on the second array. With few or many different biological samples, the repeated dye-swap experimental design is useful for reducing technical variation but can become cumbersome when many samples are being analyzed (Churchill, 2002).

Samples in the loop design are compared to one another in a 'daisy-chain' fashion (Churchill, 2002). For example, in a simple 3-sample loop, there are three comparisons

between the three pairs of RNAs like A–B, B–C, and A–C (each biological sample is hybridized to two different arrays, each with a different dye) (Kerr and Churchill, 2001). In other words, the loop design needs two aliquots from each RNA sample, because these aliquot pairs connect the arrays and are arranged in a circular pattern. The loop designs can be an efficient alternative to the reference design (which is explored later in this section) in small loops rather than large loops having more than 10 samples (Churchill, 2002; Yang and Speed, 2002).

Reference sample designs are probably the most widely used experimental design (Yang and Speed, 2002). When treatment samples are compared with control samples, the most natural reference is the wild type, the biological controls, or a common reference obtained by pooling all samples. A pooled reference sample reduces large errors from the number of extreme gene ratios on each array. A universal reference (created from several standard cell lines or different organic tissues) enables some labs to compare results for all their experiments. Although the reference design is a somewhat inefficient approach in that fully half of the measurements arise from the reference sample, there are a number of advantages to its use. For example, all comparisons are made with equal efficiency, and this design can be extended to assay large numbers of samples as long as the reference sample is available (Yang and Speed, 2002). Moreover, the possibility of laboratory error can be reduced, and the efficiency of sample handling can be increased in large projects (Churchill, 2002; Yang and Speed, 2002; Vinciotti et al., 2005).

In conclusion, designing a microarray experiment requires that three criteria be addressed: biological replicates, technical replicates, and duplication of spotted clones on the array as mentioned above. The ideal experimental design is dependant on the

objectives of the experiment and constraints in reagents and materials. However, proper experimental design is critical in order to make the appropriate statistical analysis and to correctly interpret the results in as simple and powerful a way as possible.

CHAPTER III

GENE EXPRESSION PROFILING OF PORCINE ENDOMETRIUM

THROUGHOUT THE ESTROUS CYCLE

ABSTRACT

The uterine endometrium undergoes remarkable biochemical and morphological changes throughout the reproductive cycle that are mediated through differential gene expression governed principally by sex steroid hormones. The goal of this study was to identify differentially expressed genes in the non-pregnant porcine endometrium during the course of the estrous cycle. These experiments used an in-house cDNA microarray with 19,968 spotted cDNAs cloned from pig reproductive tissues. Total RNAs from cyclic endometrium (Days 0, 3, 6, 10, 12, 14 and 18 post-estrus) were coupled to Cy5 and hybridized to the arrays along with a reference RNA pool (coupled to Cy3). After normalization and statistical analysis by using GeneSpring GX 7.3 Expression Analysis program (Agilent Technologies), a total of 4,765 transcripts were found to be differentially represented in at least 1 of the 7 timepoints by ANOVA ($p < 0.05$). Many of these genes were rather abundant in the endometrium compared to the reference RNA. Of these, 964 transcripts exhibited signal intensities that were twice as high as the reference, and 267 transcripts had signals that were four times higher than the references signal. Quantitative RT-PCR analysis on selected transcripts was used to validate some of the patterns that were obtained from the microarrays. After clustering of the data by using K-

means and Self-Organizing Maps (SOM), nine particularly interesting cluster patterns were obtained: these consisted of groups of transcripts that were maximal at day 0; days 0 and 18; days 0 and 10-14; days 3-6; days 3-12; days 3-14; days 10-12; days 10-14; and days 14-18 of the estrous cycle. Analysis with the EASE program found increases in selective binding molecules, including TATA box binding protein-associated factor (TAF4) and ATP-binding cassette A6 (ABCA6) (Day 0); immune and defense response (Days 0 and 18); protein (or protein degradation) tagging activity (Days 0 and 10-14); ion transporter activity and biosynthesis (Days 3-6); ion transporter activity (Days 3-12); sterol metabolism and steroid biosynthesis (Days 3-14); apoptosis (Days 10-12); G-protein coupled receptor protein signaling pathway (Days 10-14); and peptidase activity (Days 14-18). These data help to define some of the complexities in gene expression responsible for creating an environment conducive to sperm transport, early embryonic growth and embryo attachment.

Key words: pig, endometrium, estrous cycle, cDNA microarray, gene expression

Abbreviations: NP, NonPregnant; qRT-PCR, quantitative Reverse Transcription PCR; EASE, Expression Analysis Systemic Explorer; EST, Expressed Sequence Tag; ODC1, ornithine decarboxylase 1; VNN2, vanin 2; MMP7, matrix metalloproteinase 7; LAMC2, laminin, gamma 2; CYP26A1, cytochrome P450, family 26, subfamily A, polypeptide 1; IL24, interleukin 24; ANXA4, annexin A4; NMU, neuromedin U; UPTI, plasmin trypsin inhibitor; RBP4 ; retinol binding protein 4, plasma; TIMP2, tissue inhibitor of metalloproteinase 2; UF, uteroferrin; CCL28, chemokine (C-C motif) ligand 28.

INTRODUCTION

The primary function of the uterine endometrium is to nourish the developing embryo by providing an environment conducive to gamete maturation, placental attachment and the continued growth of the conceptus throughout the reproductive cycle. In order for these events to take place successfully, the porcine endometrium undergoes remarkable molecular and cellular changes, particularly in response to estrogen (from both ovarian and conceptus origin) and progesterone stimulation (Frank et al., 1977; Bazer and Thatcher, 1977; Pope, 1994; Roberts and Bazer, 1988; Gray, 2001a; Spencer and Bazer, 2004). The coordination of these developmental events is due to the integration of endocrine, paracrine and autocrine signals from the ovary, the conceptus and from the uterus itself. Together, they regulate the uterine transcriptome (Roberts et al., 1993; Robinson et al., 1999; Spencer and Bazer, 1995; Spencer et al., 2004). Not surprisingly, there is considerable research effort devoted toward defining and understanding gene transcription in the uterus.

Numerous published studies have focused on characterizing the transcription of specific genes in the porcine uterus during the estrous cycle and pregnancy (Vonnahme et al., 1999; Cardenas and Pope, 2003; Wollenhaupt et al., 2004; Green et al., 2006). Numerous differentially-represented transcripts have been identified; some examples include spermine/spermidine N1-acetyltransferase (SSAT) (Green et al., 1998), extracellular matrix proteins and integrins (Burghardt et al., 1997; Hettinger et al., 2001; Garlow et al., 2002; White et al., 2005), growth factors (Ka et al., 2001; Allen et al., 2002; Wollenhaupt et al., 2005; Jaeger et al., 2005; Ashworth et al., 2006), uteroferrin

(UF) (Roberts and Bazer, 1988; Naseri et al., 2004) and numerous progesterone-responsive genes that likely play key roles in establishing and maintaining pregnancy (Bowen et al., 1996; Ling and Roberts, 1993; Vonnahme et al., 2004; Spencer and Bazer, 2004; Gray et al., 2006).

Despite the tremendously useful information that has been gained by these studies, trying to understand uterine physiology on a gene-by-gene basis is exceedingly difficult due to the complexity of the uterine transcriptome. Moreover, most cytokines and growth factors have multiple actions with the molecular mechanisms including endometrial growth, angiogenesis, and implantation. Therefore, a new genomic and proteomic approach is needed to better understand the complex genomic and multifactorial etiology of uterine endometrial expression profiles (Kim et al., 2003; Ace and Okulicz, 2004; Hayes, 2004; DeSouza et al., 2005; White and Salamonsen, 2005; Horcajadas et al., 2007). The development of genomic and proteomic techniques for large-scale expression analysis has provided the means to analyze gene products on a global scale. Genome-wide approaches with microarray technologies are being used widely to evaluate global gene expression in a variety of systems from bacteria to primates (D'Hooghe et al., 2004). Indeed, if reproductive physiologists are to truly understand uterine physiology, it will be necessary to: 1. define most or all uterine-specific transcripts and 2. define the global patterns of uterine gene transcription and protein expression throughout the estrous cycle and during pregnancy.

Toward that goal, our research group has produced and sequenced several thousand cDNAs from libraries generated from female reproductive tissues and early embryos of pigs. Information regarding the EST project, and the resulting unigene set of

43

novel genes, can be found at the project website (http://genome.rnet.missouri.edu/Swine/) (Whitworth et al., 2004 and 2005; Green et al., 2006). Amplified cDNAs were used to create DNA microarrays for use in monitoring global changes in mRNA abundance throughout the estrous cycle in gilts.

The goal of this work was to define those genes that are differentially expressed in the non-pregnant (NP) porcine endometrium. This experiment used total RNAs extracted from cyclic endometrium (Days 0, 3, 6, 10, 12, 14 and 18 post-estrus) hybridized to an in-house cDNA microarray consisting of 19,968 spotted cDNAs representing 14,129 distinct genes. These data will begin to define the complex patterns of gene expression responsible for creating an environment conducive to sperm transport, early embryonic growth and embryo attachment.

MATERIALS AND METHODS

Experimental Animals and Tissue Collection

Twenty purebred Yorkshire gilts were used in this study. Unmated gilts were hysterectomized on Days 0, 3, 6, 10, 12, 14, and 18 post-estrus (n=3 per stage; except Day 0 where two pigs were used) (Fig. 2). The first day of estrus is designated Day 0. At 24 hours after the last feeding, sodium thiopental anesthesia (8 mg/lb BW, Veterinary Pentothal® by Abbott Lab.) was administered intravenously. Gilts were maintained under anesthesia with a closed circuit system of halothane (2-5%; USP by Halocarbon Lab.) and oxygen (400~1000 cc/min) for the duration of the surgery. Ovariectomy-hysterectomies were performed, and the uterine endometrium and the oviduct were individually collected from cycling gilts. All gilts were housed in the UMC Animal Science Research Center (ASRC) and their care complied with the UMC Animal Care and Use Committee (ACUC) and the *Guide for the Care and Use of Laboratory Animals*. Each endometrial sample was harvested immediately after the surgery, snap frozen in liquid nitrogen and stored at -80°C until RNA extraction.

Total RNA Extraction and cDNA Preparation

Total RNA from each endometrial sample (Days 0, 3, 6, 10, 12, 14, and 18) was extracted by using the RNA STAT-60™ reagent (Tel-Test, Friendswood, TX), according to the manufacturer's instructions. RNA quality was confirmed by the ratio of its absorbance at 260 and 280 nm and by visualization on ethidium bromide stained agarose gels. High-quality total RNAs were further purified by using the RNeasy Mini kit

(Qiagen Inc., Valencia, CA), according to the manufacturer's instructions. In addition, a reference RNA pool, which consisted of a mixture of non-reproductive (heart, kidney, liver, spleen, pituitary, hypothalamus, skeletal muscle, small intestine) and reproductive tissues (corpus luteum, follicles, oviduct, endometrium, placenta and fetus), was purified in an identical manner. The purified endometrial and reference RNAs (15 μg) were indirectly labeled with 3-aminoallyl-2′-deoxyuridine-5′-triphosphate (aa-dUTP) (Sigma, St. Louis, MO) by reverse transcription with Superscript II RT (Invitrogen, Carlsbad, CA) and 1 μl poly dT oligonucleotide (50 μM) (Whitworth et al., 2005). A standard protocol (Hegde, et al., 2000) for labeling with aa-dUTP was followed, with minor modifications: the labeling mixture contained a 25mM dATP, dCTP, and dGTP, and 15mM dTTP and 10mM aa-dUTP. 2μl 50 μM oligo dT primer was employed in cDNA preparation.

Complementary DNA Microarray

Previously our research team reported the creation of cDNA microarrays containing more than 19k spots. The clones used on the array arose from porcine EST projects at the University of Missouri-Columbia (Whitworth, 2005; Agca, 2006). Aminoallyl-labeled cDNAs from the endometrial and reference samples were purified by using the Qiagen QIAquick PCR purification kit (Qiagen, Valencia, CA) and dried by using a Centravap vacuum centrifugation system (Labconco, Kansas City, MO). The dried aa-cDNA samples were resuspended in 0.1 M sodium carbonate buffer (Na_2CO_3, pH 9.0). The aa-cDNAs from the endometrial sample and reference RNA pool were labeled with Cy5 and Cy3 monoreactive dyes (Amersham Biosciences, Piscataway, NJ),

respectively, for 1 hour at room temperature. The samples were purified by using Qiagen

PCR Purification Kit and dried by Centravap (Labconco) to remove uncoupled dye.

Labeling efficiencies of the cDNA reactions, prior to microarray hybridization, were

calculated by determining the amount of nucleotides per amount of dye (Hegde et al.,

2000 and http://pga.tigr.org/PDF/BiotechniquesCookbook_II.pdf). All cyclic endometrial

cDNA samples (labeled with Cy5) and reference samples (labeled with Cy3) possessed

dye incorporation per sample greater than 1600 pmol. Labeling efficiencies were less

than 50, which is nearly optimal for hybridization. These efficiencies were calculated by

using the protocol 'Amino-allyl labeling of RNA for microarrays' provided by TIGR

(http://www.tigr.org/tdb/microarray/protocolsTIGR.shtml). The labeled cDNAs were

resuspended in 26 μl of 1X hybridization buffer (48% formamide, 4.8X SSC, 0.1%SDS

and 20 μg polyA-DNA in water) and denatured at 95°C for 3 minutes, followed by rapid

cooling on ice for 30 sec. The labeled probe mixtures were applied to the microarray

slides under 22 x 40 mm Lifter Slips (Erie Scientific, Portsmouth, NH). The slides were

hybridized at 42°C for 16 hours and then washed at room temperature in a low stringency

wash buffer containing 1X SSC and 0.1% SDS, followed by a high stringency wash in

0.1X SSC and 0.1% SDS. The slides were subjected to a final wash in 0.1X SSC and then

were rinsed in water before being dried by centrifugation at 1000 rpm for 5 minutes. The

slides were placed in a light-tight slide box until they were scanned by using a Genepix

4000B scanner (Axon Instruments, Union City, CA). The scanned files were loaded into

GeneSpring GX 7.3.1 software (Agilent Technologies-Silicon Genetics, Redwood City,

CA) for statistical data analysis and to create visual depictions of the results.

Data Analysis by using GeneSpring GX 7.3.1.

All raw data as GenePix Results Files (*.gpr) were imported into GeneSpring GX 7.3.1. Normalization of locally weighted linear regression (LOWESS), the fiftieth percentile per chip and median per gene were performed on all good spots. Then the data were filtered based on spot quality (good quality spots needed to be present in at least one of the experimental groups) and signal intensity. Comparisons were made across the estrous time points. A cross-Gene error model based on both biological and technical replicates was allowed to define the amount of variability. This model was used as the basis for standard deviation (SD), standard error (SE), and t-test p-value calculations (all data manipulations are reviewed in the GeneSpring GX User Manual).

Relative expression levels were derived by comparing normalized/filtered data between the reference and the endometrial samples. Analysis of variance (ANOVA) ($p<0.05$) with a multiple testing correction was performed by using the Benjamini and Hochberg False Discovery Rate multiple correction test on each comparison. Gene trees and condition trees provided measures of similarity (Pearson correlation) in gene expression patterns between each microarray in the experiment. Each distance between the seven different estrous stages, or between the twenty individual animals, is actually a measure of dissimilarity ranging from 0 (the same) to 1 (different). K-means clustering (standard correlation) and Self-Organizing Maps (SOM) of the differentially expressed genes was performed to identify groups of genes possessing similar expression patterns in the endometrium during the porcine estrous cycle.

Quantitative Real-Time Reverse Transcription PCR (qRT-PCR)

Transcriptional changes for thirteen candidate cDNAs, representing differentially expressed genes during the estrous cycle, were selected for confirmation by quantitative real-time PCR. Clone names, annotation and Genbank accession numbers as well as the Genbank accession number for the annotation are listed in Table 1. Oligonucleotides were designed by using Primer Express® software 2.0 (Applied Biosystems) and were obtained from Integrated DNA technologies (Skokie, IL). Firstly, cDNA from each endometrial sample was diluted to 5 ng/µL, and then serial dilutions were performed to final concentrations of 0.5, 0.05, and 0.005 ng/µL for each sample. Quantitative RT-PCR was performed on 0.05 ng/µL concentration by using the QuantiTect SYBR Green PCR Kit (Qiagen) on the ABI Prism 7500 system (Applied Biosystems) by following the manufacturer's instructions and standard protocols (Whitworth et al., 2005; Agca et al., 2006). All amplifications were performed in triplicate on each plate, and each plate was replicated two times, resulting in six threshold cycle (C_T) measurements/gene. A housekeeping gene (p4mm3-015-H07, EST accession # CO945226; YWHAG; NM_012479) was chosen, because it showed a steady expression pattern in the porcine endometrium during the estrous cycle (days from 0 to 18). YWHAG is orthologous to the *Homo sapiens* tyrosine 3-monooxygenase/tryptophan 5-monooxygenase activation protein, gamma polypeptide (YWHAG) gene. Whitworth et al., (2005) had previously used it as a 'housekeeping' gene in pig embryo experiments. Threshold cycle (C_T) for the target gene was subtracted from the C_T of the housekeeping gene in the experimental sample to obtain the change (Δ) in C_T (ΔC_T). A ΔC_T value for the target gene was also determined for the reference sample. The relative amount of each mRNA relative to the reference was calculated by assuming an amplification efficiency of 2 and by using the

equation $2^{-\Delta\Delta CT}$ which was calculated from "$_\Delta C_{T,\,sample}$ - $_\Delta C_{T,\,reference}$." Data of $2^{-\Delta\Delta CT}$ values were analyzed by a least-squares analysis of variance by using the General Linear Models procedure of SAS 9.1 (SAS Institute Inc., NC). Contrasts were performed within group of stages to estimate differences between days of the estrous cycle.

Expression Analysis Systemic Explorer (EASE)

The software program, Expression Analysis Systemic Explorer (EASE, http://david.niaid.nih.gov/david/_ease.htm), helps interpret gene lists from microarray results based on the most prominent gene ontology (Hosack et al., 2003; Whitworth et al., 2005). All Genbank accession numbers of selected genes in the clustered expression patterns (Table 3) were loaded into the EASE program and analyzed to find over-represented categories. EASE (version 2.0) then generated an annotation table for each gene list and provided an EASE score (essentially a P-value) to identify the most significant biological themes within each gene list.

RESULTS

Microarray expression results from estrous cycle stages

ANOVA, with the Benjamini and Hochberg false discovery rate multiple testing correction, was performed in GeneSpring GX on 18,806 spots (after removing control and empty spots) to identify differentially represented genes in each RNA sample. A list of all genes on the array can be found on our website (http://genome.rnet.missouri.edu/Swine/Publications/). A total of 4,190 genes were found to differ significantly (p<0.05) over the course of the estrous cycle, and their spot intensity was at least 100 fluorescent units higher in expression level from the endometrial raw data. Examples of some of the genes having statistically significant changes in signal across the stages were listed in Table 2. Many of the genes have been described previously in the endometrium and the relative changes in abundance are consistent with previous reports (Green et al., 1998; Allen et al., 2002; Naseri et al., 2004; White et al., 2005; Kavser et al., 2006). 964 of 4,190 differentially expressed transcripts (p < 0.05) were also rather abundant in the endometrium because their signals were over twice as high as the spot intensity coming from the reference samples, in at least 1 of the 7 timepoints. When monitored on a day by day basis, the prevalence of abundant transcripts varied over the course of the estrous cycle (Day 0: 129; Day 3: 238; Day 6: 265; Day 10: 511; Day 12: 561; Day 14: 548; and Day 18: 331 genes) (See Appendix I). Among 4,190 genes (p < 0.05), 267 genes were in fact four times higher than the reference samples. The abundant transcripts were sorted by signal intensities compared to the reference RNA and the 25 most abundant genes present at each stage are represented in Appendix I.

The gene and condition trees showed that the estrous stages and the twenty individual animals were clustered in an expected manner; for example, the earliest stages were grouped together and the later stages also demonstrated similar expression patterns as shown by the value of distance, which is actually a measure of dissimilarity ranging from 0 (the same) to 1 (different) (Fig. 3-A & B). The similarity of gene expression patterns by K-means and Self-Organizing Map (SOM) clustering (Fig. 4-A to -I) showed that there were a large number of transcripts that changed throughout the estrous cycle and that the detected differences were not simply due to changes at one or only a few timepoints.

Biological Themes Identified by using EASE

The simplified gene ontology in GeneSpring GX was used to categorize significantly differentially expressed genes (4,190 genes having $p < 0.05$) into three biological categories: 1,991 genes were categorized in biological processes, 1,693 genes in cellular components and 2,159 genes in the molecular function (Venn Diagram in Fig. 5-A). Most differentially expressed genes in biological processes were involved in cellular (1,159 genes), physiological (1,130 genes), and regulation of biological (412 genes) process (Fig. 5-B). Cell related (1,149 genes), organelle (758 genes), and protein complex (294 genes) were abundantly expressed in cellular component (Fig. 5-C). Finally, 1,047 binding related genes, catalytic activity (516 genes), and signal transducer (183 genes) or transporter activity (148 genes) had molecular function in Gene Ontology (Fig. 5-D). Biological themes categorized in this manner by Gene Ontology are rather

broad. Therefore, the EASE program was used to identify pathways that changed significantly during the estrous cycle.

Gene Ontology comparisons between endometrial transcripts in the nine cluster profiles

In Table 3, a high proportion of the differentially expressed genes at Day 0 of the estrous cycle were found to be involved in immune functions, as was reflected in changing immune markers and cytokine populations. Days 0 and 18 genes were also involved in responses to external stimuli as well as exhibiting endopeptidase and proteasome activity. Days 3-6 genes were disproportionately involved in catalysis, specifically in hydrogen ion transporter activity and polyamine biosynthesis. Days 3-14 genes were involved in sterol biosynthesis and intermediate filament, possibly associated with uterine morphological changes via cell proliferation and differentiation under the influence of progesterone. Days 10-12 genes were involved in ATPase activity, development, and receptor tyrosine-kinase signaling pathways that may facilitate conceptus elongation and endometrial morphological changes. Days 10-14 genes were associated with signal transduction and morphogenesis and they may help prepare the conceptus for attachment and placentation (Table 3).

Real-time PCR verification of microarray results

As shown in Table 1, thirteen genes were selected from both the nine interesting patterns (Fig. 4) and from the abundant gene lists (Table A-G in Appendix I) for validation by using quantitative RT-PCR. These genes were identical or orthologous to: *H. sapiens* vanin 2 (VNN2; NM_078488, CO940823), *H. sapiens* laminin, gamma 2 (LAMC2; NM_018891, CO991514), *H. sapiens* ornithine decarboxylase 1 (ODC1;

NM_002539, CN026972), *H. sapiens* cytochrome P450 (CYP26A1; NM_000783, CO993312), *H. sapiens* annexin A4 (ANXA4; NM_001153, CO994549), *H. sapiens* interleukin 24 (IL24; NM_006850, CO994632), *H. sapiens* neuromedin U (NMU; NM_006681, CO994261), *H. sapiens* matrix metalloproteinase 7 (MMP7; NM_214207, CO991589), *Sus scrofa* uterine plasmin trypsin inhibitor (UPTI; L14282, CO986361), *S. scrofa* mucosa-associated epithelial chemokine CCL28 (CCL28; NM_001024695, CO988554), *H. sapiens* retinol binding protein 4 (RBP4; NM_006744, CO994296), and *S. scrofa* uteroferrin (UF; NM_214209, CO948659). The normalized ratio from the microarray raw data was calculated by using GeneSpring GX 7.3.1. Statistically significant differences in the ratio are known as a Type I Error (common false discovery rates are 0.05). The normalized ratio from the microarray raw data was calculated by using GeneSpring GX 7.3.1. The p-value associated with each normalized ratio indicates the probability of obtaining the sample data when there are no mean differences between estrous stages; a low p-value (commonly $p < 0.05$) provides the evidence for significant mean differences between estrous stages.

All genes showed significant differences during the estrous stages (Table 4), except *Homo sapiens* tyrosine 3-monooxygenase/tryptophan 5-monooxygenase activation protein, gamma polypeptide, mRNA (YWHAG; NM_012479, accession # of the porcine representative sequence: CO945226), which served as a 'housekeeping' gene. All quantitative RT-PCR results were tested for significant differences by using Tukey's test at $\alpha = 0.05$ by the GLM procedure of SAS 9.1 (SAS Institute Inc., NC). Each gene was differentially expressed at specific times during the estrous cycle. However, the

expression level of these transcripts as measured by RT-PCR had patterns consistent with

the microarray results (Table 4).

DISCUSSION

The mammalian uterine endometrium undergoes many striking physiological changes during the estrous cycle and pregnancy that arise in response to an array of endocrine, paracrine, and autocrine signals (Roberts and Bazer, 1988; Spencer et al., 1993; Gray et al., 2001; Tarleton et al., 2001). These changes help create the microenvironment required for the movement of gametes, capacitation of sperm, fertilization, successful embryonic development and subsequent fetal growth (Geisert et al., 1982a, b, and c; Roberts and Bazer, 1988; Roberts, 1993; Spencer and Bazer, 2004). Most of the overt changes in the uterine endometrium are a reflection of temporally- and spatially-specific gene expression during the estrous cycle and pregnancy. In this study, a gene expression profiling experiment illustrated some of the broad changes in mRNA populations that take place in the uterine endometrium.

The results of the gene and condition trees, on both estrous cycle stages and the individual animals, indicated that the groups tended to cluster together in an expected manner based on the stage of the cycle (Fig. 2-A and -B). Another expectation was that genes known to be responsive to estrogen and/or progesterone should be found in the differentially-expressed gene lists based on the changing concentrations of circulating steroid during the estrous cycle [estrus (maximal E_2 concentrations), metestrus (newly formed corpus luteum; low E_2 and low P_4), diestrus (fully functional CL; high progesterone, P_4), and proestrus (declining P_4; increasing E_2). In assessing the results, it was clear that this expectation was met. For example, retinol binding protein 4 (RBP4; NM_006744, CO994296), uteroferrin (UF; NM_214209, CO948659), uterine

plasmin/trypsin inhibitor (UPTI; L14282, CO986361), and fibroblast growth factor receptor 2 (FGFR2; NM_022970, CN031722) are known progesterone-responsive genes and were found to be upregulated in both the array results and in the qPCR analyses (Table 2 and 4) (Fazleabas et al., 1982; Clawitter et al., 1990; Groothuis et al., 1997; Groothuis et al., 2002; Wollenhaupt et al., 2005). Known estrogen-induced genes were also represented in the data; for example, matrix metalloproteinase 7 (MMP7, matrilysin; NM_214207, CO991589) is an MMP family member that is involved in the breakdown of the extracellular matrix during normal physiological processes including during embryonic development, reproduction, and tissue remodeling. When E_2 is dominant the endometrium undergoes rapid proliferation. If embryos are not present in the tract by the end of the second week after estrus, subsequent luteolysis causes circulating P4 levels to decline, which results in the remodeling of the functional region of the endometrium particularly as estrogen concentrations begin to rise in association with growing follicules (Brenner and Slayden, 1994). The MMPs have been associated with remodeling of the extracellular matrix (ECM) and degradation of the ECM (reviewed in Hulboy et al., 1997). As shown in Fig 3-B and Table 4, MMP7 was expressed according to circulating E_2 levels which is highest between proestrus (Day 18) and estrus (Day 0). Indeed, MMP7 is upregulated in human cervical-vaginal tissues (Gorodeski, 2007) and it may be associated with laminin gamma 2 (LAMC2; NM_018891, CO991514), which is an ECM glycoprotein and major noncollagenous constituent of basement membranes. MMP7 and LAMC2 have a similar expression pattern in endometrium during the estrous cycle, especially between Days 18 to 0 (estrus). During this period, the endometrium undergoes

rapid restructuring that is reflected in an increased mitotic index and in the synthesis of ECM materials (Maatta et al., 2004; Gorodeski, 2007).

While many genes are regulated by reproductive hormones, the results from this work did suggest a appropriate housekeeping gene for use in uterine transcriptional profiling. Often glyceraldehyde-3-phosphate dehydrogenase (GAPDH), beta-actin and cyclophilin are constitutively expressed in many different tissues and many studies have used these genes as a control or housekeeping gene to evaluate and compare RNA transcription of target genes. However, steroid hormones including E_2 transcriptionally regulate GAPDH and beta-actin in the uterus (Weisinger et al., 1999; Ing and Robertson, 1999; Ing and Zhang, 2004). For these experiments, a uniformly expressed clone (p4mm3-015-H07; CO945226) was identified in the endometrium whose mRNA concentrations remained essentially unchanged throughout the estrous cycle. This gene encoded tyrosine 3-monooxygenase/tryptophan 5-monooxygenase activation protein, gamma polypeptide (YWHAG, NM_012479) protein, which plays a role in signal transduction by binding to phosphoserine-containing proteins (Fu et al., 1994) and is induced by growth factors in human vascular smooth muscle cells (Autieri and Carbone, 1999). In humans, this gene is relatively highly expressed in brain, skeletal muscle, and heart and expressed in reproductive tissues such as testis and ovary (Horie, et al., 1999). We have also identified YWHAG in a germinal vesicle EST library (Whitworth et al., 2004) and during transcriptional profiling of pig embryogenesis (Whitworth et al., 2005). In those studies, the YWHAG transcript was found not to change significantly and was used as a normalization control for qPCR experiments. Consequently, because YWHAG

transcripts were found not to change much in uterine endometrium, it was used as a housekeeping gene in these experiments (Table 1) to standardize qRT-PCR results.

The mammalian endometrium undergoes a complex series of cyclical changes under the overall control of E_2 and P4 during the estrous (or menstrual) cycle. However, most of the biological molecular pathways that are responsible for those changes still remain unknown. The identification of novel gene and molecular pathways is essential in order to better understand the important biological processes taking place in the uterine endometrium during the estrous cycle and pregnancy.

To establish lists of similarly upregulated genes (many of which are likely to be functionally relevant), k-means and Self Organizing Maps were created in GeneSpring to gain preliminary insight into clustered genes. The subsequent clusters were further refined by the "find similar" function that allowed the further identification of transcript profiles that mimicked a defined profile. In addition to the clustering work, the ANOVA genes were also filtered based on relative abundance in the endometrium (i.e. having a signal that exceeded the reference by at least 2-fold in at least one of the time-points). From these results, we chose thirteen differentially expressed and/or abundant endometrial genes whose mRNA concentrations throughout the estrous cycle were confirmed by quantitative real-time PCR. In each case, these transcripts exhibited the same trends in both the microarray and RT-PCR results (Table 4). Five genes, including UF (NM_214209, CO948659), RBP4 (NM_006744, CO994561), TIMP2 (NM_003255, CO954667), MMP7 (NM_214207, CO991589), and UPTI (L14282, CO986361), had expression patterns that were consistent with previous results (Roberts and Bazer, 1988;

Bazer et al., 1991; Harney et al., 1993; Stallings-Mann et al., 1990; reviewed in Curry and Osteen, 2003).

A number of predictions can be made regarding some putative functional roles for the genes in each cluster: Those highest at D0 and at D0&D18 (cluster groups 1 and II) may be helping facilitate sperm transport and/or remodeling of the endometrium after loss of P4 stimulation. Those genes that are upregulated between D3-12 and D3-14 (cluster groups 5 and 6) probably represent P4-responsive genes that help create a luminal environment capable of promoting the growth of the embryos once it is in the lumen. The genes upregulated at D3-6 (cluster group 4) may be helping to create a luminal environment that facilitates blastocyst hatching and growth once the embryos enter the lumen around D6. These may also represent genes involved in the proliferation of the endometrium that takes place at this stage and may also be a class of genes transiently responsive to newly synthesized P4 arising from the corpora lutea. Those genes that peak at D10-12, D10-14 and at D14-18 (cluster groups 7-9) may be involved in preparing the endometrium to respond to conceptus-derived estrogen if the animal were to be pregnant. These genes are also likely to be involved in producing some of the uterine histotroph (including growth factors) required to nourish the elongating conceptuses. Finally, the genes found in cluster group 3 (highest at D0 & D10-14) were perhaps the most enigmatic. However, the EASE analysis suggested an involvement in protein turnover for this cluster.

Some of the individual genes chosen for follow-up had either not been described in porcine endometrium or had not been characterized extensively in this tissue. One of the genes in this category was interleukin 24 (IL-24). IL-24 is also known as Melanoma

60

differentiation-associated protein 7 (mda-7) based on its presence in melanoma cells. It was initially described as a tumor suppressing protein capable of inducing apoptosis these cells (Jiang, et al., 1995 and 1996; Su et al., 1998). IL-24/mda-7 expression is normally restricted to tissues associated with the immune system, such as the spleen, thymus, and peripheral blood leukocytes, suggesting that it has cytokine-like properties (Hung et al., 2001). IL-24/mda-7 belongs to the IL-10 family, which signals through two heterodimeric receptors including IL-20R1/IL-20R2 and IL-22R1/IL-20R2 (Dumoutier et al., 2001; Wang et al., 2002; Caudell et al., 2002). Therefore, IL-24/mda-7 displays at least two distinct biological functions: a cytokine at low concentrations (Caudell et al., 2002; Gopalkrishnan et al., 2004) and cancer cell-specific growth-inhibitory properties that do not negatively affect normal cells (Jiang, et al., 1996; Su et al., 1998; Mhashilkar et al., 2001; Gupta et al., 2006; Gopalan et al., 2007). Although IL-24 and IL-10 belong to the same family of cytokines, the recent observations highlight the different roles on immune function. IL-10 has anti-inflammatory and immune suppressive roles; however, IL-24/mda-7 functions as an immunomodulatory and pro-inflammatory role (Caudell et al., 2002). Recent research supports the possibility that cytokines such as IL-24/mda-7 activate antigen-presenting cells to present tumor antigens and trigger an antitumor immune response (Caudell et al., 2002; Tong et al., 2005). Interestingly, IL-24 was significantly differentially expressed in the porcine cyclic endometrium from Days 10 to 14 (Table 4). Although this study was focused in the cyclic endometrium, it is hypothesized that IL-24 might activate pro-inflammatory responses during the pregnancy. Early pregnancy establishment in the pig is accompanied by a localized uterine acute inflammatory response, especially during the period of porcine trophoblast attachment

61

(Vonnahme et al., 2004; Leonard et al., 2006). Clearly, further studies are required to clarify the role of IL-24 in regulating the immune response in the uterus.

Vanin 2 (VNN2; NM_078488, CO940823) is a member of the Vanin family of proteins which share extensive sequence similarity with each other and/or with human biotinidase (BTD) (Galland et al., 1998). This encoded protein is secreted, but can also be membrane-associated, by highly vascularized organs such as spleen, kidney, thymus or in tissues containing vanin-1-postive epithelia cells (Galland et al., 1998). Interestingly, vanin-1 is co-expressed with the transcription factors including steroidogenic factor-1 (SF-1) and SRY (sex determining region Y) -box 9 (SOX-9) in Sertoli cells, and is lowly expressed with SF-1 in Leydig cells in developing testes (Wilson et al., 2005). Estrogens are the end products obtained from the irreversible conversion of androgens by aromatase P450 (reviewed in Conley and Hinshelwood, 2001). Wilson and his colleagues (2005) reported that vanin-1 is expressed by the sex- and cell-type-specific manner to provide a suitable environment for male cell development in testicular cells throughout a mouse mutant experiment. In Sertoli cells, vanin-1 is highly co-expressed with SF-1, and E_2 is transformed by aromatase. As previously reported biological roles including significantly high capacity of aromatization at proliferative endometrial tissues (Tseng et al., 1982), vanin2 might have an important role in the endometrium during the estrous cycle. This transcript was differentially expressed at Day 0, 14, and 18 during the estrous cycle (Table 4). In particular, signal intensities of VNN2 were highest at Day 18 during the estrous cycle. Moreover, we found that porcine VNN2 (accession # for the porcine representative sequence, CO940823) was relatively abundant in a cDNA library derived from the oviducts of gilts at estrus (unpublished results). It is hypothesized that VNN2

might be required to provide an appropriate uterine environment during the late diestrus, proestrus, and estrus. Also, it may participate in the regulation of leukocyte trafficking, because the molecular homology is high with glycosylphosphatidyl inositol-anchored protein (GPI-80) and Vanin-1 which have a similar function and are expressed on stromal and epithelial cells of human thymoma (Sasaki et al., 2003).

LAMC2 (NM_018891, CO991514) is a number of a family of extracellular matrix glycoproteins, and the major noncollagenous constituent of basement membranes (Hormia, et al., 1995). This protein undergoes specific proteolytic processing after secretion, and its function can promote adhesion as well as migration (Yuen, et al., 2005). It is important that epithelial cell adhesion to the basement membrane is maintained to aid in the structural stability of the tissue. Up to now, several studies have suggested that LAMC2 is an important player in the cellular invasion and proliferation (Joly et al., 2006). The expression pattern of LAMC2 is similar to VNN2 in Figure 3-B and Table 4. LAMC2 may play an important role of the endometrial cell proliferation during the estrous cycle. Moreover, LAMC2 in squamous cell carcinoma of the tongue is suggested to influence the invasive activity (Katoh et al., 2002). Thus, further experiments may be required to investigate whether or not LAMC2 transcript and its encoded protein are highly expressed at the maternal-fetal interface in either epitheliochorial or hemochorial placentas. The biological functions of LAMC2 may be correlated with MMP7 expression (mentioned later).

ODC1 (NM_002539, CN026972) is the key regulator enzyme involved in polyamine biosynthesis, and it is regulated by c-myc, which is a transcriptional activator implicated not only in the control of cell proliferation and differentiation but also in

apoptosis (Trubiani et al., 1999). ODC activities are also associated with cell transformation, tumor invasion, and angiogenesis (Nemoto et al., 2002). Holinka and Gurpide (1985) reported that ODC expression was significantly higher in the estrogen-dominated follicular phase (proliferative endometrium) than the progesterone-secreting corpus luteum (secretory endometrium) in humans. ODC inhibition induces marked reductions in the intracellular levels of the polyamines (putrescine, spermidine, and spermine), which are essential for cell proliferation and tissue growth. Loss of ODC is predicted to lead to reductions and an imbalance in polyamine pools, which could result in DNA damage and cell death (Pendeville et al., 2001). In Table 4, ODC1 on days 3 − 6 was significantly increased in the cyclic endometrium. This corresponds to the time immediately before porcine blastocysts enter the uterine lumen. Therefore, it likely plays important roles in the endometrial cell proliferation and tissue growth during the estrous cycle, and to prepare an environment conducive to embryo development.

CYP26A1 (NM_000783, CO993312) is a member of the cytochrome P450 superfamily, which are monooxygenases catalyzing many reactions including synthesis of cholesterol, steroids and other lipids. This endoplasmic reticulum enzyme acts on retinoids and regulates the cellular level of retinoic acid which is involved in gene regulation in both embryonic and adult tissues. P4 regulates retinoic acid metabolism both spatially and temporally with multiple related genes, including CYP26A1 (Jeong JW, 2005). Indeed, CYP26A1 was up-regulated during Days 10 − 14, which corresponded to maximal P4 concentrations in blood (Table 4). Most recently, the expression of CYP26A1 in endometrial epithelial cells was regulated by P4 in uteri of ovariectomized

mice and was not significantly influenced by co-administration of E_2 (Fritzsche et al., 2007).

CCL28 (NM_001024695, CO988554) is *sus scrofa* chemokine (C-C motif) ligand 28 of the porcine mucosa-associated epithelial chemokine (MEC) family. CCL28 is abundantly expressed by epithelia in the bronchi, colon, salivary gland, and mammary gland, and at lower levels in the small intestine (reviewed in Campbell et al, 2003). Its receptor is CCR10 found on nearly all IgA-secreting plasma cells present at mucosal sites (Lazarus et al., 2003; Kunkel et al., 2003). This gene had a very fascinating expression pattern as shown by Figure 3-E, and it was significantly up-regulated during Days 3–12 (Table 4). At present, the function of CCL28 is not known; however, CCL28 and its receptor, CCR10, may play a constant role in mucosal immune defense. Interestingly, this gene expression shows a P_4-responsive pattern; however, it was almost dramatically down-regulated (nine fold) at Day 14 during the estrous cycle. It is possible that the downregulation of CCL28 facilitates the initiation of $PGF_{2\alpha}$ pulsatility that begins soon after Day 12. Another possibility may that this gene is still a P_4-responsive gene, because the endometrial concentration of P_4 receptors (PRs) reached the lowest point on Day 12 and PRs lost in luminal epithelial cells during Days 12-14 (Geisert et al., 1994).

ANXA4 (NM_001153, CO994549) is an annexin family of calcium-dependent phopholipid binding proteins whose function is only partially understood (Piljic and Schultz, 2006). To date, in human endometrial microarray experiments, ANXA4 has been shown to be differentially up-regulated during the secretory phase of the human menstrual cycle, when compared with the proliferative phase (Kao et al., 2002; Ponnampalam et al., 2004; Mirkin et al., 2005). ANXA4 is abundant in the kidney,

trachea, lung, intestine and stomach and is thought to be a marker for polarized epithelial cells, because it belongs to a ubiquitous family of structurally related proteins capable of binding anionic phospholipid membranes in a calcium-dependent manner (Ponnampalam and Rogers, 2006). As shown in Fig 3-F and Table 4, ANXA4 expression was significantly increased during the secretory phase (Days 10-14). In cyclic endometrium of gilts, ANXA4 transcription showed it is regulated by progesterone. This result is supported by the experiment on ANXA4 transcription and translation in human endometrium (Ponnampalam and Rogers, 2006). In human endometrium, ANXA4 protein was localized in glandular and luminal epithelium, and the staining signal was strong during the secretory phase (Ponnampalam and Rogers, 2006). This gene was initially identified in this study using the porcine reproductive microarray, and the expression pattern is consistent with results from human endometrial experiments.

To our knowledge, this is the first systematic study describing the use of cDNA microarrays to examine gene expression patterns in the endometrium throughout the porcine estrous cycle. This study analyzed and identified several differentially expressed genes that showed evidence for a role in the endometrial biology. More importantly, however, it provided a wealth of profiling data that identified functionally-related gene clusters at key times during the cycle that likely participate in the different functional roles of the uterus in facilitating gamete transport and embryo/conceptus growth and development. Future experiments will build upon these results and they will hopefully aid in an improved understanding of uterine gene transcriptional changes that will improve our knowledge of uterine physiology.

Table 1. Primer sequences used for qRT-PCR

cDNA ID (Clone ID in GenBank)	Annotation (synonym)	Genbank access no. of annotation	Primer Sequences
p4mm3-015-h07 (CO945226)	Homo sapiens tyrosine 3-monooxygenase/tryptophan 5-monooxygenase activation protein, gamma polypeptide, mRNA (YWHAG)	NM_012479	F- TGACTCACATTCATGATATTCCATCA R- CTCCGTGTTTCTCTAAGGAATTATTTC
peov1-008-c09 (CO940823)	Homo sapiens vanin 2 (VNN2), transcript variant 1, mRNA	NM_078488	F- GGCTCAGATGTTCCGTTCTTG R- ATCAATCTGGCACCTGGAAAA
pd3ov4-001-h05 (CO991514)	Homo sapiens laminin, gamma 2 (LAMC2), transcript variant 1, mRNA	NM_018891	F- GCTTGTGGGAAAGTTGGAGAA R- TTTGAGTGGCCTCCAGCAA
p4civv1-010-d05 (CN026972)	Homo sapiens ornithine decarboxylase 1 (ODC1), mRNA	NM_002539	F- TGCCAACGCACAAGCTACA R- CCCTTGCAACCATGCTACTAGA
pd6end2-014-g09 (CO993312)	Homo sapiens cytochrome P450, family 26, subfamily A, polypeptide 1 (CYP26A1), transcript variant 2, mRNA	NM_000783	F- GGGAGATCATCCACAGGGTACA R- TGACTGGCGGCTCCTAAATG
pd12-14end-004-g02 (CO994549)	Homo sapiens annexin A4 (ANXA4), mRNA	NM_001153	F- TGGAGTCTCCCGATGTGTCA R- CATCCGGGCAAACTTCAAGA
pd12-14end-005-g02 (CO994632)	Homo sapiens interleukin 24 (IL24), transcript variant 1, mRNA	NM_006850	F- ACTCCACACAGCAGCAAGGA R- AGGAGGCTGCAAGGATGG
pd12-14end-005-c10 (CO994598)	Homo sapiens neuromedin U (NMU), mRNA	NM_006681	F- TGGCTTACAATAGGACCTTGGAA R- TCCACAACTGCATGAGAGAAGAA
pd3end3-003-f03 (CO988554)	Sus scrofa mucosa-associated epithelial chemokine CCL28 precursor, mRNA	NM_001024695	F- CACTCGGAAGCTATACTTCCCATT R- TCTAGAAGCCTTCTGGAAATATGATG
pd3ov4-003-a01 (CO991589)	Homo sapiens matrix metallopeptidase 7 (matrilysin, uterine) (MMP7), mRNA	NM_214207	F- GTGTATATAACATTTATTGACATCCACCAA R- TTCAATGACGTGACTGTGTCTTACTC
p8mm4-007-F12 (CO948659)	Sus scrofa tartrate-resistant acid phosphatase mRNA, (Uteroferrin)	NM_214209	F- TGACCCAGGAGAGAGCTTTCC R- CTCGCCCAGCCTGACTTC
pd12-14end-004-h03 (CO994561)	Homo sapiens retinol binding protein 4, plasma (RBP4), mRNA	NM_006744	F- CCCTCCATGTTGCTACAAAATG R- CGGCTGATCACTCACAATGGT
pnatal4-012-g09 (CO954667)	Homo sapiens TIMP metallopeptidase inhibitor 2 (TIMP2), mRNA	NM_003255	F- CTCTTGATGCAGGCGAAAAAC R- TGGACTGGGTCACGGAGAAG
pd10en3-001-f02 (CO986361)	Pig uterine plasmin trypsin inhibitor (UPTI), mRNA	L14282	F- TGCAGGGAAAGGGACATTTT R- TTCTGCCATTCCCATTCTGAGT

Figure 2. Experimental design on the tissue collection time and microarray hybridization.

Biological replication: three non-pregnant gilts / stage (but, two animals at Day 0)

Technical replication: two hybridizations / gilt (but, three hybridizations / gilt at Day 0)

Stages	Estrus	Metestrus	Diestrus	Diestrus	Diestrus	Diestrus	Proestrus	Estrus
Day	0	3	6	10	12	14	18	0
Pig ID	O130	O117	O073	O112	O200	O176	O151	
	W030	W036	O167	O187	W272	O193	O173	
		W285	W243	W282	W247	W260	O188	

68

Figure 3. The gene and condition trees of the seven different estrous stages (A) and twenty individual animals (B) based on 4765 ANOVA passed (p < 0.05) genes. Distance are ranged from 0 (same condition) to 1 (different condition).
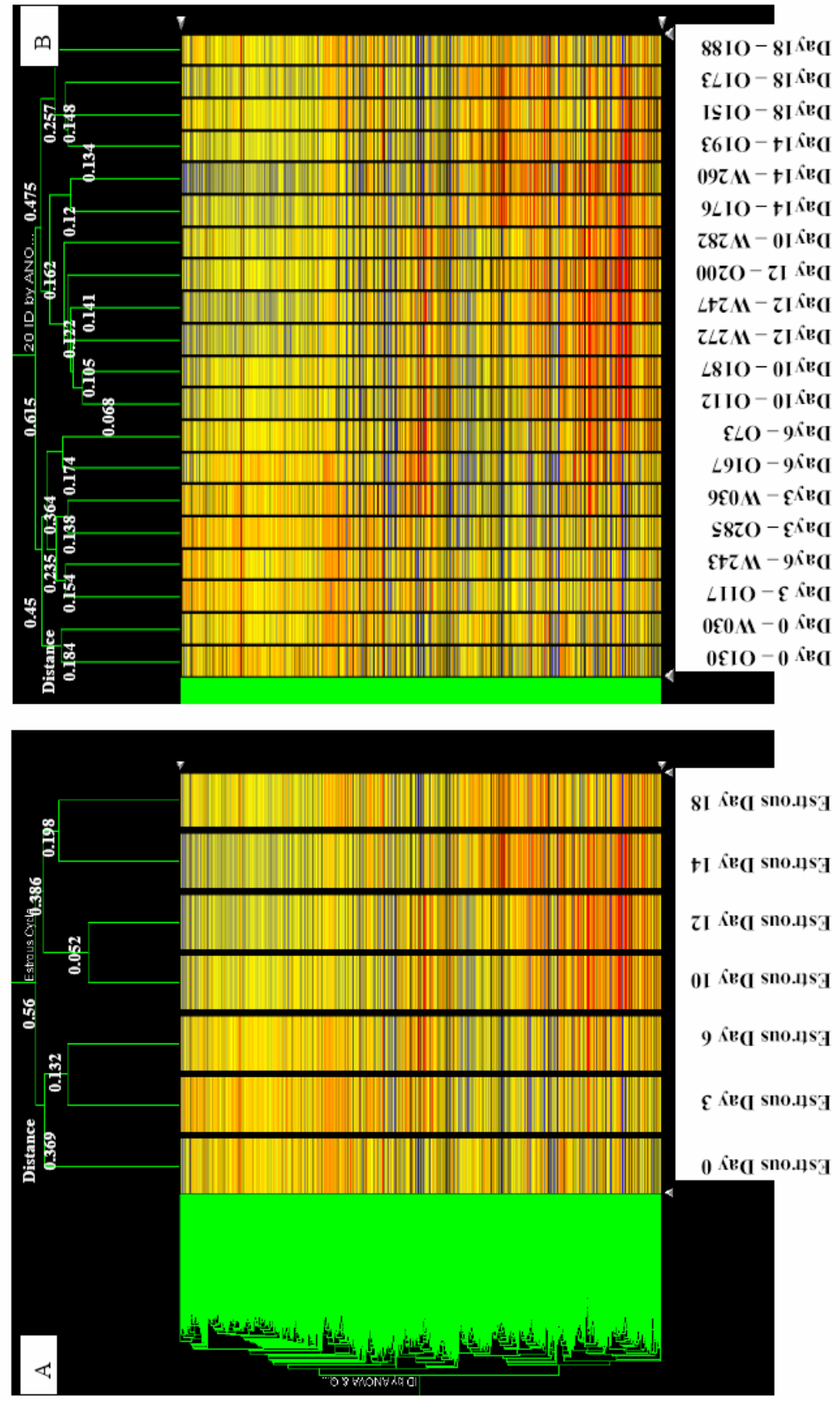
Figure 4. The nine interesting patterns with similar gene expression profiles by K-means and SOM clustering, and inspected gene expression profile (green expression line throughout the estrous cycle in each figure from A to I). X-axis: the porcine estrous cycle, Y-axis: the normalized expression ratio calculated by Cy5 (Cyclic endometrial RNAs) /Cy3 (Reference RNAs).
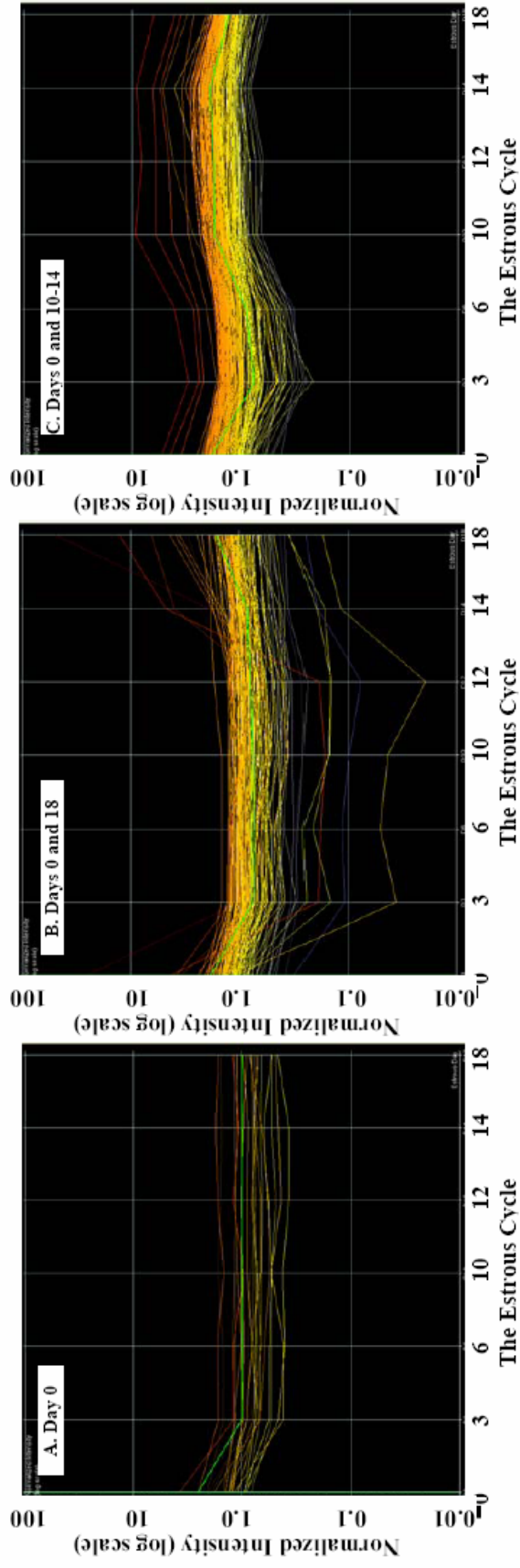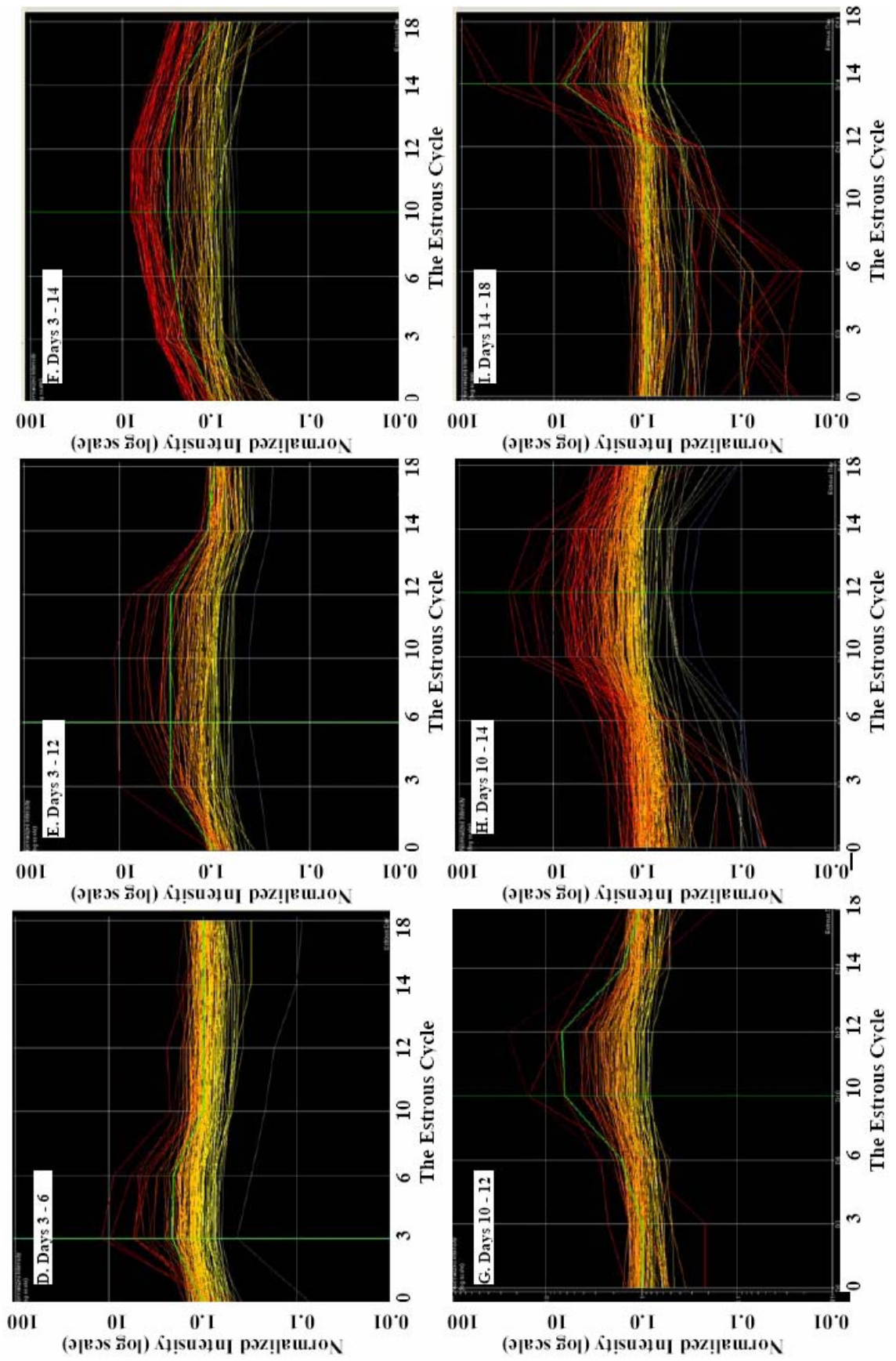
Figure 5. Venn diagram comparing the three Gene Ontology (A) categories of gene list (4,190 genes, p < 0.05) by GeneSpring GX shows biological process (B; 1,991 genes), cellular component (C; 1,693 genes), and molecular function (D; 2,159 genes).
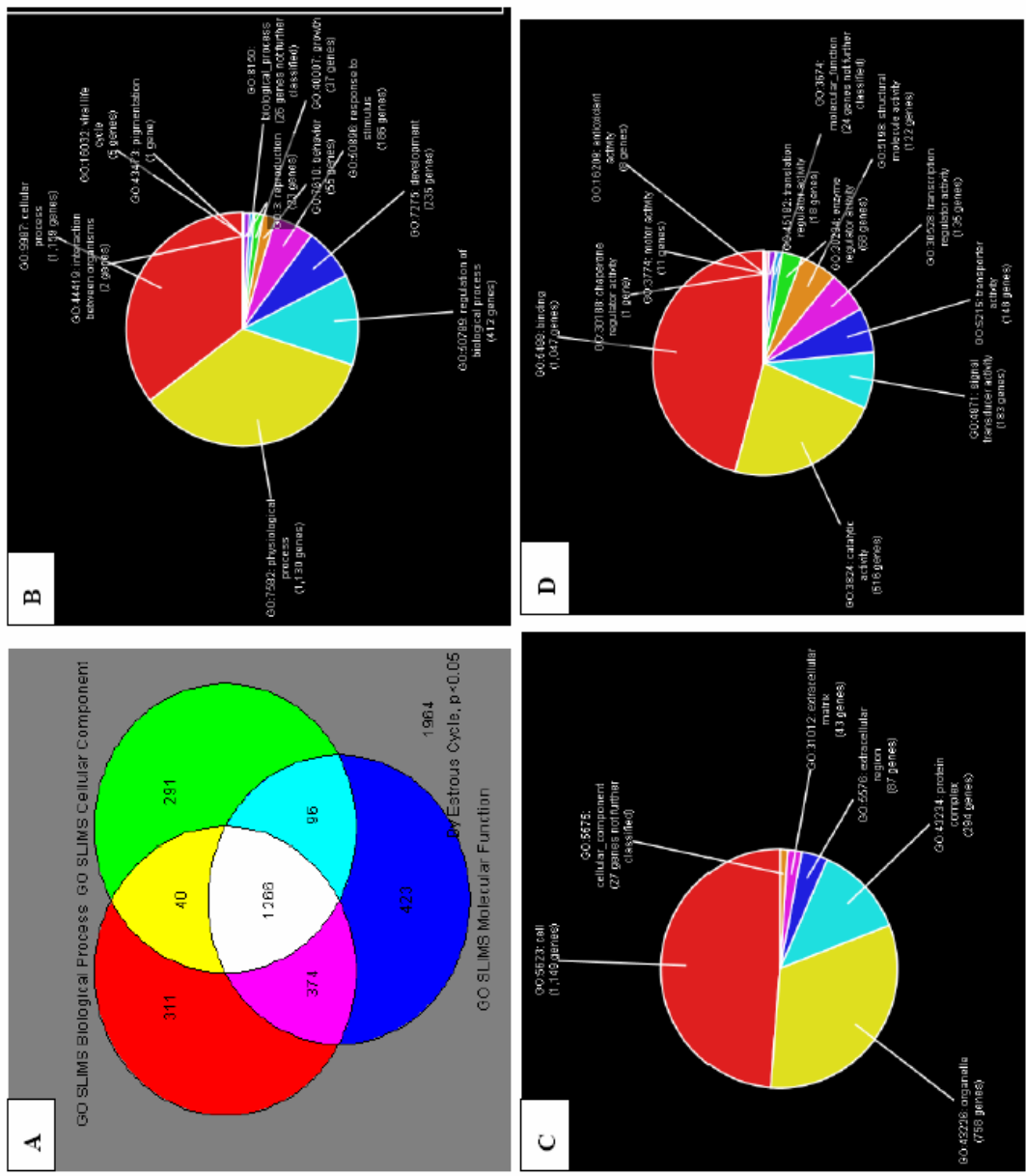
Table 2. Examples of 4,190 genes having statistically significant differences ($p < 0.05$) in the cyclic endometrium.

GenBank ID Clone ID	p-value*	The Porcine Estrous Cycle**							Description
		0	3	6	10	12	14	18	
NM_001114934 CO942163	6.43E-12	0.09	0.06	0.10	0.28	0.53	9.81	4.12	PREDICTED: Macaca mulatta similar to DIPB protein (LOC717072), mRNA
NM_006744 CO994296	1.04E-09	0.02	0.08	0.02	0.13	0.28	7.48	2.40	Homo sapiens retinol binding protein 4, plasma (RBP4), mRNA
NM_214209 CO948659	1.70E-09	1.55	0.19	0.56	4.58	7.95	46.34	31.70	Sus scrofa uteroferrin (UF), mRNA
NM_014895 CO937090	3.19E-09	0.77	0.69	0.68	1.35	2.46	9.82	4.24	Homo sapiens KIAA1009 (KIAA1009), mRNA
NM_001430 CO947516	3.52E-09	1.18	0.71	1.35	5.50	6.91	5.05	2.58	Homo sapiens endothelial PAS domain protein 1 (EPAS1), mRNA
NM_005184 CO953457	4.49E-09	1.56	3.97	5.14	6.77	5.77	3.34	2.63	Homo sapiens calmodulin 3 (phosphorylase kinase, delta) (CALM3), mRNA
NM_022970 CN031722	4.49E-09	1.96	0.87	2.02	4.71	4.78	4.41	1.96	Homo sapiens fibroblast growth factor receptor 2 (keratinocyte growth factor receptor) (FGFR2), transcript variant 3, mRNA
NM_001257 CO994638	5.46E-09	0.71	1.16	3.06	5.16	7.11	5.92	3.14	Homo sapiens cadherin 13, H-cadherin (heart) (CDH13), mRNA
NM_001901 CO944463	5.98E-09	0.62	0.66	0.59	2.67	3.01	5.23	1.59	Homo sapiens connective tissue growth factor (CTGF), mRNA
L14282 CO986361	2.06E-08	0.12	0.05	1.38	4.77	5.16	10.22	1.91	Porcine uterine plasmin trypsin inhibitor (UPTI), mRNA
NM_002970 CO994773	2.06E-08	1.63	4.20	5.86	7.93	7.51	4.62	2.75	Homo sapiens spermidine/spermine N1-acetyltransferase 1 (SAT1), mRNA
NM_007014 CO987720	2.81E-08	0.73	1.25	2.17	5.23	4.60	0.85	0.67	Homo sapiens WW domain containing E3 ubiquitin protein ligase 2 (WWP2), transcript variant 1, mRNA
NM_001014391 CO986261	3.32E-08	1.51	1.50	1.51	2.93	3.19	7.01	3.72	Bos taurus claudin-4 (CLDN4), mRNA
NM_175851 CO994753	4.47E-08	0.32	0.20	0.31	0.24	1.13	54.60	112.02	Homo sapiens ADAM metallopeptidase with thrombospondin type 1 motif, 20 (ADAMTS20), transcript variant 2, mRNA
NM_001682 CO940373	6.07E-08	0.30	0.06	0.10	0.09	0.35	0.98	0.83	Homo sapiens ATPase, Ca++ transporting, plasma membrane 1 (ATP2B1), transcript variant 2, mRNA
NM_006667 CO994264	6.34E-08	0.30	0.43	0.83	2.01	1.97	1.26	0.58	Homo sapiens progesterone receptor membrane component 1 (PGRMC1), mRNA

GenBank ID Clone ID	p-value*	The Porcine Estrous Cycle**							Description
		0	3	6	10	12	14	18	
NM_001024695 CO988554	4.93E-07	1.05	9.88	10.40	11.26	7.47	0.56	0.71	Sus scrofa chemokine CCL28 (CCL28), mRNA
NM_001153 CO994549	8.19E-07	0.56	1.57	2.73	8.27	10.09	3.77	1.63	Homo sapiens annexin A4 (ANXA4), mRNA
NM_001647 CO956860	1.44E-06	1.91	1.48	2.35	2.29	2.53	11.46	6.01	Homo sapiens apolipoprotein D (APOD), mRNA
NM_001039590 CN032108	1.54E-06	1.64	2.57	2.93	5.07	4.84	2.21	1.57	Homo sapiens ubiquitin specific peptidase 9, X-linked (USP9X), transcript variant 3, mRNA

*, p-value cutoff 0.05 and multiple testing correction by Benjamini and Hochberg False Discovery Rate

**, the normalized ratio during the oestrous cycle

Table 3. Gene Ontology comparisons by the EASE program between ANOVA (p < 0.05) passed genes reflected in the nine clustering profiles shown as Figure 3-A to I.

Expression Pattern	System	Gene Category	EASE Score*	Example of Gene
A. Day 0	Molecular Function	Binding	4.43E-02	NM_003185; NM_006769; NM_014268; NM_014574; NM_025208; NM_080284; NM_176799
B. Days 0 and 18	Biological Process	Immune response	3.37E-07	NM_000204; NM_000633; NM_000715; NM_000895; NM_014268; NM_025240; NM_148919; NM_148954
	Molecular Function	Hydrolase activity	3.79E-03	NM_000204; NM_000521; NM_000528; NM_000895; NM_002801; NM_004396; NM_005168; NM_005606; NM_006209; NM_006868; NM_018837; NM_078488
C. Days 0 and 10 - 14	Molecular Function	Protein (degradation) tagging activity	4.46E-02	NM_002954; NM_018955
D. Days 3 - 6	Molecular Function	Ion transporter activity	7.61E-05	NM_001862; NM_001865; NM_002489; NM_002495; NM_003615; NM_004549; NM_005005; NM_006356; NM_015965; NM_134431
	Cellular Component	Inner membrane	1.34E-03	NM_001634; NM_001862; NM_001865; NM_002539; NM_005005; NM_012459; NM_015965
E. Days 3 - 12	Molecular Function	Ion transporter activity (primary active transporter activity)	1.80E-06	NM_001677; NM_002488; NM_004718; NM_005001; NM_005603; NM_005984; NM_006886; NM_013387; NM_014402
F. Days 3 - 14	Biological Process	Sterol metabolism (Steroid biosynthesis)	1.14E-03	NM_000859; NM_002004; NM_003105; NM_006745
G. Days 10 - 12	Biological Process	Programmed cell death (Apoptosis)	6.67E-02	NM_003478; NM_006850; NM_032346; NM_199320

Expression Pattern	System	Gene Category	EASE Score*	Example of Gene
H. Days 10 - 14	Biological Process	G-protein coupled receptor protein signaling	5.06E-03	AF045766; NM_002074; NM_002923; NM_004613; NM_006681; NM_016592; NM_032412
I. Days 14 - 18	Molecular Function	Peptidase activity	8.03E-03	NM_001304; NM_001335; NM_005482; NM_006988; NM_015702; NM_030789; NM_153696

Table 4. The relative quantitation of significantly differentially expressed genes from microarray and real-time PCR analysis.

Genes (Genbank access no.)	Analysis[1]	The Pig Estrous Cycle						
		Day 0	Day 3	Day 6	Day 10	Day 12	Day 14	Day 18
VNN2 (NM_078488, CO940823)	Microarray	4.26 ± 0.40**	0.19 ± 0.09**	0.18 ± 0.10*	0.16 ± 0.01**	0.18 ± 0.16*	4.67 ± 2.11**	12.61 ± 2.57**
	RT-PCR	14.53 ± 1.11^b	0.39 ± 0.02	0.37 ± 0.04	0.08 ± 0.01	0.52 ± 0.07	14.77 ± 2.04^b	39.31 ± 10.5^a
LAMC2 (NM_018891, CO991514)	Microarray	2.06 ± 0.51*	0.53 ± 0.22	0.61 ± 0.16	0.77 ± 0.07*	0.60 ± 0.16	1.43 ± 0.68	3.53 ± 0.71**
	RT-PCR	32.41 ± 3.95^a	4.42 ± 0.89^{cd}	2.44 ± 0.32^d	2.40 ± 0.48^d	1.42 ± 0.15^d	9.90 ± 0.74^c	17.80 ± 1.17^b
MMP7 (NM_214207, CO991589)	Microarray	25.39 ± 7.13**	0.98 ± 0.88	0.96 ± 2.18	0.36 ± 0.05**	0.39 ± 0.02**	1.85 ± 5.86	48.53 ± 14.74**
	RT-PCR	77.13 ± 2.86^b	1.92 ± 0.19	9.12 ± 0.57	0.34 ± 0.01	0.22 ± 0.01	30.81 ± 3.38	250.05 ± 25.60^a
ODC1 (NM_002539, CN026972)	Microarray	0.79 ± 0.04**	5.27 ± 2.19**	4.47 ± 2.82*	1.31 ± 0.18	0.97 ± 0.13	0.69 ± 0.08*	0.89 ± 0.07
	RT-PCR	1.31 ± 0.27	11.91 ± 1.43^a	11.64 ± 1.52^a	2.93 ± 0.36	1.15 ± 0.10	1.23 ± 0.11	1.69 ± 0.20
CYP26A1 (NM_000783, CO993312)	Microarray	0.20 ± 0.03**	1.31 ± 0.69	5.708 ± 0.7*	2.69 ± 0.26**	2.59 ± 0.74*	1.09 ± 0.93	0.14 ± 0.02**
	RT-PCR	0.12 ± 0.02	6.57 ± 0.23	67.23 ± 4.27^a	5.74 ± 0.45	4.47 ± 0.28	4.06 ± 0.25	0.15 ± 0.04
CCL28 (NM_1024695, CO988554)	Microarray	1.05 ± 0.13	9.87 ± 2.10**	10.39 ± 2.88**	$11.26 \pm .39$**	7.46 ± 3.67**	0.55 ± 0.11*	0.71 ± 0.15
	RT-PCR	1.98 ± 0.19	17.79 ± 1.63^a	21.12 ± 2.12^a	19.89 ± 2.13^a	8.94 ± 1.10^b	0.63 ± 0.04	0.72 ± 0.06
ANXA4 (NM_001153, CO994549)	Microarray	0.56 ± 0.10*	1.57 ± 0.32	2.72 ± 1.36	8.27 ± 0.79**	10.09 ± 0.37**	3.77 ± 0.68**	1.62 ± 0.28*
	RT-PCR	1.55 ± 0.02^f	2.89 ± 0.08^{ef}	5.74 ± 0.26^c	12.65 ± 0.75^a	9.912 ± 0.21^b	4.81 ± 0.31^{cd}	3.35 ± 0.17^{de}
IL24 (NM_006850, CO994632)	Microarray	0.95 ± 0.08	1.02 ± 0.05	2.35 ± 2.52	15.33 ± 2.64**	24.73 ± 3.83**	2.82 ± 0.42**	1.30 ± 0.10*
	RT-PCR	0.61 ± 0.09	0.53 ± 0.08	4.63 ± 0.37	67.03 ± 4.85^a	36.63 ± 4.57^b	2.62 ± 0.13	0.77 ± 0.13
NMU (NM_006681, CO994598)	Microarray	0.11 ± 0.02**	0.14 ± 0.09**	0.90 ± 2.92	23.13 ± 5.67**	29.23 ± 0.23**	16.83 ± 3.71**	2.04 ± 3.51
	RT-PCR	0.32 ± 0.07	1.10 ± 0.18	24.08 ± 4.49	177.67 ± 32.55^a	67.53 ± 11.21^b	84.57 ± 16.26^b	29.18 ± 6.08^{bc}

Genes (Genbank access no)	Analysis[1]	The Pig Estrous Cycle						
		Day 0	Day 3	Day 6	Day 10	Day 12	Day 14	Day 18
UF (NM_214209, CO948659)	Microarray	1.55 ± 0.17**	0.19 ± 0.04**	0.65 ± 0.25	4.58 ± 0.59**	7.95 ± 1.44**	46.34 ± 4.65**	31.69 ± 17.14**
	RT-PCR	3.13 ± 0.13	0.45 ± 0.21	1.44 ± 0.11	8.63 ± 0.57	51.19 ± 16.45^{b}	97.56 ± 4.27^{a}	89.92 ± 8.09^{a}
RBP4 (NM_006744, CO994561)	Microarray	0.02 ± 0.00**	0.11 ± 1.07	0.04 ± 0.02**	0.15 ± 0.03**	0.27 ± 0.33	6.27 ± 0.90**	2.66 ± 1.42
	RT-PCR	0.05 ± 0.00	0.08 ± 0.01	0.07 ± 0.01	0.39 ± 0.05	0.87 ± 0.10	14.67 ± 1.93^{a}	10.27 ± 1.23^{b}
TIMP2 (NM_003255, CO954667)	Microarray	1.17 ± 0.12	0.73 ± 0.02**	0.93 ± 0.03	1.45 ± 0.10**	2.44 ± 0.31**	6.14 ± 0.67**	3.57 ± 17.14**
	RT-PCR	2.25 ± 0.43	0.72 ± 0.09	0.52 ± 0.08	4.02 ± 0.73	4.75 ± 0.78	15.01 ± 1.95^{a}	9.56 ± 1.38^{b}
UPTI (L14282, CO986361)	Microarray	0.11 ± 0.03**	0.05 ± 0.01**	1.38 ± 1.94	4.77 ± 0.19**	5.16 ± 0.70**	10.22 ± 3.27**	1.91 ± 0.84
	RT-PCR	0.04 ± 0.01	0.01 ± 0.00	1.65 ± 0.22^{d}	8.99 ± 0.50^{a}	3.86 ± 0.57^{c}	6.62 ± 0.39^{b}	1.24 ± 0.17^{de}

[1], values in Microarray results were normalized to all array spots by using LOWESS, and values in Real-Time PCR were normalized to a housekeeping gene.

- Each cell represents the mean ± S.E.M.
- Symbols * and ** indicate differences at p-value < 0.05 and p-value < 0.01, respectively with GeneSpring GX 7.3.1.
- The same letters including [a], [b], [c], [d], [e], and [f] are not significantly different at α = 0.05 with Tukey's Student Range Test by GLM procedure of SAS

APPENDIX   I

Twenty Five Most Abundant Transcripts and their GO at Each Estrous Stage

Of the significantly differentially expressed genes defined by ANOVA, 964 of these were abundant transcripts in that their signals were over twice as high as the spot intensity coming from the reference samples in at least 1 of the 7 timepoints (Day 0: 121; Day 3: 234; Day 6: 255; Day 10: 464; Day 12: 529; Day 14: 326; and Day 18: 318 genes) (Table A to G). Of these, an additional 267 genes were four times higher than the reference samples. The endometrial genes having at least two times higher intensities than reference sample were sorted by signal intensities on the endometrial RNA abundances within each estrous stage, and the twenty-five genes that had the largest ratio were represented in Tables A to G.

The two fold-up increased gene lists were ranked according to their EASE score, which measures the relative enrichment of a GO term annotated to a particular gene group of a specific estrous stage (described in more detail in the body of the thesis).

Gene Ontology comparisons between two fold-up expressed genes at each estrous stage

The genes from Table A to G were interpreted on the most prominent gene ontology by using EASE 2.0. As shown in Table A, 121 genes at Day 0 represented structural molecular activity in molecular function including Homo sapiens laminin, gamma 2 (LAMC2; NM_018891). 234 genes at Day 3 represented cytosolic ribosom in

cellular component and biosynthesis in biological process including Homo sapiens ribosomal protein L22 (RPL22; NM_000983). 255 genes at <u>Day 6</u> represented cytosolic small ribosomal subunit in cellular component and amine biosynthesis in biological process including Homo sapiens ornithine decarboxylase 1 (ODC1; NM_002539). 464 genes at <u>Day 10</u> represented alcohol metabolism in biological process and integral to plasma membrane in cellular component including Homo sapiens neuromedin U (NMU; NM_006681). 529 genes at <u>Day 12</u> represented morphogenesis and organogenesis in biological process including Homo sapiens fibroblast growth factor receptor 2 (FGFR2; NM_000141). 326 genes at <u>Day 14</u> represented cell surface receptor linked signal transduction and steroid metabolism in biological process including Homo sapiens retinol binding protein 4 (RBP4; NM_006744). Finally, 318 genes at <u>Day 18</u> resented extracellular matrix in cellular component including Homo sapiens TIMP metallopeptidase inhibitor 2 (TIMP2; NM_003255).

Gene lists are displayed in Tables A-I for each of the different stages of the cycle. Associated tables summarizing the EASE results are also included.

Table A. Abundant genes at Day 0 based on ANOVA passed genes (p<0.05)

Clone Name	GenBank Id	Gbid	p-value	Ratio (Cy5/Cy3)*	Cy5=Endo**	Description
p4mm3-019-c04	NM_001003	CO945454	0.000163	2.3	18010.3	Homo sapiens ribosomal protein, large, P1 (RPLP1), transcript variant 1, mRNA
p4mm3-020-d11	XM_495885	CO945528	5.61E-06	2.4	16005.6	PREDICTED: Homo sapiens similar to ribosomal protein S12 (LOC440055), mRNA
pnatal4-003-b02	NM_001011	CO953900	0.00219	2.0	15301.6	Homo sapiens ribosomal protein S7 (RPS7), mRNA
p4mm3-004-e08	NM_001030	CO944444	0.0174	2.2	15005.3	Homo sapiens ribosomal protein S27 (metallopanstimulin 1) (RPS27), mRNA
p4mm3-011-c09	NM_001011	CO944904	0.00137	2.1	13955.7	Homo sapiens ribosomal protein S7 (RPS7), mRNA
pnatal4-003-C03	US***	non	0.0464	2.0	13622.7	M13reverse Sheep spleen\brain pSport1 library Ovis aries cDNA clone Oa_splbn_11
p8mm4-020-g01	CO949682	CO949682	0.000503	2.1	13603.0	866262 MARC 4PIG Sus scrofa cDNA 3', mRNA sequence /clone_end=3' /gb=CF78
p2mm4-004-b01	NM_001022	CO942817	0.00187	2.1	13571.7	Homo sapiens ribosomal protein S19 (RPS19), mRNA
p4civp1-006-E02	CN025285	CN025285	0.0105	2.2	11118.0	UMC-p4civp1-006-e02 In-Vitro-4-Cell-Embryo p4civp Sus scrofa cDNA 3', mRNA se
pd12-14end-010-A11	NM_214028	CO994967	0.0313	2.7	11007.0	Sus scrofa inhibin beta-subunit (INHBA), mRNA
p2mm4-001-h04	NM_015367	CO942676	0.0418	2.5	10029.3	Homo sapiens BCL2-like 13 (apoptosis facilitator) (BCL2L13), nuclear gene encodin
pputal1-003-e08	NM_005617	CO955520	0.00162	2.3	9960.4	Homo sapiens ribosomal protein S14 (RPS14), transcript variant 3, mRNA
pputal1-003-d07	NM_000994	CO955510	0.0131	2.1	9678.4	Homo sapiens ribosomal protein L32 (RPL32), transcript variant 1, mRNA
pputal1-003-d01	NM_001035006	CO955505	0.0192	2.0	9111.7	Homo sapiens ribosomal protein L17 (RPL17), transcript variant 2, mRNA
BF712863	BF712863	BF712863	2.64E-05	2.4	9010.7	****No Hits Found****
pnatal4-019-e10	NM_133507	CO955182	0.00289	2.8	8343.3	Homo sapiens decorin (DCN), transcript variant E, mRNA
pnatal4-002-c06	NM_000967	CO953835	0.0426	2.0	8197.7	Homo sapiens ribosomal protein L3 (RPL3), transcript variant 1, mRNA
BF712988	BF712988	BF712988	0.0042	1.9	8096.4	****No Hits Found****
BF712987	BF712987	BF712987	0.0458	2.0	7915.3	****No Hits Found****
pfeto1-012-e08	XM_593621	CO952992	0.00421	2.0	7636.7	PREDICTED: Bos taurus similar to GrpE protein homolog 1, mitochondrial precursor
p2mm4-017-e05	NM_001011	CO943728	0.000937	2.1	7470.0	Homo sapiens ribosomal protein S7 (RPS7), mRNA
pd12-14end-003-D11	NM_003849	CO994443	0.0364	2.0	7292.4	Homo sapiens succinate-CoA ligase, GDP-forming, alpha subunit (SUCLG1), mRNA
p4mm3-002-a11	NM_002305	CO944291	2.20E-06	3.2	7201.6	Homo sapiens lectin, galactoside-binding, soluble, 1 (galectin 1) (LGALS1), mRNA
pd12-14end-008-E04	NM_133507	CO994865	0.0219	2.3	7103.7	Homo sapiens decorin (DCN), transcript variant E, mRNA
pblivp1-001-d09	NM_000978	CN027962	0.00979	2.1	6995.0	Homo sapiens ribosomal protein L23 (RPL23), mRNA

*, normalized ratio = Cy5 (Endometrial sample) / Cy3 (Reference sample)

**, Cy5 signal intensities correspond to the endometrial mRNAs purified from different estrous days during the estrous cycle

***, US means unaccepted sequences.

Table A-1. Gene Ontology of abundant genes at Day 0 based on ANOVA passed genes (p<0.05)

System	Gene Category	EASE Score*	Example of Genes (GenBank ID)
Molecular Function	Structural molecule activity	1.22E-08	NM_000094; NM_000224; NM_000967; NM_000978; NM_001003; NM_001004; NM_001011; NM_001022; NM_001030; NM_001306; NM_002948; NM_002954; NM_005617; NM_006082; NM_007104; **NM_018891** **(LAMC2)**; NM_182848; NM_199442
Cellular Component	cytosolic ribosome (sensu Eukarya)	6.96E-06	NM_000967; NM_001003; NM_001004; NM_001011; NM_001022; NM_001030; NM_005617; NM_007104
Cellular Component	Ribosome	2.11E-05	NM_000967; NM_000978; NM_001003; NM_001004; NM_001011; NM_001022; NM_001030; NM_002948; NM_002954; NM_005617; NM_007104
Cellular Component	ribonucleoprotein complex	5.67E-05	NM_000967; NM_000978; NM_001003; NM_001004; NM_001011; NM_001022; NM_001030; NM_002948; NM_002954; NM_005617; NM_006275; NM_006387; NM_007104
Biological Process	protein biosynthesis	9.61E-04	NM_000967; NM_000978; NM_001003; NM_001004; NM_001011; NM_001022; NM_001030; NM_001568; NM_002948; NM_002954; NM_005617; NM_007104

*, essentially a p-value

82

Table B. Abundant genes at Day 3 based on ANOVA passed genes (p<0.05)

EST Clone ID	GenBank Id	Gbid	p-value	Ratio (Cy5/Cy3)*	Cy5=Endo**	Description
pd12-14end-007-G07	NM_001326	CO994801	6.53E-07	4.2	25980.2	Homo sapiens cleavage stimulation factor, 3' pre-RNA, subunit 3, 77kDa (CSTF3), tran
peov3-014-D12	CO942151	CO942151	4.73E-07	5.4	24583.3	UMC-peov3-014-d12 Oviduct from a gilt in estrus peov Sus scrofa cDNA 3', mRNA seq
pnatal4-002-h08	XR_017657	CO953885	5.08E-07	2.3	23315.0	PREDICTED: Homo sapiens similar to ribosomal protein S2 (LOC646294), mRNA
p4mm3-019-c04	NM_001003	CO945454	0.000163	2.4	21583.5	Homo sapiens ribosomal protein, large, P1 (RPLP1), transcript variant 1, mRNA
pd12-14end-006-G09	AY550075	non	1.12E-05	2.0	21060.8	Sus scrofa 40S ribosomal protein S3a mRNA, partial cds
pgvo4-011-B06	XR_017397	CN032507	0.000519	2.0	18324.0	PREDICTED: Homo sapiens similar to 60S ribosomal protein L7a (LOC644029), mRN
p4mm3-004-e08	NM_001030	CO944444	0.0174	2.2	18236.5	Homo sapiens ribosomal protein S27 (metallopanstimulin 1) (RPS27), mRNA
pd3ov4-002-A03	XM_001088323	CO991524	1.90E-06	3.8	17888.3	PREDICTED: Macaca mulatta similar to Diamine acetyltransferase 1 (Spermidine/sper
p4mm3-020-d11	XM_495885	CO945528	5.61E-06	2.1	17680.8	PREDICTED: Homo sapiens similar to ribosomal protein S12 (LOC440055), mRNA
pblivv4-019-H04	NM_001006	CN031222	0.000308	2.2	17524.3	Homo sapiens ribosomal protein S3A (RPS3A), mRNA
pd12-14end-008-H02	NM_006098	CO994886	1.71E-06	2.2	17248.2	Homo sapiens guanine nucleotide binding protein (G protein), beta polypeptide 2-like 1
p4mm3-011-c09	NM_001011	CO944904	0.00137	2.1	17009.3	Homo sapiens ribosomal protein S7 (RPS7), mRNA
pfeto1-015-a04	CO953154	CO953154	2.63E-05	2.1	16962.3	UMC-pfeto1-015-a04 Fetal ovary pfeto Sus scrofa cDNA 3', mRNA sequence.
p4mm3-007-d10	NM_002970	CO944645	4.67E-05	3.6	16857.5	Homo sapiens spermidine/spermine N1-acetyltransferase 1 (SAT1), mRNA
pd12-14end-003-F04	NM_014579	CO994458	5.57E-06	2.6	16572.5	Homo sapiens solute carrier family 39 (zinc transporter), member 2 (SLC39A2), mRNA
peov3-013-G12	NM_004859	CO942106	0.000231	1.9	16287.2	Homo sapiens clathrin, heavy polypeptide (Hc) (CLTC), mRNA
pd12-14end-007-D09	NM_002970	CO994773	6.65E-08	4.2	16268.2	Homo sapiens spermidine/spermine N1-acetyltransferase 1 (SAT1), mRNA
pd12-14end-010-A01	US***	non	1.86E-06	2.8	16245.2	****No Hits Found****
p2mm4-004-b01	NM_001022	CO942817	0.00187	2.0	16190.3	Homo sapiens ribosomal protein S19 (RPS19), mRNA
pd12-14end-006-B07	NM_000992	CO994667	0.0059	2.5	15816.2	Homo sapiens ribosomal protein L29 (RPL29), mRNA
pd12-14end-003-E10	NM_002970	CO994454	1.41E-05	4.0	13687.2	Homo sapiens spermidine/spermine N1-acetyltransferase 1 (SAT1), mRNA
pd12-14end-004-G09	NM_002273	CO994555	0.0149	2.5	13041.2	Homo sapiens keratin 8 (KRT8), mRNA
pputal2-003-e01	NM_001006	CO955651	0.000622	2.1	12412.0	Homo sapiens ribosomal protein S3A (RPS3A), mRNA
p2mm2-002-f09	XM_001134243	CO942465	3.04E-06	2.1	12292.0	PREDICTED: Homo sapiens similar to 40S ribosomal protein SA (p40) (34/67 kDa lam
pputal6-008-a08	NM_001010	CO956824	2.30E-05	2.1	12128.5	Homo sapiens ribosomal protein S6 (RPS6), mRNA

*, normalized ratio = Cy5 (Endometrial sample) / Cy3 (Reference sample)

**, Cy5 signal intensities correspond to the endometrial mRNAs purified from different estrous days during the estrous cycle

***, US means unaccepted sequences.

Table B-1. Gene Ontology of abundant genes at Day 3 based on ANOVA passed genes ($p<0.05$)

System	Gene Category	EASE Score*	Example of Genes (GenBank ID)
Cellular Component	Cytosol	1.86E-08	NM_000476; NM_000967; **NM_000983 (RPL2)**; NM_000991; NM_000992; NM_001003; NM_001004; NM_001006; NM_001010; NM_001011; NM_001022; NM_001030; NM_002004; NM_002300; NM_002923; NM_003372; NM_006263; NM_007104; NM_031966; NM_032918; NM_134421
Cellular Component	Cytosol ribosome (sensu Eukarya)	5.55E-08	NM_000967; **NM_000983 (RPL2)**; NM_000991; NM_000992; NM_001003; NM_001004; NM_001006; NM_001010; NM_001011; NM_001022; NM_001030; NM_007104
Molecular Function	Structural constituent of ribosome	9.47E-07	NM_000967; NM_000978; **NM_000983 (RPL2)**; NM_000991; NM_000992; NM_001003; NM_001004; NM_001006; NM_001010; NM_001011; NM_001022; NM_001030; NM_002954; NM_007104; NM_022551
Molecular Function	Structural molecule activity	1.27E-06	NM_000224; NM_000967; NM_000978; **NM_000983 (RPL2)**; NM_000991; NM_000992; NM_001003; NM_001004; NM_001006; NM_001010; NM_001011; NM_001022; NM_001030; NM_001306; NM_002273; NM_002300; NM_002954; NM_004859; NM_007104; NM_022551; NM_199328; NM_199442

*, essentially a p-value

84

Table C. Abundant genes at Day 6 based on ANOVA passed genes (p<0.05)

EST Clone ID	GenBank Id	Gbid	p-value	Ratio (Cy5/Cy3)*	Cy5=Endo**	Description
pd12-14end-007-G07	NM_001326	CO994801	6.53E-07	5.1	30995.5	Homo sapiens cleavage stimulation factor, 3' pre-RNA, subunit 3, 77kDa (CSTF3), tra
pd3ov4-002-A03	XM_001088323	CO991524	1.90E-06	5.6	30312.8	PREDICTED: Macaca mulatta similar to Diamine acetyltransferase 1 (Spermidine/spe
pd12-14end-007-D09	NM_002970	CO994773	6.65E-08	5.9	24866.0	Homo sapiens spermidine/spermine N1-acetyltransferase 1 (SAT1), mRNA
pd12-14end-003-F04	NM_014579	CO994458	5.57E-06	3.8	22204.2	Homo sapiens solute carrier family 39 (zinc transporter), member 2 (SLC39A2), mRN
pblivv4-019-H04	NM_001006	CN031222	0.000308	2.0	19544.8	Homo sapiens ribosomal protein S3A (RPS3A), mRNA
p4mm3-007-d10	NM_002970	CO944645	4.67E-05	4.9	19460.7	Homo sapiens spermidine/spermine N1-acetyltransferase 1 (SAT1), mRNA
pd12-14end-010-A01	US***	non	1.86E-06	4.0	19000.7	****No Hits Found****
peov3-012-F01	CO942005	CO942005	4.20E-07	5.9	18848.3	UMC-peov3-012-f01 Oviduct from a gilt in estrus peov Sus scrofa cDNA 3', mRNA se
p4mm3-019-c04	NM_001003	CO945454	0.000163	2.3	18806.2	Homo sapiens ribosomal protein, large, P1 (RPLP1), transcript variant 1, mRNA
peov3-014-D12	CO942151	CO942151	4.73E-07	4.0	18004.7	UMC-peov3-014-d12 Oviduct from a gilt in estrus peov Sus scrofa cDNA 3', mRNA se
peov3-014-D11	XM_001092697	CO942150	0.000934	6.2	17495.7	PREDICTED: Macaca mulatta similar to CCR4-NOT transcription complex, subunit 6-
pnatal4-002-h08	XR_017657	CO953885	5.08E-07	1.9	17011.3	PREDICTED: Homo sapiens similar to ribosomal protein S2 (LOC646294), mRNA
pnatal4-003-b02	NM_001011	CO953900	0.00219	1.9	16315.2	Homo sapiens ribosomal protein S7 (RPS7), mRNA
p2mm4-004-b01	NM_001022	CO942817	0.00187	2.2	15941.3	Homo sapiens ribosomal protein S19 (RPS19), mRNA
pd12-14end-003-E10	NM_002970	CO994454	1.41E-05	4.6	15108.8	Homo sapiens spermidine/spermine N1-acetyltransferase 1 (SAT1), mRNA
p4mm3-011-c09	NM_001011	CO944904	0.00137	1.9	14465.7	Homo sapiens ribosomal protein S7 (RPS7), mRNA
pd12-14end-003-F07	NM_001035459	CO994460	2.58E-05	3.5	14288.8	Bos taurus similar to BCL2-antagonist of cell death protein (MGC127164), mRNA
p4mm3-004-e08	NM_001030	CO944444	0.0174	2.1	14281.2	Homo sapiens ribosomal protein S27 (metallopanstimulin 1) (RPS27), mRNA
peov3-004-B11	XM_938907	CO941369	3.53E-07	5.8	12818.0	PREDICTED: Homo sapiens KIAA1240 protein, transcript variant 4 (KIAA1240), mRN
pd10en3-020-D08	NM_002970	CO987754	0.000125	4.8	12709.2	Homo sapiens spermidine/spermine N1-acetyltransferase 1 (SAT1), mRNA
pd12-14end-010-A01	US***	non	8.04E-09	5.4	12588.7	****No Hits Found****
BF713300	AJ946662	BF713300	0.000209	5.3	12339.4	AJ946662 KN404_1 Sus scrofa cDNA clone C0007747m05 3', mRNA sequence.
pd3ov3-005-E01	XM_001092044	CO990614	7.80E-06	4.8	11587.2	PREDICTED: Macaca mulatta similar to multi sex combs CG12058-PA (LOC703731)
pd12-14end-010-A11	NM_214028	CO994967	0.0313	2.1	11244.2	Sus scrofa inhibin beta-subunit (INHBA), mRNA
p4mm1-001-e09	NM_001007	CO943994	0.0308	2.0	10044.0	Homo sapiens ribosomal protein S4, X-linked (RPS4X), mRNA

*, normalized ratio = Cy5 (Endometrial sample) / Cy3 (Reference sample)

**, Cy5 signal intensities correspond to the endometrial mRNAs purified from different estrous days during the estrous cycle

***, US means unaccepted sequences.

Table C-1. Gene Ontology of abundant genes at Day 6 based on ANOVA passed genes (p<0.05)

System	Gene Category	EASE Score*	Example of Genes (GenBank ID)
Cellular Component	Cytosolic small ribosome subunit (sensu Eukarya)	1.38E-03	NM_001006; NM_001007; NM_001011; NM_001022; NM_001030
Cellular Component	Eukaryotic 48S initiation complex	1.38E-03	NM_001006; NM_001007; NM_001011; NM_001022; NM_001030
Biological Process	Amine biosynthesis	3.08E-03	NM_000860; NM_002112; **NM_002539 (ODC1)**; NM_006623; NM_148174
Cellular Component	Ribosome	3.12E-03	NM_000978; NM_001003; NM_001006; NM_001007; NM_001011; NM_001022; NM_001030; NM_002954; NM_002971; NM_005241; NM_006191

*, essentially a p-value

Table D. Abundant genes at Day 10 based on ANOVA passed genes (p<0.05)

EST Clone ID	GenBank Id	Gbid	p-value	Ratio (Cy5/Cy3)*	Cy5=Endo**	Description
pd12-14end-007-G07	NM_001326	CO994801	6.53E-07	7.4	38649.2	Homo sapiens cleavage stimulation factor, 3' pre-RNA, subunit 3, 77kDa (CSTF3), tran
pd3ov4-002-A03	XM_001088323	CO991524	1.90E-06	8.2	35657.3	PREDICTED: Macaca mulatta similar to Diamine acetyltransferase 1 (Spermidine/sper
pd12-14end-003-F04	NM_014579	CO994458	5.57E-06	5.5	28032.5	Homo sapiens solute carrier family 39 (zinc transporter), member 2 (SLC39A2), mRNA
pd12-14end-007-D09	NM_002970	CO994773	6.65E-08	7.9	26976.3	Homo sapiens spermidine/spermine N1-acetyltransferase 1 (SAT1), mRNA
pnatal3-003-d03	NM_001031789	CO953717	0.00551	2.0	24932.7	Sus scrofa cellular retinol binding protein 1 (CRBP1), mRNA
pd6end2-005-G03	CO992674	CO992674	2.01E-07	18.0	24483.8	AJ947985 KN404_1 Sus scrofa cDNA clone C0007742h10 5', mRNA sequence
pd12-14end-003-E10	NM_002970	CO994454	1.41E-05	6.8	24482.8	Homo sapiens spermidine/spermine N1-acetyltransferase 1 (SAT1), mRNA
pd12-14end-005-C10	NM_006681	CO994598	6.84E-08	23.1	23682.3	Homo sapiens neuromedin U (NMU), mRNA
pd12-14end-010-A01	US***	non	1.86E-06	5.3	23503.8	****No Hits Found****
p4mm3-007-d10	NM_002970	CO944645	4.67E-05	6.4	23045.5	Homo sapiens spermidine/spermine N1-acetyltransferase 1 (SAT1), mRNA
peov3-012-F01	CO942005	CO942005	4.20E-07	7.9	22761.0	UMC-peov3-012-f01 Oviduct from a gilt in estrus peov Sus scrofa cDNA 3', mRNA seq
p8mm4-006-B01	S2009695	non	8.53E-08	7.2	20526.3	EST387105 MAGE resequences, MAGN Homo sapiens cDNA, mRNA sequence /gb=/
pd12-14end-007-F07	NM_207047	CO994791	4.41E-08	6.5	18017.5	Homo sapiens endosulfine alpha (ENSA), transcript variant 7, mRNA
peov3-004-B11	XM_938907	CO941369	3.53E-07	7.5	16319.0	PREDICTED: Homo sapiens KIAA1240 protein, transcript variant 4 (KIAA1240), mRN/
pd12-14end-003-F07	NM_001035459	CO994460	2.58E-05	4.7	15630.7	Bos taurus similar to BCL2-antagonist of cell death protein (MGC127164), mRNA
p4mm3-006-b05	NM_002004	CO944562	9.88E-08	7.9	15627.8	Homo sapiens farnesyl diphosphate synthase (farnesyl pyrophosphate synthetase, dim
pd20fet-019-A01	CO939734	CO939734	3.34E-07	6.9	15512.3	UMC-pd20fet-019-a01 Day 20 fetus pd20fet Sus scrofa cDNA 3', mRNA sequence.
pd12-14end-004-G09	NM_002273	CO994555	0.0149	2.6	14114.8	Homo sapiens keratin 8 (KRT8), mRNA
pd12-14end-007-G11	NM_001903	CO994805	5.95E-06	5.5	13983.5	Homo sapiens catenin (cadherin-associated protein), alpha 1, 102kDa (CTNNA1), mRI
pd12-14end-007-F09	CO994793	CO994793	5.68E-06	5.1	13315.7	UMC-pd12_14end-007-f09 Endometrium pregnant gilt day 12 & 14 pd12_14end Sus s
pd12-14end-005-H09	NM_174142	CO994648	2.74E-06	6.5	13283.8	Bos taurus phytanoyl-CoA hydroxylase (PHYH), mRNA
pd12-14end-010-A01	US***	non	8.04E-09	6.8	12915.8	****No Hits Found****
pd12-14end-006-B07	NM_000992	CO994667	0.0059	2.7	12742.0	Homo sapiens ribosomal protein L29 (RPL29), mRNA
pd3ov3-005-E01	XM_001092044	CO990614	7.80E-06	6.2	12628.5	PREDICTED: Macaca mulatta similar to multi sex combs CG12058-PA (LOC703731),
pd10en3-020-D08	NM_002970	CO987754	0.000125	5.6	12627.5	Homo sapiens spermidine/spermine N1-acetyltransferase 1 (SAT1), mRNA

*, normalized ratio = Cy5 (Endometrial sample) / Cy3 (Reference sample)

**, Cy5 signal intensities correspond to the endometrial mRNAs purified from different estrous days during the estrous cycle

***, US means unaccepted sequences.

87

Table D-1. Gene Ontology of abundant genes at Day 10 based on ANOVA passed genes (p<0.05)

System	Gene Category	EASE Score*	Example of Genes (GenBank ID)
Biological Process	Alcohol metabolism	4.13E-03	NM_000155; NM_000860; NM_002004; NM_002112; NM_002300; NM_003105; NM_004462; NM_005391; NM_005502
Cellular Component	Integral to plasma membrane	6.05E-03	AF045766; NM_000701; NM_001306; NM_001677; NM_001769; NM_001776; NM_002353; NM_003105; NM_003304; NM_003876; **NM_004512 (IL11RA)**; NM_005415; NM_005502; NM_005603; NM_006667; NM_014579; NM_020348; NM_147162; NM_182685
Molecular Function	Lipid transporter activity	6.82E-03	NM_001443; NM_001647; NM_003105; NM_005502; NM_005603
Biological Process	Lipid metabolism	1.31E-02	NM_000860; NM_001443; NM_001647; NM_002004; NM_003105; NM_004462; NM_005502; NM_005603; NM_006214; NM_006412; NM_016371; NM_017436
Biological Process	Amine biosynthesis	1.68E-02	NM_000860; NM_002112; NM_005504; NM_006623; NM_148174

*, essentially a p-value

88

Table E. Abundant genes at Day 12 based on ANOVA passed genes (p<0.05)

EST Clone ID	GenBank Id	Gbid	p-value	Ratio (Cy5/Cy3)*	Cy5=Endo**	Description
pd3ov4-002-A03	XM_0010088323	CO991524	1.90E-06	8.2	36541.7	PREDICTED: Macaca mulatta similar to Diamine acetyltransferase 1 (Spermidine/...
pd12-14end-007-G07	NM_001326	CO994801	6.53E-07	6.3	34512.5	Homo sapiens cleavage stimulation factor, 3' pre-RNA, subunit 3, 77kDa (CSTF3),
pd6end2-005-G03	CO992674	CO992674	2.01E-07	26.2	29272.8	AJ947985 KN404_1 Sus scrofa cDNA clone C0007742h10 5', mRNA sequence
pd12-14end-003-F04	NM_014579	CO994458	5.57E-06	5.2	28343.5	Homo sapiens solute carrier family 39 (zinc transporter), member 2 (SLC39A2), mf
pnatal3-003-d03	NM_001031789	CO953717	0.00551	2.3	26565.5	Sus scrofa cellular retinol binding protein 1 (CRBP1), mRNA
pd12-14end-010-A01	US***	non	1.86E-06	5.2	24298.2	****No Hits Found****
peov3-004-B03	NM_001008408	CO941364	0.0129	2.1	24297.8	Homo sapiens RNA binding motif protein 33 (RBM33), mRNA
pd12-14end-007-D09	NM_002970	CO994773	6.65E-08	7.5	24126.7	Homo sapiens spermidine/spermine N1-acetyltransferase 1 (SAT1), mRNA
peov3-012-F01	CO942005	CO942005	4.20E-07	7.8	22838.2	UMC-peov3-012-f01 Oviduct from a gilt in estrus peov Sus scrofa cDNA 3', mRNA
p4mm3-007-d10	NM_002970	CO944645	4.67E-05	6.7	22716.2	Homo sapiens spermidine/spermine N1-acetyltransferase 1 (SAT1), mRNA
p8mm4-006-B01	S2009695	non	8.53E-08	7.8	22136.5	EST387105 MAGE resequences, MAGN Homo sapiens cDNA, mRNA sequence /...
pd12-14end-005-C10	NM_006681	CO994598	6.84E-08	29.2	20688.3	Homo sapiens neuromedin U (NMU), mRNA
pd12-14end-007-F07	NM_207047	CO994791	4.41E-08	5.5	15794.3	Homo sapiens endosulfine alpha (ENSA), transcript variant 7, mRNA
pd12-14end-003-E10	NM_002970	CO994454	3.50E-06	6.3	15352.6	Homo sapiens spermidine/spermine N1-acetyltransferase 1 (SAT1), mRNA
BF713300	AJ946662	BF713300	2.09E-04	7.0	15125.3	AJ946662 KN404_1 Sus scrofa cDNA clone C0007747m05 3', mRNA sequence.
pd12-14end-007-G11	NM_001903	CO994805	5.95E-06	6.1	14769.0	Homo sapiens catenin (cadherin-associated protein), alpha 1, 102kDa (CTNNA1),
pd12-14end-003-E10	NM_002970	CO994454	1.41E-05	5.9	14758.8	Homo sapiens spermidine/spermine N1-acetyltransferase 1 (SAT1), mRNA
peov3-004-B11	XM_938907	CO941369	3.53E-07	7.0	14301.0	PREDICTED: Homo sapiens KIAA1240 protein, transcript variant 4 (KIAA1240), m
pd12-14end-003-F07	NM_001035459	CO994460	2.58E-05	3.8	13590.0	Bos taurus similar to BCL2-antagonist of cell death protein (MGC127164), mRNA
pd10en3-001-f02	L14282	CO986361	6.32E-08	5.2	13514.7	plasmin trypsin inhibitor
pd12-14end-007-F09	CO994793	CO994793	5.68E-06	5.7	13356.0	UMC-pd12_14end-007-f09 Endometrium pregnant gilt day 12 & 14 pd12_14end Si
pd12-14end-004-G02	**NM_001153**	CO994549	3.04E-06	10.1	13024.8	Homo sapiens annexin A4 (ANXA4), mRNA
pd10en3-013-H05	CO987252	CO987252	6.58E-06	16.8	12994.7	UMC-pd10en3-013-h05 Endometrium gilt D10 of estrous cycle pd10en Sus scrofa
pd12-14end-005-H09	NM_174142	CO994648	2.74E-06	8.4	12994.7	Bos taurus phytanoyl-CoA hydroxylase (PHYH), mRNA
p4mm3-006-b05	NM_002004	CO944562	9.88E-08	7.6	12935.3	Homo sapiens farnesyl diphosphate synthase (farnesyl pyrophosphate synthetase,

*, normalized ratio = Cy5 (Endometrial sample) / Cy3 (Reference sample)

**, Cy5 signal intensities correspond to the endometrial mRNAs purified from different estrous days during the estrous cycle

***, US means unaccepted sequences.

Table E-1. Gene Ontology of abundant genes at Day 12 based on ANOVA passed genes (p<0.05)

System	Gene Category	EASE Score*	Example of Genes (GenBank ID)
GO Biological Process	morphogenesis	5.76E-05	NM_000090; NM_000104; NM_000141 (FGFR2); NM_000224; NM_000266; NM_000478; NM_000618; NM_001402; NM_001430; NM_001443; NM_001664; NM_001901; NM_001920; NM_002166; NM_002191; NM_002448; NM_002615; NM_002825; NM_003027; NM_003118; NM_004463; NM_005077; NM_005180; NM_005686; NM_006214; NM_006271; NM_006471; NM_006623; NM_022970; NM_133503; NM_133504; NM_133507
GO Cellular Component	integral to plasma membrane	6.50E-03	AF045766; NM_000701; NM_001306; NM_001677; NM_001769; NM_001776; NM_002353; NM_003105; NM_003304; NM_003876; NM_004512 (IL11RA); NM_005415; NM_005502; NM_005603; NM_006667; NM_014579; NM_020348; NM_147162; NM_182685
GO Molecular Function	lipid transporter activity	6.82E-03	NM_001443; NM_001647; NM_003105; NM_005502; NM_005603
GO Biological Process	lipid metabolism	1.31E-02	NM_000860; NM_001443; NM_001647; NM_002004; NM_003105; NM_004462; NM_005502; NM_005603; NM_006214; NM_006412; NM_016371; NM_017436
GO Biological Process	amine biosynthesis	1.68E-02	NM_000860; NM_002112; NM_005504; NM_006623; NM_148174
GO Cellular Component	plasma membrane	2.29E-02	AF045766; NM_000701; NM_001306; NM_001677; NM_001769; NM_001776; NM_001901; NM_001903; NM_002353; NM_003105; NM_003304; NM_003876; NM_004512 (IL11RA); NM_005273; NM_005415; NM_005502; NM_005603; NM_006667; NM_006751; NM_014579; NM_018362; NM_020348; NM_147162; NM_182685; NM_199328

*, essentially a p-value

Table F. Abundant genes at Day 14 based on ANOVA passed genes (p<0.05)

EST Clone ID	GenBank Id	Gbid	p-value	Ratio (Cy5/Cy3)*	Cy5=Endo**	Description
peov3-013-C01	XM_920906	CO942054	6.70E-08	42.0	39813.8	PREDICTED: Mus musculus bromodomain containing 8, transcript variant 9 (Brd8),
p8mm4-007-f12	NM_214209	CO948659	4.71E-09	46.3	27803.3	Sus scrofa uteroferrin (UF), mRNA
pd12-14end-010-B02	NM_214209	CO994970	5.25E-07	26.3	24857.3	Sus scrofa uteroferrin (UF), mRNA
pd10en3-001-f02	L14282	CO886361	6.32E-08	10.2	18846.3	plasmin trypsin inhibitor
pd12-14end-007-G07	NM_001326	CO994801	6.53E-07	4.1	18366.0	Homo sapiens cleavage stimulation factor, 3' pre-RNA, subunit 3, 77kDa (CSTF3), t
pd3ov4-002-A03	XM_001088323	CO991524	1.90E-06	4.7	18313.0	PREDICTED: Macaca mulatta similar to Diamine acetyltransferase 1 (Spermidine/sp
p8mm4-007-f12	NM_214209	CO948659	4.91E-09	35.4	17703.8	Sus scrofa uteroferrin (UF), mRNA
pgvo2-009-D10	CN031976	CN031976	1.11E-07	13.5	17640.7	UMC-pgvo2-009-d10 Germinal-Vesicle-Oocyte pgvo Sus scrofa cDNA 3', mRNA se
p8mm4-006-B01	S2009695	non	8.53E-08	5.7	16433.2	EST387105 MAGE resequences, MAGN Homo sapiens cDNA, mRNA sequence /gb
p4mm3-007-d10	NM_002970	CO944645	4.67E-05	4.4	16415.8	Homo sapiens spermidine/spermine N1-acetyltransferase 1 (SAT1), mRNA
pd12-14end-003-F04	NM_014579	CO994458	5.57E-06	2.9	14955.8	Homo sapiens solute carrier family 39 (zinc transporter), member 2 (SLC39A2), mR
pd12-14end-007-D09	NM_002970	CO994773	6.65E-08	4.6	14830.7	Homo sapiens spermidine/spermine N1-acetyltransferase 1 (SAT1), mRNA
pd12-14end-010-A01	US***	non	1.86E-06	3.1	13981.3	****No Hits Found****
pd12-14end-005-C10	NM_006681	CO994598	6.84E-08	16.8	13080.7	Homo sapiens neuromedin U (NMU), mRNA
pd12-14end-007-F07	NM_207047	CO994791	4.41E-08	3.8	11449.5	Homo sapiens endosulfine alpha (ENSA), transcript variant 7, mRNA
peov3-012-F01	CO942005	CO942005	4.20E-07	4.6	11422.7	UMC-peov3-012-f01 Oviduct from a gilt in estrus peov Sus scrofa cDNA 3', mRNA s
peov3-014-D11	XM_001092697	CO942150	0.000934	4.1	10862.5	PREDICTED: Macaca mulatta similar to CCR4-NOT transcription complex, subunit t
BF713300	AJ946662	BF713300	0.000209	4.3	10359.7	AJ946662 KN404_1 Sus scrofa cDNA clone C0007747m05 3', mRNA sequence.
pnatal4-019-e10	NM_133507	CO955182	0.00289	3.2	10138.2	Homo sapiens decorin (DCN), transcript variant E, mRNA
pd12-14end-010-A11	NM_214028	CO994967	0.0313	3.4	10036.5	Sus scrofa inhibin beta-subunit (INHBA), mRNA
peov3-004-B11	XM_938907	CO941369	3.53E-07	4.8	9897.7	PREDICTED: Homo sapiens KIAA1240 protein, transcript variant 4 (KIAA1240), mR
p4mm3-006-b05	NM_002004	CO944562	9.88E-08	5.2	9477.8	Homo sapiens farnesyl diphosphate synthase (farnesyl pyrophosphate synthetase, (
p4civp1-006-E02	CN025285	CN025285	0.0105	3.0	9422.8	UMC-p4civp1-006-e02 In-Vitro-4-Cell-Embryo p4civp Sus scrofa cDNA 3', mRNA se
pd12-14end-010-B02	NM_214209	CO994970	9.74E-09	18.2	9079.3	Sus scrofa uteroferrin (UF), mRNA
pd20fet-019-A01	CO939734	CO939734	3.34E-07	4.4	8998.0	UMC-pd20fet-019-a01 Day 20 fetus pd20fet Sus scrofa cDNA 3', mRNA sequence.

*, normalized ratio = Cy5 (Endometrial sample) / Cy3 (Reference sample)

**, Cy5 signal intensities correspond to the endometrial mRNAs purified from different estrous days during the estrous cycle

***, US means unaccepted sequences.

Table F-1. Gene Ontology of abundant genes at Day 14 based on ANOVA passed genes (p<0.05)

System	Gene Category	EASE Score*	Example of Genes (GenBank ID)
GO Biological Process	cell surface receptor linked signal transduction	1.67E-03	AF045766; NM_001901; NM_002191; NM_002353; NM_002825; NM_002923; NM_004613; NM_006206; NM_006471; NM_006681 (NMU); NM_006988; NM_012242; NM_016269; NM_024945; NM_032315
GO Biological Process	steroid metabolism	1.21E-02	NM_002004; NM_003105; NM_004462; NM_005502; NM_016371
GO Biological Process	cholesterol metabolism	1.40E-02	NM_002004; NM_003105; NM_004462; NM_005502
GO Molecular Function	enzyme regulator activity	1.79E-02	NM_001153 (ANXA4); NM_002615; NM_002825; NM_002923; NM_003255 (TIMP2); NM_004463; NM_005241; NM_005863; NM_015367; NM_019084; NM_021102
GO Cellular Component	integral to membrane	1.81E-02	AF045766; NM_000478; NM_001306; NM_001769; NM_001776; NM_002353; NM_003105; NM_003304; NM_004362; NM_004462; NM_004487; NM_005415; NM_005502; NM_006206; NM_006412; NM_006471; NM_014579; NM_015367; NM_016371; NM_021102; NM_022873; NM_022897; NM_022970; NM_024315; NM_147188; NM_147200; NM_178818; NM_182685; NM_199328

*, essentially a p-value

Table G. Abundant genes at Day 18 based on ANOVA passed genes (p<0.05)

EST Clone ID	GenBank Id	Gbid	p-value	Ratio (Cy5/Cy3)*	Cy5=Endo**	Description
pd12-14end-007-F04	NM_006804	CO994788	3.96E-08	99.4	55893.7	Homo sapiens START domain containing 3 (STARD3), mRNA
pd12-14end-007-B11	NM_175851	CO994753	1.46E-07	112.0	55025.8	Homo sapiens ADAM metallopeptidase with thrombospondin type 1 motif, 20 (A
peov3-013-C01	XM_920906	CO942054	6.70E-08	30.3	40424.7	PREDICTED: Mus musculus bromodomain containing 8, transcript variant 9 (Br
p8mm4-007-f12	NM_214209	CO948859	4.71E-09	31.7	39012.2	Sus scrofa uteroferrin (UF), mRNA
peov3-001-H08	NM_024045	CO941194	0.0147	2.5	37694.0	Homo sapiens DEAD (Asp-Glu-Ala-Asp) box polypeptide 50 (DDX50), mRNA
peov3-014-E12	XM_0011114934	CO942163	2.85E-11	4.1	34333.0	PREDICTED: Macaca mulatta similar to DIPB protein (LOC717072), mRNA
pd6end2-007-E05	CO992799	CO992799	0.000234	2.7	29307.7	UMC-pd6end2-007-e05 Endometrium gilt D6 of estrous cycle pd6end Sus scrof
pd12-14end-010-B02	NM_214209	CO994970	5.25E-07	22.1	28372.3	Sus scrofa uteroferrin (UF), mRNA
peov3-004-B03	NM_001008408	CO941364	0.0129	2.5	24714.2	Homo sapiens RNA binding motif protein 33 (RBM33), mRNA
p8mm4-007-f12	NM_214209	CO948859	4.91E-09	27.1	23447.3	Sus scrofa uteroferrin (UF), mRNA
p4mm3-020-d11	XM_495885	CO945528	5.61E-06	2.7	23214.3	PREDICTED: Homo sapiens similar to ribosomal protein S12 (LOC440055), mR
pputal6-002-e03	NM_000088	CO956389	0.000414	2.1	20831.2	Homo sapiens collagen, type I, alpha 1 (COL1A1), mRNA
peov3-014-H12	CO942190	CO942190	0.00221	2.0	20188.2	UMC-peov3-014-h12 Oviduct from a gilt in estrus peov Sus scrofa cDNA 3', mRI
peov3-008-B03	NM_006591	CO941668	0.0243	2.0	19224.7	Homo sapiens polymerase (DNA-directed), delta 3, accessory subunit (POLD3),
pd10en3-016-D11	NM_000090	CO987447	0.00541	2.4	19064.3	Homo sapiens collagen, type III, alpha 1 (Ehlers-Danlos syndrome type IV, auto
peov3-014-D11	XM_0010092697	CO942150	0.000934	5.3	16797.5	PREDICTED: Macaca mulatta similar to CCR4-NOT transcription complex, subu
p4mm3-007-d10	NM_002970	CO944645	4.67E-05	2.6	16351.3	Homo sapiens spermidine/spermine N1-acetyltransferase 1 (SAT1), mRNA
pd12-14end-003-A08	CO994412	CO994412	5.22E-08	5.3	16181.8	UMC-pd12_14end-003-a08 Endometrium pregnant gilt day 12 & 14 pd12_14enc
pnatal4-019-e10	NM_133507	CO955182	0.00289	3.7	15957.2	Homo sapiens decorin (DCN), transcript variant E, mRNA
p8mm4-002-d03	NM_003145	CO948250	0.0194	2.4	15511.8	Homo sapiens signal sequence receptor, beta (translocon-associated protein be
pd12-14end-004-C04	NM_006744	CO994513	1.81E-08	3.0	14831.3	Homo sapiens retinol binding protein 4, plasma (RBP4), mRNA
pd12-14end-007-G07	NM_001326	CO994801	6.53E-07	2.4	14620.3	Homo sapiens cleavage stimulation factor, 3' pre-RNA, subunit 3, 77kDa (CSTF
pd3ov3-010-B12	CO990980	CO990980	7.27E-08	3.3	14488.8	UMC-pd3ov3-010-b12 Oviduct gilt D3 of estrous cycle pd3ov Sus scrofa cDNA :
pnatal4-003-g12	NM_152991	CO953955	0.00133	2.4	13903.8	Homo sapiens embryonic ectoderm development (EED), transcript variant 2, mF
p8mm4-006-B01	S2009695	non	8.53E-08	3.0	12726.7	EST387105 MAGE resequences, MAGN Homo sapiens cDNA, mRNA sequenc

*, normalized ratio = Cy5 (Endometrial sample) / Cy3 (Reference sample)

**, Cy5 signal intensities correspond to the endometrial mRNAs purified from different estrous days during the estrous cycle

Table G-1. Gene Ontology of abundant genes at Day 18 based on ANOVA passed genes (p<0.05)

System	Gene Category	EASE Score*	Example of Genes (GenBank ID)
GO Cellular Component	extracellular	1.10E-03	NM_000088; NM_000089; NM_000090; NM_000094; NM_000552; NM_001647; NM_001920; NM_001996; NM_002193; NM_003255 (TIMP2); NM_004477; NM_004613; NM_006486; NM_006744 (RBP4); NM_006763; NM_006988; NM_007293; NM_007349; NM_018891 (LAMC2); NM_021102; NM_133504; NM_133507
GO Cellular Component	extracellular matrix	1.62E-03	NM_000088; NM_000089; NM_000090; NM_000094; NM_000552; NM_001920; NM_001996; NM_003255(TIMP2); NM_006486; NM_006988; NM_018891 (LAMC2); NM_133504; NM_133507
GO Molecular Function	structural molecule activity	1.85E-03	NM_000088; NM_000089; NM_000090; NM_000094; NM_000224; NM_001306; NM_001924; NM_001996; NM_002300; NM_002823; NM_002954; NM_006013; NM_006082; NM_006471; NM_006486; NM_014895; NM_018477; NM_018891 (LAMC2); NM_182848; NM_199442
GO Cellular Component	fibrillar collagen	7.54E-03	NM_000088; NM_000089; NM_000090
GO Biological Process	development	7.86E-03	NM_000088; NM_000089; NM_000090; NM_000094; NM_000224; NM_000245; NM_001430; NM_001920; NM_002166; NM_002193; NM_002615; NM_002823; NM_003114; NM_003199; NM_003483; NM_004039; NM_004362; NM_004463; NM_005156; NM_005241; NM_005252; NM_006471; NM_007349; NM_018891 (LAMC2); NM_133504; NM_133507; NM_173171
GO Cellular Component	collagen	7.88E-03	NM_000088; NM_000089; NM_000090; NM_000094

*, essentially a p-value

APPENDIX   II

DIFFERENTIAL EXPRESSION OF *Ornithine Decarboxylase-1* (*ODC-1*) AND *Neuromedin U* (*NMU*) IN THE NON-PREGNANT (NP) AND PREGNANT (P) UTERINE ENDOMETRIUM OF SWINE

ABSTRACT

Female reproductive organs undergo extensive temporal and spatial changes in gene expression throughout the estrous cycle and pregnancy. Recently, microarray results from our group identified the polyamine biosynthetic enzyme *ornithine decarboxylase-1* (*ODC-1*, NM_002539) and the smooth muscle contractile neuropeptide *neuromedin U* (*NMU*, NM_006681) as being differentially expressed in non-pregnant (NP) endometrium. The former was maximal on days 3 and 6; the latter was maximal on days 10 to 14. The goal of this experiment was to use real-time PCR to examine the expression of these transcripts in the early pregnant (P) uterus and to determine if they differ from NP animals. When *ODC-1* and *NMU* were compared to *tyrosine 3-monooxygenase/tryptophan 5-monooxygenase activation protein, gamma polypeptide* (YWHAG, NM_012479), *ODC-1* was maximal at D3-6 as expected, but there were no differences in ODC-1 mRNA amounts between the NP and P endometrium. *NMU* mRNA was elevated at D10-14 in the NP endometrium; the abundance on D10 and D12 were significantly higher in the P endometrium compared to the NP endometrium.

When comparisons were made to the reference sample during the pregnancy, the *ODC-1* transcript declined steadily from day 10 to day 18. Comparisons between P and NP endometrium on days 10, 12 and 14 revealed that *ODC-1* transcripts were 1.2 to 3. 4 fold higher in the NP endometrium compared to the P endometrium. The *NMU* transcript was maximal on P day 10 and declined to a steady-state level on days 14 to 18. The *NMU* transcripts were more abundant in the NP uterus on day 14 (2.5 fold higher than the P uterus). In contrast, NMU transcript amounts were more abundant in the P endometrium on days 10 (1.7 fold higher than in the NP). These data suggest that *ODC-1* and *NMU* represent genes that may differ in expression at selected timepoints between P and NP animals and may be important for successful embryo development.

INTRODUCTION

During the estrous cycle and pregnancy, the physiological (endocrine-, paracrine-, and autocrine-induced) changes of the mammalian uterus provide an essential microenvironment for maturation of gametes, successful embryonic development and fetal growth. Such changes are a reflection of temporally and spatially-specific gene expression in the uterus. In swine, prenatal mortality can reach approximately 30 to 50% of potential embryos by term, because those range of the ova released from the ovary do not survive through gestation (Pope, 1994; Geisert and Schmitt, 2002). Moreover, early embryonic loss tends to be greatest during the first 30 days of gestation – ranging from 20 to 30% (Hanly, 1961; Perry and Rowlands, 1962; Pope, 1994). More specifically, the majority of early embryonic loss occurs during the period of conceptus implantation from days 13 to 20.

To examine the complex patterns of gene expression responsible for creating a microenvironment in the uterus, we previously reported that 964 genes were differentially expressed during the course of the estrous cycle and were at least twice as high in signal intensity compared to a reference RNA pool in at least 1 of the 7 timepoints. Another 267 genes were over four times higher than the reference in the porcine NP endometrium. Moreover, we had found that transcripts for *ODC-1* ((NM_002539, CN026972) and *NMU* (NM_006681, CO994598) were significantly higher in NP endometrium on days 3-6 and 10-14 during the estrous cycle, respectively. *ODC-1* is the first enzyme and the key regulator of the polyamine biosynthetic pathway (Trubiani et al., 1999). It acts to decarboxylate L-ornithine to form putrescine (Fig 6). *ODC-1* inhibition induces marked

reductions in the intracellular levels of the polyamines (putrescine, spermidine, and spermine), which are essential for cell proliferation and tissue growth. Loss of *ODC-1* might lead to reductions and an imbalance in polyamine pools, which could result in DNA damage and cell death (Pendeville et al., 2001). In contrast, *ODC-1* is known to be overexpressed in various cancers and associated with promoting tumor growth and angiogenesis (Nemoto et al., 2002). Holinka and Gurpide (1985) reported that *ODC* expression was significantly higher in the estrogen-dominated follicular phase (proliferative endometrium) than the progesterone-secreting corpus luteum (secretory endometrium) in human.

NMU is a neuropeptide that is ubiquitously distributed, but is highly expressed in the gastrointestinal tract and pituitary (reviewed in Brighton et al., 2004). *NMU* was originally isolated from porcine spinal cord and subsequently characterized by its ability to induct contractions in rat uterine smooth-muscle (Minamino et al., 1985). Until now, *NMU* has been implicated in the regulation of smooth-muscle contraction, blood pressure and local blood flow, ion transport in the gut, stress responses, cancer, gastric acid secretion, pronociception, and feeding behavior (Brighton et al., 2004).

ODC and *NMU* are thought to have potentially important roles in the porcine endometrium between the NP and P animals. In this study, we examined the expression for both transcripts of *ODC* and *NMU* in the early pregnant uterus to determine if they differ from NP animals.

Figure 6. *Ornithine* and *polyamine* pathway.
Ornithine decarboxylase (ODC); *Spermidine/spermine-N1-acetyltransferase (SSAT)*;
Polyamine oxidase (PAO).
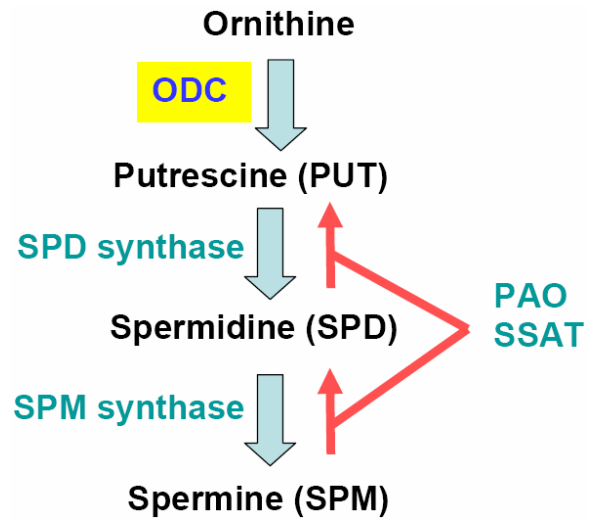
MATERIALS AND METHODS

Animal and Tissue Preparation

Unmated purebred Yorkshire gilts were ovary-hysterectomized on Days 0, 3, 6, 10, 12, 14, and 18 post-estrus (n=3 per stage; except Day 0 where there were only two). The first day of estrus was designated Day 0. Mated gilts were also ovariectomized-hysterectomized on days 10, 12, 14, 18, 23 and 28 post-mating (n=3 per stage) (Figure 7). Gilts assigned to the pregnant status were mated when detected in estrus and 10 and 24 hrs later. Pregnancy was confirmed visually by the presence of conceptuses in the uterine lumen. The guidelines for the care and use of the animals approved by the UMC-ACUC were strictly followed. Each collected uterine sample was snap frozen in liquid nitrogen and stored at -80℃ until RNA extraction.

Figure 7. Experimental design on the endometrial tissue collection time (3 pig / Day)

Biological replication: three non-pregnant gilts / stage (but, two animals at Day 0)
Technical replication: two hybridizations / gilt (but, three hybridizations / gilt at Day 0)
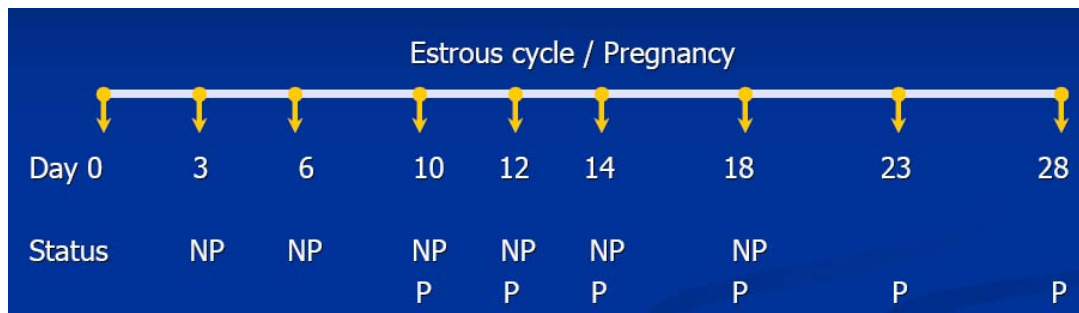
RNA Extraction and cDNA Synthesis

Total RNA from each sample was extracted by using the STAT-60™ reagent (Tel-Test, Friendswood, TX), according to the manufacturer's instructions. The RNA reference samples were comprised of an RNA pool composed of RNA from both reproductive (fetus, uterus, ovary, and placenta) and non-reproductive (liver, brain, skeletal muscle, heart, kidney, liver, spleen) tissues. RNA quality was confirmed by relative absorbance at 260 and 280 nm and by visualization on ethidium bromide stained agarose gels. See 'Materials and Methods in Chapter III' for more information.

Quantitative Real-Time Reverse Transcription (RT)-PCR

Primers for *ODC-1* (NM_002539, p4civv1-010-d05; sense-TGCCAACGCACA AGCTACA; antisense- CCCTTGCAACCATGCTACTAGA) and *NMU* (NM_006681, pd12-14end-005-C10; sense- TGGCTTACAATAGGACCTTGGAA; antisense-TCCAC AACTGCATGAGAGAAGAA) were designed by using the Primer Express program (Applied Biosystems, Foster City, CA). All RT-PCR results were statistically calculated by using Tukey's test at $\alpha = 0.05$ by the GLM procedure of SAS 9.1 (SAS Institute Inc., NC). See 'Materials and Methods in Chapter III' for more information.

Expression of *ODC-1* and *NMU* mRNA in total endometrium was compared to a housekeeping gene, YWHAG or a reference RNA sample, since preliminary results suggested that YWHAG mRNA differed significantly in the pregnant endometrium when compared to nonpregnant endometrium.

Expression of ODC-1 and NMU mRNA in Total Endometrium based on YWHAG

When *ODC-1* and *NMU* were compared to a housekeeping gene, *YWHAG* (Fig. 8-A and -B) during quantitative RT-PCR, *ODC-1* was highly expressed only days 3 - 6 in the porcine endometrium during the estrous cycle. This result was consistent with a previous microarray experiment, as shown in the scanned spot image of cDNA microarray in Fig. 8). There were no significant differences of mRNA expression in other stages between NP and P endometrium. However, expression of *ODC-1* mRNA was significantly different between Days in the pregnant endometrium (p-value < 0.0001).

NMU transcripts were maximal in both NP and P endometrium on days 10-18 compared to earlier stages of the estrous cycle (Fig. 8-B). Pregnant endometrium possessed higher amounts of *NMU* transcripts compared to NP endometrium on days 10-18. Expression of *NMU* mRNA was significantly different based on pregnancy status (p-value < 0.0007), and Days (p-value < 0.0001).

Comparisons with P and NP endometrium on days 10-18 based on the reference

sample

In Fig 9-A, *ODC-1* transcripts were 1.2 to 3.4 fold higher in the NP endometrium than the P. *ODC-1* transcripts were lower than the reference sample in both the NP and P endometrium, and they declined steadily from day 10 to day 18 when compared to the reference sample. There were significant differences between NP and P (p-value < 0.0001), and Days (p-value < 0.0001).

In Fig 9-B, *NMU* transcripts were abundant in the endometrium on days 10 to 14 compared to the reference and they also declined steadily from days 10 to 18. There was a trend for *NMU* to be higher in the P compared to NP endometrium at day 10 whether *NMU* transcripts were compared to YWHAG or not reference. The opposite relationship seemed to be occurring at day 14 in that the transcripts were numerically higher in the NP compared to the P endometrium. However, there were no significant differences between NP and P endometrium at day 14, although there were significantly different between Days (p-value < 0.0001).

DISCUSSION

ODC expression in humans has been reported to be higher in the estrogen-dominated follicular phase (proliferative endometrium) than in the progesterone-secreting luteal phase (secretory endometrium) (Holinka and Gurpide, 1985). Because *ODC-1* on days 3 – 6 was significantly expressed in the cyclic endometrium from both microarray and qRT-PCR, it was hypothesized that this gene might play important roles to nurture early porcine embryos in pregnant pigs. However, *ODC-1* expression was significantly altered during days 10 – 18 in pregnant pigs, although its expression was low. Therefore, it likely plays important roles to increase the endometrial cell proliferation and tissue growth during the estrous cycle and early pregnancy, although we did not investigate the expression of *ODC-1* mRNA during days 3-6 in pregnant endometrium.

NMU is originally purified from porcine spinal cord, and its biological function in the uterus seems to be involved mainly in smooth muscle contraction. In other organs, *NMU* has been reported to reduce food intake and body weight (Howard et al., 2000), regulate stress responses (Hanada et al., 2001), and modify ion transport in the gastrointestinal tract (Brown et al., 1988). The actions of this peptide are extensively studied; however, only two receptors (*NMU* -R1 and *NMU* -R2) have been identified (Howard et al., 2000). *NMU* -R1 is expressed in spleen/lymphocytes (Hedrik et al., 2000) and *NMU* promotes the secretion of various cytokines in a mouse Th2 cell clone (Johnson et al., 2004). *NMU* may be involved in the regulation of innate and adaptive immunity. Interestingly, our results showed that *NMU* was upregulated during days 10-14 in both NP and P endometrium. At that time, porcine embryos are extensively developed and are producing estrogen as the signal for maternal recognition of pregnancy. At this time, the

conceptus trophoblasts are also beginning to initiate attachment on the endometrial epithelial cells. Moriyama et al. (2005) reported that *NMU* is expressed abundantly in the epidermis. Therefore, it was hypothesized that *NMU* in the uterus may have two different biological functions: firstly *NMU* may function as smooth muscle contraction only in the uterine myometrium, and secondly it may act to influence immune responses, including inflammation, in the uterine endometrium. In the future, we need to investigate where and when *NMU* receptors are expressed during the estrous cycle and the early pregnancy.

Figure 8. Fold changes of *ODC-1* and *NMU* expression based on YWHAG between NP and P endometrium.

Figure 4. The *ODC-1* and *NMU* expression pattern based on Reference between NP and P uterus.
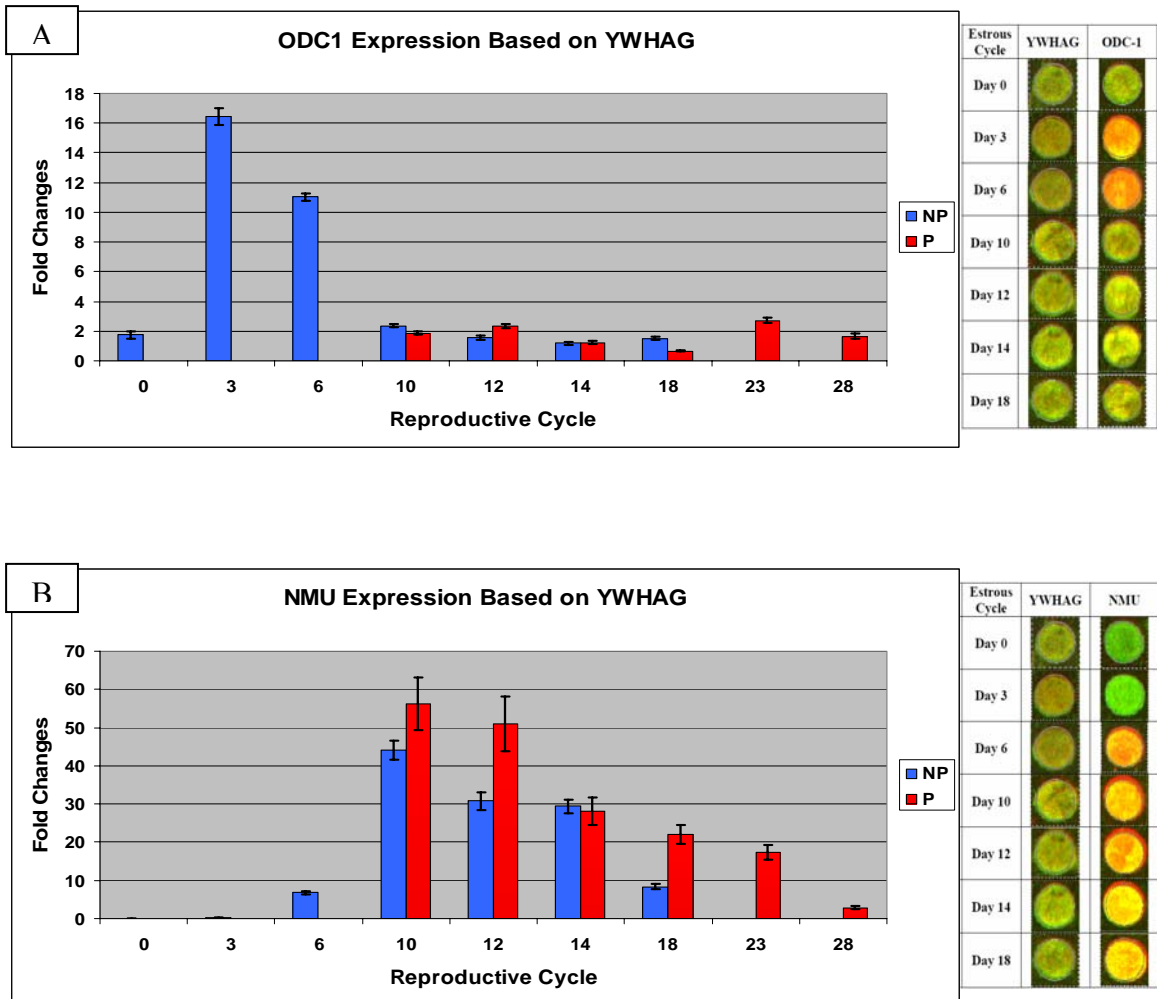
Figure 4. The *ODC-1* and *NMU* expression pattern based on Reference between NP and P uterus.
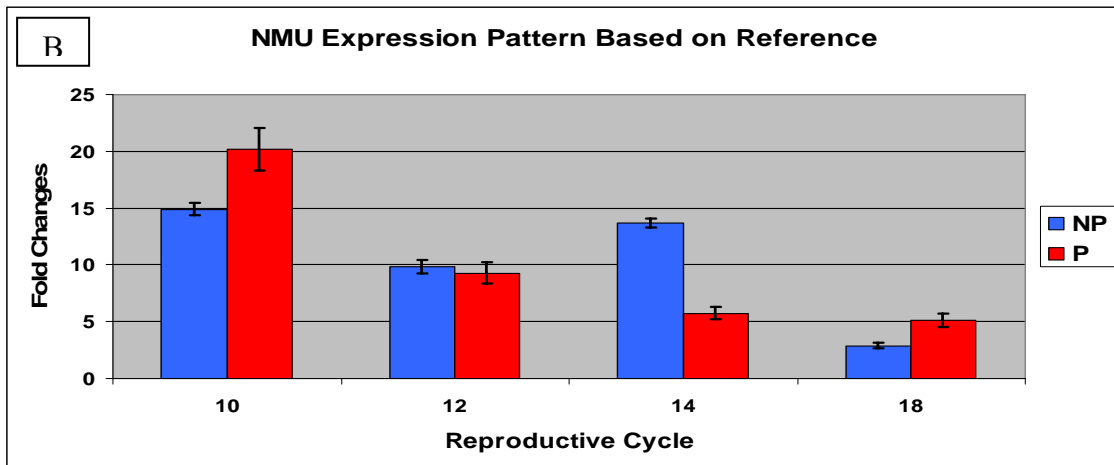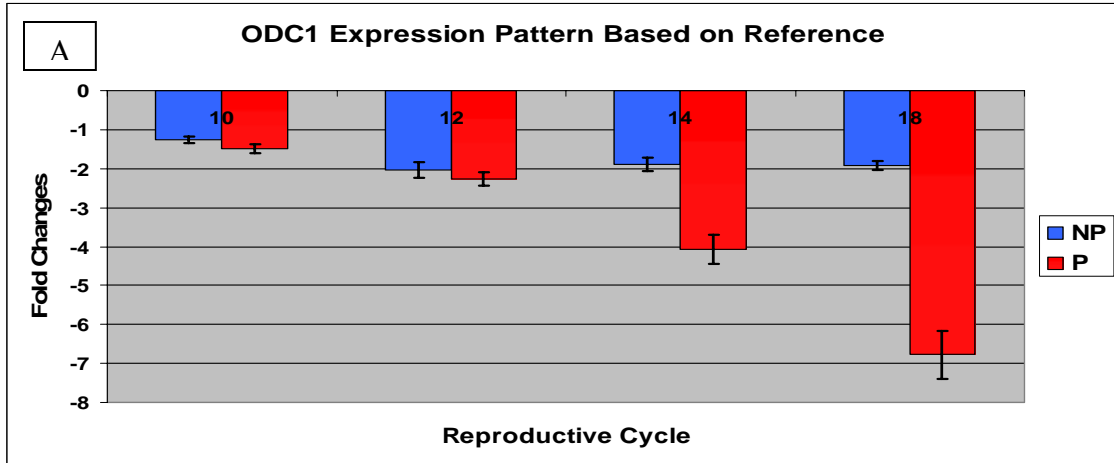
BIBLIOGRAPHY

Ace CI and Okulicz WC. 2004. Microarray profiling of progesterone-regulated endometrial genes during the rhesus monkey secretory phase. Reprod Biol Endocrinol. 2(1):54

Adams, KL, Bazer FW, and Roberts RM. 1981. Progesteroneinduced secretion of a retinol-binding protein in the pig uterus. J Reprod Fertil. 62(1):39-47

Agca C, Ries JE, Kolath SJ, Kim JH, Forrester LJ, Antoniou E, Whitworth KM, Mathialagan N, Springer GK, Prather RS, and Lucy MC. 2006. Luteinization of porcine preovulatory follicles leads to systematic changes in follicular gene expression. Reproduction. 132(1):133-45

Akinlosotu BA, Diehl JR, and Gimenez T. 1988. Prostaglandin E_2 counteracts the effects of $PGF_{2\alpha}$ in indomethacin treated cycling gilts. Prostaglandins. 35:81-93

Allen MR, Zhang BR, Hettinger AM, Goad DW, Malayer JR, and Geisert RD. 2002. Detection of bradykinin and bradykinin-beta(2) receptors in the porcine endometrium during the estrous cycle and early pregnancy. Biol Reprod. 66(3): 574-579

Anderson LL. 1978. Growth, protein content and distribution of early pig embryos. Anat Rec. 190:143-153

Andronowska A, Wasowska B, Calka J, and Doboszynska T. 2005. Localization and correlation between NADH-diaphorase and nitric oxide synthease isoforms in the porcine uterus during the estrous cycle. Cell Tissue Res. 321(2): 243-250

Araki Y, Nohara M, Yoshida-Komiya H, Kuramochi T, Ito M, Hoshi H, Shinkai Y, and Sendai Y. 2003. Effect of a null mutation of the oviduct-specific glycoprotein gene on mouse fertilization. Biochem. J. 374:551-557

Ashworth MD, Ross JW, Hu J, White FJ, Stein DR, Desilva U, Johnson GA, Spencer TE, and Geisert RD. 2006. Expression of porcine endometrial prostaglandin synthase during the estrous cycle and early pregnancy, and following endocrine disruption of pregnancy. 74(6): 1007-1015

Attur MG, Dave MN, Stuchin S, Kowalski AJ, Steiner G, Abramson SB, Denhardt DT, and Amin AR. 2001. Osteopontin an intrinsic inhibitor of inflammation in cartilage, Arthritis Rheum. 44: 578-584

Autieri MV and Carbone CJ. 1999. 14-3-3 Gamma interacts with and is phosphorylated by multiple protein kinase C isoforms in PDGF-stimulated human vascular smooth muscle cells. DNA Cell Biol. 18: 555-564

Badinga L, Michel FJ, and Simmen RCM. 1999. Uterine-associated serine protease inhibitors stimulate deoxyribonucleic acid synthesis in porcine endometrial glandular epithelial cells of pregnancy. Biol Reprod. 61:380-387

Bartol FF, Wiley AA, Spencer TE, Vallet JL, and Christenson RK. 1993. Early uterine development in pigs. Reprod. Fert. 48(Suppl. 1): 99-116

Bartol FF, Wiley AA, and Goodlett DR. 1988. Ovine uterine morphogenesis: histochemical aspects of endometrial development in the fetus and neonate. J Anim Sci. 66: 1303-1313

Bartol FF, Wiley AA, Coleman DA, Wolfe DF, and Riddel MG. 1988. Ovine uterine morphogenesis: effects of age and progestin administration and withdrawal on neonatal endometrial development and DNA synthesis. J Anim Sci. 66: 3000-3009

Bartol FF, Wiley AA, Floyd JG, Ott TL, Bazer FW, Gray CA, and Spencer TE. 1999. Uterine differentiation as a foundation for subsequent fertility. J. Reprod. Fertil. 54(Suppl.): 287-302

Bazer FW and Thatcher WW. 1977. Theory of maternal recognition of pregnancy in swine based on estrogen controlled endocrine versus exocrine secretion of prostaglandin $F_{2\alpha}$ by the uterine endometrium. Prostaglandins. 14:397-400

Bazer FW, Geisert RD, and Zavy MT. 1993. Fertilization, cleavage, and implantation. *Reproduction in farm animals, 6th Edition*. Lea&Febiger. *pp*.188-212

Bazer FW, Geisert RD, Thatcher WW and Roberts RM. 1982. The establishment and maintenance of pregnancy. In Control of Pig Reproduction pp 227-252 Eds DJA Cole and GR Foxcroft. Butterworth Scientific, London.

Bazer FW, Spencer TE, and Ott TL. 1996. Placental interferons. Am J Reprod Immunol. 35(4):297-308.

Bazer FW, Worthington-White D, Fliss MF, Gross S. 1991. Uteroferrin: a progesterone-induced hematopoietic growth factor of uterine origin. Exp Hematol. 19(9): 910-915.

Bethin KE, Nagai Y, Sladek R, Asada M, Sadovsky Y, Hudson TJ, and Muglia LJ. 2003. Microarray analysis of uterine gene expression in mouse and human pregnancy. Mol Endocrinol. 17(8):1454-1469

Bigsby RM and Cunha GR. 1985. Effects of progestins and glucocorticoids on deoxyribonucleic acid synthesis in the uterus of the neonatal mouse. Endocrinology. 117: 2520-2526

Bischof RJ, Brandon MR, and Lee C-S. 1995. Cellular immune responses in the pig uterus during pregnancy. J Reprod Immunol. 29:161-178

Boatman DE and Magnoni GE. 1995. Identification of a sperm penetration factor in the oviduct of the golden hamster. Biol. Reprod. 52:199-207

Bongso A, fong CY, and Ratnam S. 1994. Human embryonic behavior in a sequential human-oviduct-endometrial co-culture system. Fertil Steril. 61:976-978

Bowen JA, Bazer FW, and Burghardt RC. 1996. Spatial and temporal analyses of integrin and Muc-1 expression in porcine uterine epithelium and trophectoderm in vivo. Biol Reprod. 55(5):1098-106.

Brady SM, Long TA, and Benfey PN. 2006. Unraveling the dynamic transcriptome. Plant Cell. 18:2101-2111

Brenner RM and Slayden OD. 1994. Cyclic changes in the primate oviduct and endometrium. In: Knobil E, Neill JD (eds.), The Physiology of Reproduction. New York: Raven Press. pp 541–569

Brighton PJ, Szekeres PG, Willars GB. 2004. Neuromedin U and its receptors: structure, function, and physiological roles. Pharmacol Rev. 56(2): 231-248

Brown DR, and Quito FL. 1988. Neuromedin U octapeptide alters ion transport in porcine jejunum. Eur. J. Pharmacol. 155:159–162

Buhi WC, Ducsay CA, Bazer FW, and Roberts RM. 1982. Iron transfer between the purple phosphatase uteroferrin and transferrin and its possible role in iron metabolism of the fetal pig. J Biol Chem. 257:1712-1723

Bull H, Murray PG, Thomas D, Fraser AM, and Nelson PN. 2002. Acid phosphatases. J Clin Pathol. 55: 65-72

Burgess JK. 2001. Gene expression studies using microarrays. Clin Exp Pharmacol Physiol. 28:321-328

Burghardt RC, Bowen JA, Newton GR, and Bazer FW. 1997. Extracellular matrix and the implantation cascade in pigs. J Reprod Fertil Suppl. 52: 151-164

Campbell DJ, Kim CH, and Butcher EC. 2003. Chemokines in the systemic organization of immunity. Immunol Rev. 195: 58-71

Cardenas H and Pope WF. 2003. Distribution and changes in amounts of the androgen receptor in the pig uterus during the estrous cycle, early pregnancy and after treatment with sex steroids. J Endocrinol. 177(3): 461-469

Carson DD, Lagow E, Thathiah A, Al-Shami R, Farach-Carson MC, Vernon M, Yuan L, Fritz MA & Lessey B 2002 Changes in gene expression during the early to mid-luteal (receptive phase) transition in human endometrium detected by high-density microarray screening. Molecular Human Reproduction 8 871–879

Carson DD. 2002. The glycobiology of implantation. Frontiers in Bioscience. 7:d1535-1544

Carter AM and Enders AC. 2004. Comparative aspects of trophoblast development and placentation. Repro Bio Endo. 2:46

Caudell EG, Mumm JB, Poindexter N, Ekmekcioglu S, Mhashilkar AM, Yang XH, Retter MW, Hill P, and et al., 2002. The protein product of the tumor suppressor gene, melanoma differentiation-association gene 7, exhibits immunostimulatory activity and is designated IL-24. J Immunol. 168: 6041-6046

Chabot V, Lambert RD, Laforest JP, St-Jacques S, Matte JJ, Guay F, Palin MF, and Lessard M. 2004. Effect of oestrous cycle and early pregnancy on uterine production and expression of immune regulatory factors in gilts. Ani Reprod Sci. 81:137-149

Chakraborty PK, England DC, and Stormshak E. 1972. Effect of 1703-estradiol on pituitary gonadotropins and luteal function in gilts. J Anim Sci. 34:427-429

Chegini N. 1996. Oviductal-derived growth factors and cytokines: implications in preimplantation. Semin Reprod Endocrinol. 14:219 –229

Christenson LK, Farley DB, Anderson LH, and Ford SP. 1994. Luteal maintenance during early pregnancy in the pig: role for prostaglandin E_2. Prostaglandins. 47:61-75

Churchill GA. 2002. Fundamentals of experimental design for cDNA microarrays. Nat Genet. 32 Suppl: 490-495

Clawitter J, Trout WE, Burke MG, Araghi S, and Roberts RM. 1990. A novel family of progesterone-induced, retinol-binding proteins from uterine secretions of the pig. J Biol Chem. 265(6): 3248-3255

Clawitter J, Trout WE, Burke MG, Arahi S, and Roberts RM. 1990. A novel family of progesterone-induced, retinol-binding proteins from uterine secretions of the pig. J Biol Chem. 265: 3248-3255

Conley A and Hinshelwood M. 2001. Mammalian aromatases. Reproduction. 121: 685-695

Cross JC, Werb Z, and Fisher S. 1994. Implantation and the placenta: Key pieces of the development puzzle. Science. 266: 1508-1518

Cunha GR. 1976. Stromal induction and specification of morphogenesis and cytodifferentiation of the epithelia of the mullerian ducts and urogenital sinus during development of the uterus and vagina in mice. J Exp Zool. 196: 361-370

Curry TE and Osteen KG. 2003. The matrix metalloproteinase system: changes, regulation, and impact throughout the ovarian and uterine reproductive cycle. Endocr Rev. 24:428-465

Curtis SW, Clark J, Myers P, and Korach KS. 1999. Disruption of estrogen signaling does not prevent progesterone action in the estrogen receptor α knockout mouse uterus. Proc Natl Acad Sci U S A. 96: 3646-3651

D'Hooghe TM, Kyama C, Debrock S, Meuleman C, and Mwenda JM. 2004. Future directions in endometriosis research. Ann N Y Acad Sci. 1034: 316-325.

Dantzer V, Bjorkman N, and Hasselager E. 1981. An electron microscopic study of histotroph in the interareolar part of the porcine placenta. Placenta. 2:19-28

Dantzer V. 1985. Electron microscopy of the initial stages of placentation in the pig. Anat Embryol, 172:281-293

Davis DL and Blair RM. 1993. Studies of uterine secretions and products of primary cultures of endometrial cells in pigs. J Reprod Fertil Suppl. 48:143-155

Davis DL, Pakrasi PL, and Dey SK. 1983. Prostaglandins in swine blastocysts. Biol Reprod. 28:1114–1118

DeSouza L, Diehl G, Yang EC, Guo J, Rodrigues MJ, Romaschin AD, Clogan TJ, and Siu KW. 2005. Proteomic analysis of the proliferative and secretory phases of the human endometrium: protein identification and differential protein expression. Proteomics. 5(1): 270-281

Dockery P, Pritchard K, Warren MA, Li TC, and Cooke ID. 1996. Changes in nuclear morphology in the human endometrial glandular epithelium in women with unexplained infertility. Hum Reprod. 11: 2251-2256

Dubey RK, Rosselli M, Imthurn B, Keller PJ, and Jackson EK. 2000. Vascular effects of environmental estrogens: implications for reproductive and vascular health. Hum Reprod Update. 6:351-363.

Dudley A, Aach J, Steffen MA, and Church GM. 2002. Measuring absolute expression with microarrays with calibrated reference sample and an extended signal intensity range. Proc. Natl Acad. Sci. USA. 99: 7554-7559

Duggan DJ, Bittner M, Chen Y, Meltzer P, and Trent JM. 1999. Expression profiling using cDNA microarrays. Nat. Genet. 21:10-14

Dumoutier L, Leemans C, Lejeune D, Kotenko SV, and Renauld JC. 2001. Cutting edge: STAT activiation by IL-19, IL20 and mda-7 through IL-20 receptor complexes of two types. J Immunol. 167: 3545-3549

Ek-Rylander B, Flores M, Wendal M, Heinegard D, and Andersson G. 1994. Dephosphorylation of osteopontin and bone sialoprotein by osteoclastic tartrate-resistant acid phosphatase. Modulation of osteoclast adhesion in vitro. J Biol Chem. 269:14853-14856.

Farmer SJ, Fliss AE, and Simmen RCM. 1990. Complementary DNA cloning and regulation of expression of the messenger RNA encoding a pregnancy-associated porcine uterine protein related to human antileukoproteinase. Mol Endocrinol. 4:1095-1104

Fazleabas AT, Baser FW, and Roberts RM. 1982. Purification and properties of a progesterone-induced plasmin/trypsin inhibitor from uterine secretions of pigs and its immunochemical localization in the pregnant uterus. J Biol Chem. 257:6886-6897

Fazleabas AT, Baser FW, Hansen PJ, Geisert RD, and Roberts RM. 1985. Differential patterns of secretory protein localization within the pig uterine endometrium. Endocrinology. 116: 240-245

Fazleabas AT, Bell SC, Fleming S, Sun J, and Lessey BA. 1997. Distribution of integrins and the extracellular matrix proteins in the baboon endometrium during the menstrual cycle and early pregnancy. Biol Reprod. 56:348-356

Fazleabas AT, Geisert RD, Baser FW, and Roberts RM. 1983. The relationship between the release of plasminogen activator and estrogen by blastocysts and secretion of plasmin inhibitor by uterine endometrium in the pregnant pig. Biol Reprod. 29: 225-238

Fisher LW and Fedarko NS. 2003. Six genes expressed in bones and teeth encode the current members of the SIBLING family of proteins. Connect Tissue Res. 44:(suppl 1)33-40

Ford SP and Christenson RK. 1979. Blood flow to uteri of sows during the estrous cycle and early pregnancy: local effect of the conceptus on the uterine blood supply. Biol Reprod. 21: 617-624

Ford SP, Vonnahme KA, and Wilson ME. 2002. Uterine capacity in the pig reflects a combination of uterine environment and conceptus genotype effects. J Anim Sci. 80(E. Suppl.1):E66-E73

Forster T, Costa Y, Roy D, Cooke HJ, and Maratou K. 2004. Triple-target microarray experiments: a novel experimental strategy. BMC Genomics. 5:13

Franczak A, Wocławek-Potocka I, Oponowicz A, Kurowicka B, and Kotwica G. 2004. Oxytocin stimulates prostaglandin $F_{2\alpha}$ secretion and prostaglandin F synthase protein expression in porcine myometrial tissue. Reprod Biol. 4:177-184

Frank M, Bazer FW, Thatcher WW, and Wilcox CJ. 1977. A study of prostaglandin F2, as a luteolysin in swine. III. Effects of estradiol valerate on prostaglandin F, progestins, estrone and estradiol concentrations in utero-ovarian vein of nonpregnant gilts. Prostaglandins. 14:1183-1196.

Frank M, Bazer FW, Thatcher WW, and Wilcox CJ. 1978. A study of prostaglandin F2 as a luteolysin in swine. IV. An explanation for the luteotrophic effect of estradiol. Prostaglandins 1978; 15:151-160.

Friess AE, Sinowatz F, Skolek-Winnisch R, and Trautner W. 1981. The placenta of the pig. II. The ultrastructure of the areolae. Anat. Embryol. 163:43-53

Fritzsche B, Vermot J, Neumann U, Schmidt A, Schweigert FJ, Dolle P, and Ruhl P. 2007. Regulation of expression of the retinoic acid metabolizing enzyme CYP26A1 in uteri of ovariectomized mice after treatment with ovarian steroid hormones. Mol Reprod Dev. 74(2): 258-264

Fu H, Xia K, Pallas DC, Cui C, Conroy K, Narsimhan RP, Mamon H, Collier RJ, and Roberts TM. 1994. Interaction of the protein kinase Raf-1 with 14-3-3 Proteins. Science. 266: 126-129

Galland F, Malergue F, Bazin H, Mattei MG, Aurrand-Lions M, Theillet C, and Naquet P. 1998. Two human genes related to murine vanin-1 are located on the long arm of human chromosome 6. Genomics. 53 (2): 203-213

Gandolfi F, Modina S, Brevini TAL, Galli C, Moor RM, and Lauria A. 1991. Oviduct ampullary epithelium contributes a glycoprotein to the zona pellucida, perivitelline space and blastomeres membrane of sheep embryos. Euro J Basic and Appl Histo. 35:383–392

Gardner ML, First NL, and Casida LE. 1963. Effect of exogenous estrogens on corpus luteum maintenance in gilts. J Anim Sci. 22:132-134.

Garlow JE, Ka H, Johnson GA, Burghardt RC, Jaeger LA, and Bazer FW. 2002. Analysis of oteopontin at the maternal-placental interface in pigs. Biol Reprod. 66:718-725

Gasc JM, Renoir JM, Radanyi C, Joab I, Tuohimaa P, and Baulieu EE. 1984. Progesterone receptor in the chick oviduct: an immunohistochemical study with antibodies to distinct receptor components. J Cell Biol. 99:1193-1201

Gawronska B, Bodek G, and Ziecik AJ. 2000. Distribution of NADPH-diaphorase and nitric oxide synthase (NOS) in different regions of porcine oviduct during theeEstrous cycle. J Histochem Cytochem. 48(6): 867-875

Geisert RD and Schmitt RAM. 2002. Early embryonic survival in the pig: Can it be improved?. J Anim Sci. 80(E. Suppl.1): E54-E65

Geisert RD and Yelich JV. 1997. Regulation of conceptus development and attachment. J Reprod Fertil Suppl. 52:133-149

Geisert RD, Brookbank JW, Roberts RM and Bazer FW. 1982b. Establishment of pregnancy in the pig: II. Cellular remodeling of the porcine blastocyst during elongation on day 12 of pregnancy. Biol Reprod. 27:941-955

Geisert RD, Pratt TN, Bazer FW, Mayes JS, and Watson GH. 1994. Immunocytochemical localization and changes in endometrial progestin receptor protein during the porcine oestrous cycle and early pregnancy. Reprod Fertil Dev. 6(6):749-760

Geisert RD, Renegar RH, Thatcher WW, Roberts RM, and Bazer FW. 1982a. Establishment of pregnancy in the pig: I. Interrelationships between preimplantation development of the pig blastocyst and uterine endometrial secretions. Biol Reprod. 27:925-939

Geisert RD, Ross JW, Ashworth MD, White FJ, Johnson GA, and DeSilva U. 2006. Maternal recognition of pregnancy signal or endocrine disruptor: the two faces of oestrogen during establishment of pregnancy in the pig. Reprod Suppl. 62:131-145

Geisert RD, Thatcher WW, Roberts RM, and Bazer FW. 1982c. Establishment of pregnancy in the pig. III. Endometrial secretory response to estradiol valerate administered on day 11 of the estrous cycle. Biol Reprod. 27:957-965

Geisert RD, Zavy MT, Wettemann RP, and Biggers BG. 1987. Length of pseudopregnancy and pattern of uterine protein release as influenced by time and duration of oestrogen administration in the pig. J Reprod Fertil. 79:163-172.

Ghosh D and Sengupta J. 1998. Recent developments in endocrinology and paracrinology of blastocyst implantation in the primate. Hum Reprod Update. 4:153-168

Gopalan B, Shanker M, Chada S, and Ramesh R. 2007. MDA-7/IL-24 suppresses human ovarian carcinoma growth in vitro and in vivo. Mol Cancer. 6: 11.

Gopalkrishnan RV, Sauane M, and Fisher PB. 2004. Cytokine and tumor cell apoptosis inducing activity of mda-7/IL-24. Int Immunopharmacol. 4: 635-647

Gorodeski GI. 2007. Estrogen decrease in tight junctional resistance involves matrix-metalloproteinase-7-mediated remodeling of occludin. Endocrinology. 48(1): 218-231.

Grant SA, Hunter MG, and Foxcroft GR. 1989. Morphological and biochemical characteristics during ovarian follicular development in the pig. J. Reprod. Fertil. 86:171-183.

Gray CA, Abbey CA, Beremand PD, Choi Y, Farmer JL, Adelson DL, Thomas TL, Bazer FW, and Spencer TE. 2006. Identification of endometrial genes regulated by early pregnancy, progesterone, and interferon tau in the ovine uterus. Biol Reprod. 74(2):383-94.

Gray CA, Adelson DL, Bazer FW, Burghardt RC, Meeusen Els NT, and Spencer TE. 2004. Discovery and characterization of an epithelial-specific galectin in the endometrium that forms crystals in the trophectoderm. Proc Natl Acad Sci USA. 101(21): 7982-7987

Gray CA, Bartol FF, Tarleton BJ, Wiley AA, Johnson GA, Bazer FW, and Spencer TE. 2001a. Developmental biology of uterine glands. Biol Reprod. 65:1311-1323

Gray CA, Burghardt RC, Johnson GA, Bazer FW and Spencer TE. 2002. Evidence that absence of endometrial gland secretions in uterine gland knockout ewes compromises conceptus survival and elongation. Reproduction. 124(2): 289-300

Green JA, Kim JG, Whitworth KM, Agca C, Prather RS. 2006. The use of microarrays to define functionally-related genes that are differentially expressed in the cycling pig uterus. Soc Reprod Fertil Suppl. 62:163-176

Green ML, Blaeser LL, Simmen FA, and Simmen RC. 1996. Molecular cloning of spermidine/spermine N1-acetyltransferase from the periimplantation porcine uterus by messenger ribonucleic acid differential display: temporal and conceptus-modulated gene expression. Endocrinology. 137(12):5447-5455.

Green ML, Chung TE, Reed KL, Modric T, Badinga L, Yang J, Simmen FA, and Simmen RC. 1998. Paracrine inducers of uterine endometrial spermidine/spermine N1-acetyltransferase gene expression during early pregnancy in the pig. Biol Reprod. 59(5):1251-1258.

Groothuis PG, Blair RM, Simmen RC, Vallet JL, Grieger DM, and Davis DL. 1997. Uterine response to progesterone in prepubertal gilts. J Reprod Fertil. 110(2): 237-243

Groothuis PG, McGuire WJ, Vallett JL, Grieger DM, and Davis DL. 2002. Retinol and estradiol regulation of retinol binding protein and prostaglandin production by porcine uterine epithelial cells in vitro. J Anim Sci. 80(10): 2688-2694

Guidice LC. 1994. Growth factors and growth modulations in human uterine endometrium: their potential relevance to reproductive medicine. Fertil Steril. 61:1-17

Gunnet JW and Freeman ME. 1984. Hypothalamic regulation of mating-induced prolactin release. Effect of electrical stimulation of the medial preoptic area in conscious female rats. Neuroendocrinology. 38:12-16

Guo H, Cai CQ, Schroeder RA, and Kuo PC. 2001. Osteopontin is a negative feedback regulator of nitric oxide synthesis in murine macrophages, J Immunol. 166: 1079-1086

Gupta A, Huet YM, and Day SK. 1989. Evidence for prostaglandin and leucotrienes as mediators of phase I of estrogen action in implantation in the mouse. Endocrinology. 124:546-548

Gupta P, Su ZZ, Lebedeva IV, Sarkar D, Sauane M, Emdad L, Bachelor MA, Grant S, Curiel DT, Dent P, and Fisher PB. 2006. mda-7/IL-24: multifunctional cancer-specific apoptosis-inducing cytokine. Pharmacol Ther. 111(3): 596-628

Hafez ESE and Ludwig H. 1977. Scanning electron microscopy of the endometrium. In: Wynn, R.M., Editor, 1977. *Biology of the Uterus*, Plenum Press, New York/London, pp. 309-340.

Halleen JM, Jaija H, Stepan JJ, Vihko P, Vaananen HK. 1998. Studies on the protein tyrosine phosphatase activity of tartrate-resistant acid phosphatase. Arch Biochem Biophys. 352:97-102.

Hanly S. 1961. Prenatal mortality in farm animals. J. Reprod. Fertil. 2:182-194.

Hao Y, Mathialagan N, Walters E, Mao J, Lai L, Becker D, Li W, Critser J, and Prather RS. 2006. Osteopontin reduces polyspermy during in vitro fertilization of porcine oocytes. Biol Reprod. 75: 726-733

Hanada R, Nakazato M, Murakami N, Sakihara S, Yoshimatsu H, Toshinai K, Hanada T, Suda T, Kangawa K, Matsukura S, and Sakata T. 2001. A role for neuromedin U in stress response. Biochem. Biophys. Res. Commun. 289:225–228

Harada M, Suganuma N, Furuhashi M, Nagasaka T, Nakashima N, Kikkawa F, Tomoda Y, and Furui K. 1996. Detection of apoptosis in human endometric tissues. Mol Hum Reprod. 2: 307-315

Harney JP, Ali M, Vedeckis WV, and Bazer FW. 1990. Retinol-binding protein: a major secretory product of the pig conceptus. Biol Reprod. 42:523-532

Harney JP, Ott TL, Geisert RD, and Bazer FW. 1993. Retinol-binding protein gene expression in cycle and pregnant endometrium of pigs, sheep, and cattle. Biol Reprod. 49:1066-1073

Harvey MB, Leco KJ, Arcellana-Panlilio MY, Zhang X, Edwards DR, and Schultz GA. 1995. Roles of growth factors during preimplantation development. Hum Reprod. 10:712-718

Hayes ES. 2004. Biology of primate relaxin: a paracrine signal in early pregnancy? Reprod Biol Endocrinol. 16: 2-36

Hearn JP. 1986. The embryo-maternal dialogue during early pregnancy in primates. J Reprod Fertil. 76:809-819.

Hedrick JA, Morse K, Shan L, Qiao X, Pang L, Wang S, Laz T, Gustafson EL, Bayne M, and Monsma FJ. 2000. Identification of a human gastrointestinal tract and immune system receptor for the peptide neuromedin U. Mol. Pharmacol. 58:870–875

Hegde P, Qi R, Abernathy K, Gay C, Dharap S, Gaspard R, Hughes JE, Snesrud E, Lee N, and Quackenbush J. 2000. A concise guide to cDNA microarray analysis. BioTechniques. 29(3): 548-562

Held G, Grinstein G, and Tu Y. 2003. Modeling of DNA microarray data by using physical properties of hybridization Proc. Natl Acad. Sci. USA. 100: 7575-7580

Hettinger AM, Allen MR, Zhang BR, Goad DW, Malayer JR, and Geisert RD. 2001. Presence of the acute phase protein, bikunin, in the endometrium of gilts during estrous cycle and early pregnancy. Biol Reprod. 65(2): 507-513

Hill JL, Walker SK, Brown GH, and Nancarrow CD. 1996. The effects of an ovine oviductal estrus-associated glycoprotein on early embryo development. Theriogenology. 46:1367-1377

Holinka CF and Gurpide E. 1985. Ornithine decarboxylase activity in human endometrium and endometrial cancer cells. In Vitro Cell Dev Biol. 21(12): 697-706

Horcajadas JA, Pellicer A, and Simon C. 2007. Wide genomic analysis of human endometrial receptivity: new times, new opportunities. Hum Reprod Update. 3(1): 77-86

Horie M, Suzuki M, Takahashi EI, and Tanigami A. 1999. Cloning, expression, and chromosomal mapping of the human 14-3-3 gamma Gene (YWHAG) to 7q11.23. Genomics. 60(2): 241-243

Hormia M, Falk-Marzillier J, Plopper G, Tamura RN, Jones JCR, and Quaranta V. 1995. Rapid spreading and mature hemidesmosome formation in HaCaT keratinocytes induced by incubation with soluble laminin-5r, J. Invest. Dermatol. 105: 557-561

Hosack DA, Dennis J, G., Sherman BT, Lane HC, and Lempicki RA. 2003. Identifying biological themes within lists of genes with EASE. Genome Biology. 4:R70

Howard AD, Wang R, Pong SS, Mellin TN, Strack A, Guan XM, Zeng Z, Williams Jr DL, Feighner SD, Nunes CN, et al. 2000. Identification of receptors for neuromedin U and its role in feeding. Nature. 406:70–74.

Huang EY, Madireddi MT, Gopalkrishnan RV, Leszczyniecka M, Su Z, Lebedeva IV, Kang D, Jiang H, Lin JJ, Alexandre D, Chen Y, Vozhilla N, Mei MX, Christiansen KA, Sivo F, Goldstein NI, Mhashilkar AB, Chada S, Huberman E, Pestka S, Fisher PB. 2001. Genomic structure, chromosomal localization and expression profile of a novel melanoma differentiation associated (mda-7) gene with cancer specific growth suppressing and apoptosis inducing peroperties. Oncogene. 20: 7051-7063.

Hulboy DL, Rudolph LA, and Matrisian LM. 1997. Matrix metalloproteinases as mediators of reproductive function. Mol Hum Reprod. 3: 27-45

Hunter RH. 1998. Have the fallopian tubes a vital role in promoting fertility? Acta Obstet Gynecol Scand. 77:475-486.

Hunter RHF. 1988. The Fallopian Tubes: Their Role in Fertility and Infertility. Berlin, Springer.

Ing NH and Robertson JA. 1999. Regulation of hormone receptor gene expression in endometrium. In: Carson DD, editor. Embryo Implantation: Molecular, Cellular and Clinical Aspects. New York: Springer. pp. 287–298.

Ing NH and Zhang Y. 2004. Cell-specific expression of estrogen-responsive genes in the uteri of cyclic, early pregnant and ovariectomized ewes. Theriogenology. 62(3-4): 403-414

Ing NH, Francis H, McDonnell JJ, Amann JF, and Roberts RM. 1989. Progesterone induction of the uterine milk proteins: major secretory proteins of sheep endometrium. Biol Reprod. 41(4):643-654.

Jaeger LA, Spiegel AK, Ing NH, Johnson GA, Bazer FW, and Burghardt RC. 2005. Functional effects of transforming growth factor beta on adhesive properties of porcine trophectoderm. Endocrinology. 146(9): 3933-3942

Jeong JW, Lee KY, Kwak I, White LD, Hilsenbeck SG, Lydon JP, and DeMayo FJ. 2005. Identification of murine uterine genes regulated in a ligand-dependent manner by the progesterone receptor. Endocrinology. 146(8): 3490-3505

Jiang H, Lin JJ, Su ZZ, Goldstein NI, and Fisher PB. 1995. Subtraction hybridization identifies a novel melanoma differentiation associated gene, mda-7, modulated during human melanoma differentiation, growth and progression. Oncogene. 11: 2477-2486

Jiang H, Su ZZ, Lin JJ, Goldstein NI, Young CS, and Fisher PB. 1996. The melanoma differentiation associated gene mda-7 suppresses cancer cell growth. Proc Natl Acad Sci USA. 93: 9160-9165

Jin W, Riley RM, Wolfinger RD, White KP, Passador-Gurgel G, and Gibson G. 2001. The contributions of sex, genotype and age to transcriptional variance in Drosophila melanogaster. Nat Genet. 29:389–395

Johnson EN, Appelbaum ER, Carpenter DC, Cox RF, Disa J, Foley JJ, Ghosh SK, Naselsky DP, Pullen MA, Sarau HM, et al. 2004. Neuromedin U elicits cytokine release in murine Th2-type T cell clone D10.G4.1. J. Immunol. 173:7230–7238

Johnson GA, Bazer FW, Jaeger LA, Ka H, Garlow JE, Prarrer C, et al. 2001. Muc-1, integrin, and osteopontin expression during the implantation cascade in sheep. Biol Reprod. 65:820-828

Johnson GA, Burghardt RC, Bazer FW and Spencer TE. 2003b. Osteopontin: roles in implantation and placentation. Biol Reprod. 69: 1458-1471

Johnson GA, Burghardt RC, Joyce MM, Spencer TE, Bazer FW, Gray CA and Pfarrer C. 2003. Osteopontin is synthesized by uterine glands and a 45-kDa cleavage fragment is localized at the uterine-placental interface throughout ovine pregnancy. Biol Reprod. 69: 92-98

Johnson GA, Spencer TE, Burghardt RC, and Bazer FW. 1999. Ovine osteopontin: I. Cloning and expression of mRNA in the uterus during the peri-implantation period. Biol Reprod. 61:884-891

Joly D, Berissi S, Bertrand A, Strehl L, Patey N, and Knebelmann B. 2006. Laminin 5 regulates polycystic kidney cell proliferation and cyst formation. J Biol Chem. 281(39): 29181-29189

Ka H, Jaeger LA, Johnson GA, Spencer TE, and Bazer FW. 2001. Keratinocyte growth factor is up-regulated by estrogen in the porcine uterine endometrium and functions in trophectoderm cell proliferation and differentiation. Endocrinology. 142(6): 2303-2310

Kafatos FC, Jones CW, and Efstratiadis A. 1979. Determination of nucleic acid sequence homologies and relative concentrations by a dot hybridization procedure. Nucleic Acids Res. 7:1541-1552

Kamb A and Ramaswami M. 2001. A simple method for statistical analysis of intensity differences in microarray-derived gene expression data. BMC Biotechnol. 1:8

Kane MT, Morgan PM, and Coonan C. 1997. Peptide growth factors and preimplantation development. Hum. Reprod. Update 3(2): 137-157

Kao LC, Tulac S, Lobo S, Imani B, Yang JP, Germeyer A, Osteen K, Taylor RN, Lessey BA, and Giudice LC. 2002. Global gene profiling in human endometrium during the window of implantation. Endocrinology. 143(6):2119-2138

Kapur RP and Johnson LV. 1988. Ultrastructural evidence that specialized regions of the murine oviduct contribute a glycoprotein to the extracellular matrix of mouse oocytes. Anatomical Record. 221:720–729

Katoh K, Nakanishi Y, Akimoto S, Yoshimura K, Takagi M, Sakamoto M, and Hirohashi S. 2002. Correlation between Laminin-5 gamma 2 Chain Expression and Epidermal Growth Factor Receptor Expression and Its Clinicopathological Significance in Squamous Cell Carcinoma of the Tongue. Oncology. 62(4): 318-326

Kauma SW. 2000. Cytokines in implantation. J. Reprod. Fertil. Suppl. 55:31-42
Kerr MK and Churchill GA. 2001. Statistical design and the analysis of gene expression microarray data. Genet. Res. 77:123-128.

Kerr MK. 2003. Design considerations for efficient and effective microarray studies. Biometrics. 59:822-828

Kidder HE, Casida LE, and Grummer RH. 1995. Some effects of estrogen injections on the estrual cycle of gilts. J Anim Sci. 14:470-474.

Kim S, Choi Y, Bazer FW, and Spencer TE. 2003. Identification of genes in the ovine endometrium regulated by interferon tau independent of signal transducer and activator of transcription 1. Endocrinology. 144(12): 5203-5214

Kimura H, Matsuda J, Ogura A, Asano T, and Naiki M. 1994. Affinity binding of hamster oviductin to spermatozoa and its influence on in vitro fertilization. Mol. Reprod.

King BF. 1984. The fine structure of the placenta and chorionic vesicles of the bush baby, *Galago crassicaudata*. Amerian J Anatomy. 169(1):101-116

King GJ. 1993. Comparative placentation in ungulates. J Exp Zool. 266:588-602

King RS and Killian GJ. 1994. Purification of bovine estrus-associated protein and localization of binding on sperm. Bio Repro. 51:34–42

King RS, Anderson SH, and Killian GJ. 1994. Effect of bovine oviductal estrusassociated protein on the ability of sperm to capacitate and fertilize oocytes. J. Androl. 15:468-478

Knight JW, Bazer FW, Thatcher WW, Franke DE, and Wallace HD. 1977. Conceptus development in intact and unilaterally hysterectomized-ovariectomized gilts: Interrelations among hormonal status, placental development, fetal fluids and fetal growth. J. Anim. Sci. 44:620-637

Kniss DA, Rovin B, Fertel RH, and Zimmerman PD. 2001. Blockade NF-kB activation prohibits TNF-α-induced cyclooxygenase-2 gene expression in ED 27 trophoblast-like cell. Placenta. 22:80-89

Kohane IS, Kho AT, and Butte AJ. 2003. Microarrays for an integrative genomics. A Bradfor Book, the MIT Press: pp. 1-36

Kouba AJ, Abeydeera LR, Alvarez IM, Day BN, and Buhi WC. 2000. Effects of the porcine oviduct-specific glycoprotein on fertilization, and embryonic development in vitro. Biol. Reprod. 63:242-250

Kraeling RR, Rampacek GB, and Fiorello NA. 1985. Inhibition of pregnancy with indomethacin in mature gilts and prepubertal gilts induced to ovulate. Biol Reprod. 32:105-110

Krzymowski T and Stefanczyk-Krzymowska S. 2004. The oestrous cycle and early pregnancy – a new concept of local endocrine regualtion. Vet J. 168(3): 285-296

Kubo H, Spindle H, and Pederson RA. 1981. Inhibiton of mouse blastocyst attachment and outgrowth by protease inhibitors. J Exp Zool. 216:445-451

Kunkel EJ, Kim CH, Lazarus NH, Vierra MA, Soler D, Bowman EP, Butcher EC. 2003. CCR10 expression is a common feature of circulating and mucosal epithelial tissue IgA Ab-secreting cells. J Clin Invest.111: 1001-1010.

Lacroix MC, Devinoy E, Servely JL, Puissant C, and Kann G. 1996. Expression of the growth hormone gene in ovine placenta: detection and cellular localization of the protein. Endocrinology. 137:4886-4892

Lagow E, DeSouza MM, and Carson DD. 1999. Mammalian reproductive tract mucins. Human Reproduction Update. 4:280–292

Lauffer RB, Antanaitis BC, Aisen P, and Que L. 1983. 1H NMR studies of porcine uteroferrin. Magnetic interactions and active site structure. J Biol Chem. 258 (23): 14212-14218

Lazarus NH, Kunkel EJ, Johnston B, Wilson E, Youngman KR, and Butcher EC. 2003. A common mucosal chemokine (mucosae-associated epithelial chemokine/CCL28) selectively attracts IgA plasmablasts. J Immunol. 170: 3799-3805

Lenhart JA, Ryan PL, Ohleth KM, Palmer SS, and Bagnell CA. 2001. Relaxin increases secretion of matrix metalloproteinase-2 and matrix metalloproteinase-9 during uterine and cervical growth and remodeling in the pig. Endocrinology. 142(9): 3941-3949

Lennon GG and Lehrach H. 1991. Hybridization analyses of arrayed cDNA libraries. Trends Genet. 7:314-317

Leonard S, Murrant C, Tayade C, van den Heuvel M, Watering R, and Croy BA. 2006. Mechanisms regulating immune cell contributions to spiral artery modification -- facts and hypotheses -- a review. Placenta. 27 Suppl A: S40-46

Lessey BA, Damjanovich L, Coutifaris C, Castelbaum A, Albelda SM, and Buck CA. 1992. Integrin adhesion molecules in the human endometrium: Correlation with the normal and abnormal menstrual cycle. J Clin Invest. 90: 188-195

Lessey BA. 2002. Adhesion molecules and implantation. J Reprod Immunol. 55(1-2):101-112
Lim HJ, Paria BC, Das SK, Dinchuk JE, Langenbach R, Trzaskos JM, and Dey SK. 1997. Mulitple female reproductive failures in cyclooxygenases 2-deficient mice. Cell. 91:197-208

Ling P and Roberts RM. 1993. Overexpression of uteroferrin, a lysosomal acid phosphatase found in porcine uterine secretions, results in its high rate of secretion from transfected fibroblasts. Biol Reprod. 49(6): 1317-1327

Lubahn DB, Moyer JS, Golding TS, Couse JF, Korach KS, and Smithies O. 1993. Alteration of reproductive function but not prenatal sexual development after insertional disruption of the mouse estrogen receptor gene. Proc Natl Acad Sci U S A. 90: 11162-11166

Maatta M, Salo S, Tasanen K, Soini Y, Liakka A, Bruckner-Tuderman L, Autio-Harmainen H. 2004. Distribution of basement membrane anchoring molecules in normal and transformed endometrium: altered expression of laminin gamma2 chain and collagen type XVII in endometrial adenocarcinomas. J Mol Histol. 35(8-9): 715-722

Madore E, Harvey N, Parent J, Chapdelaine P, Arosh JA, and Fortier MA. 2003. An aldose reductase with 20α-hydroxysteroid dehydrogenase activity is most likely the enzyme responsible for the production of prostaglandin F$_{2\alpha}$ in the bovine endometrium. J Biol Chem. 278:11205-11212

Martus NS, Verhage HG, Mavrogianis PA, and Thibodeaux JK. 1998. Enhancement of bovine oocyte fertilization in vitro with a bovine oviductal specific glycoprotein. J. Reprod. Fertil. 113:323-329

McCormack JT, Friederichs MG, Limback SD, and Greenwald GS. 1998. Apoptosis during spontaneous luteolysis in the cyclic Golden Hamster: biochemical and morphological evidence. Biology of Reproduction. 58: 255-260

Mhashilkar AM, Schrock RD, Hindi M, Liao J, Sieger K, Kourouma F, Zou-Yang XH, Onishi E, et al. 2001. Melanoma differentiation associated gene-7 (mda-7): a novel anti-tumor gene for cancer gene therapy. Mol Med. 7: 271-282

Minamino N, Sudoh T, Kangawa K, and Matsuo H. 1985. Neuromedins: novel smooth-muscle stimulating peptides identified in porcine spinal cord. Peptides. 6 Suppl 3: 245-248

Mirkin S, Arslan M, Churikov D, Corica A, Diaz JI, Williams S, Bocca S, and Oehninger S. 2005. In search of candidate genes critically expressed in the human endometrium during the window of implantation. Hum Reprod. 20: 2104-2117

Moonga BS, Moss DW, Patchell A, and Zaidi M. 1990. Intracellular regulation of enzyme secretion from rat osteoclasts and evidence for a functional role in bone resorption. J Physiol. 429: 29-45

Moriyama M, Sato T, Inoue H, Fukuyama S, Teranishi H, Kangawa K, Kano T, Yoshimura A, and Kojima M. 2005. The neuropeptide neuromedin U promotes inflammation by direct activation of mast cells. J Exp Med. 202(2): 217-224

Mullins DE, Bazer FW, and Roberts RM. 1980. Secretion of progesterone-induced inhibitor of plasminogen activator by the porcine uterus. Cell. 20: 865-872

Murray FA, Bazer FW, Wallace HD, and Warnick AC. 1972. Quantitative and qualitative variation in the secretion of protein by the porcine uterus during the estrous cycle. Biol Reprod. 7:314-320

Nandha KA, Benito-Orfila MA, Smith DM, Bloom SR. 1993. Characterization of the rat uterine neuromedin U receptor. Endocrinology. 133(2): 482-486

Naseri JI, Truong NT, Horentrup J, Kuballa P, Vogel A, Rompel A, Spener F, and Krebs B. 2004. Porcine purple acid phosphatase: heterologous expression, characterization, and proteolytic analysis. Arch Biochem Biophys. 432(1): 25-36

Nebekura H, Koike H, Ohtsuka T, Yamaguchi M, Miyakawa I, and Mori N. 1994. Fallopian tube prostaglandin production with and without endometriosis. Int J Fertil Menopausal Stud. 39:57-63

Nemoto T, Hori H, Yoshimoto M, Seyama Y, and Kubota S. 2002. Overexpression of ornithine decarboxylase enhances endothelial proliferation by suppressing endostatin expression. Blood. 99(4): 1478-1481

Nomura S, Wills AJ, Edwards DR, Heath JK, and Hogan BL. 1988. Developmental expression of 2ar (osteopontin) and SPARC (osteonectin) RNA as revealed by in situ hybridization. J Cell Biol. 106:441-450

O'Day-Bowman MB, Mavrogianis PA, Reuter LM, Johnson DE, Fazleabas AT, and Verhage HG. 1996. Association of oviduct-specific glycoproteins with human and baboon (Papio anubis) ovarian oocytes and enhancement of human sperm binding to human hemizonae following in vitro incubation. Biol. Reprod. 54:60-69

Ogasawara Y, Okamoto S, Kitamura Y, and Matsumoto K. 1983. Proliferative patterns of uterine cells from birth to adult-hood in intact, neonatally castrated, and/or adrenalectomized mice, assayed by incorporation of [^{125}I] iododeoxyuridine. Endocrinology. 113: 582-587

Omigbodun A, Ziolkiewicz P, Tessler C, Hoyer JR, and Coutifaris C. 1997. Progesterone regulates osteopontin expression in human trophoblasts: a model of paracrine control in the placenta. Endocrinology. 138:4308-4315

Palludan B, Wegger J, and Moustgard J. 1970. Placental transfer of iron. Danish Roy Vet Agric Univ Yearbook, Copenh. Pp.62-90

Paria BC, Reese J, Das SK, and Dey SK. 2002. Deciphering the cross-talk of implantation: advances and challenges. Science. 296:2185-2188

Pendeville H, Carpino N, Marine JC, Takahashi Y, Muller M, Martial JA, and Cleveland JL. 2001. The ornithine decarboxylase gene is essential for cell survival during early murine development. Mol Cell Biol. 21(19): 6459-6558

Perry JS and Rowlands IW. 1962. Early pregnancy in the pig. J Reprod Fertil. 4:175-188

Perry JS. 1981. The mammalian fetal membranes. J Reprod Fertil. 62:321-335

Piljic A, Schultz C. 2006. Annexin A4 self-association modulates general membrane protein mobility in living cells. Mol Biol Cell. 17(7):3318-3328.

Ponnampalam AP and Rogers PA. 2006. Cyclic changes and hormonal regulation of annexin IV mRNA and protein in human endometrium. Mol Hum Reprod. 12(11):661-9

Ponnampalam AP, Weston GC, Trajstman AC, Susil B, and Rogers PA. 2004. Molecular classification of human endometrial cycle stages by transcriptional profiling. Mol Hum Reprod. 10: 879-893

Pope WF. 1994. Embryonic mortality in swine. *Embryonic Mortality in Domestic Species*. Edited by M.T. Zavy and R. D. Geisert. CRC Press, Boca Raton, FL. 53-77

Przala J, Gregoraszczuk EL, Kotwica G, Stefanczyk-Krzymowska S, Ziecik AJ, Blitek A, Ptak A, Rak A, Wojtowicz A, Kaminski T, Siawrys G, Smolinska N, Franczak A, Kurowicka B, Oponowicz A, Wasowska B, Chlopek J, Kowalczyk AE, Kaczmarek MM, and Waclawik A. 2006. Mechanisms ensuring optimal conditions of implantation and embryo development in the pig. Reprod Biol. 6:Suppl. 59-87

Quackenbush J. 2001. Computational analysis of microarray data. Nat Rev Genet. 2(6): 418-428

Quackenbush J. 2002. Microarray data normalization and transformation. Nat Gent. 32 Suppl: 496-501

Quackenbush J. 2006. Microarray analysis and tumor classification. N Engl J Med. 354: 2463-2472

Raub TJ, Bazer FW, and Roberts RM. 1985. Localization of the iron transport glycoprotein, Uteroferrin, in the porcine endometrium and placentae by using immunocolloidal gold. Anat. Embryol. 171:253-258

Reinhart KC, Dubey RK, Mummery CL, van Rooijen M, Keller PJ, and Marinella R. 2000. Synthesis and regulation of leukaemia inhibitory factor in cultured bovine oviduct cells by hormones. Mol Hum Reprod. 4(3): 301-308

Renegar RH, Bazer FW, and Roberts RM. 1982. Placental transport and distribution of uteroferrin in the fetal pig. Biol Reprod. 27(5): 1247-1260.

Reynolds LP and Ford SP. 1984. Contractility of the vascular bed during the oestrous cycle and early pregnancy in gilts. J Reprod Fertil. 71: 65 - 71.

Roberts RM and Bazer FW. 1988. The function of uterine secretions. J Reprod Fertil. 82: 875-892

Roberts RM, Leaman DW and Cross JC. 1992b. Role of interferons in maternal recognition of pregnancy in ruminants. Proc Soc Exp Biol Med. 200: 7-18

Roberts RM, Murray MK, Burke MG, Ketcham CM, and Bazer FW. 1987. Hormonal control and function of secretory proteins. In: Leavitt WW(Ed.) Cell and Molecular Biology of the Uterus. pp. 137 Plenum Publishing Corp., New York.

Roberts RM, Raub TJ, and Bazer FW. 1986. Role of uteroferrin in transplacental iron transport in the pig. Fed Proc. 45(10): 2513-2518.

Roberts RM, Xie S, and Trout WE. 1993. Embryo-uterine interactions in pigs during week 2 of pregnancy. J Reprod Fertil Suppl. 48:171-186

Robertson SA, Seamark RF, Guilbert LJ, and Wegmann TG. 1994. The role of cytokines in gestation. Crit. Rev. Immunol. 14(3&4):239-292

Robinson RS, Mann GE, Lamming GE, and Wathes DC. 1999. The effect of pregnancy on the expression of uterine oxytocin, oestrogen and progesterone receptors during early pregnancy in the cow. J Endocrinol. 160(1): 21-33

Robitaille G, St-Jacques S, Potier M, and Bleau G. 1988. Characterization of an oviductal glycoprotein associated with the ovulated hamster oocyte. Bio Repro. 38:687–694

Rodriguez-Martinez H, Tienthai P, Suzuki K, Funahashi H, Ekwall H, and Johannisson A. 2001. Involvement of oviduct in sperm capacitation and oocyte development in pigs. Reprod Suppl. 58:129-145

Rodriguez-Sallaberry C, Simmen FA, and Simmen RC. 2001. Polyamine- and insulin-like growth factor-I-mediated proliferation of porcine uterine endometrial cells: a potential role for spermidine/spermine N(1)-acetyltransferase during peri-implantation. Biol Reprod. 65(2):587-594

Roman-Ponce H, Caton D, Thatcher WW, and Lehrer R. 1983. Uterine blood flow in relation to endogenous hormones during estrous cycle and early pregnancy. American Journal of Physiology. 245: R843–R849.

Ross JW, Malayer JR, Ritchey JW, and Geisert RD. 2003. Characterization of the interleukin-1beta system during porcine trophoblastic elongation and early placental attachment. Biol Reprod. 69(4):1251-1259

Rosselli M, Dubey RK, Rosselli MA, Macas E, Fink D, Lauper U, Keller PJ, and Imthurn B. 1996. Identification of nitric oxide synthase in human and bovine oviduct. Mol Hum Reprod. 2:607-612

Rosselli M, Imthurn B, Macas E, and Keller PJ. 1994. Endothelin production by bovine oviduct epithelial cells. J Reprod Fertil. 101:27-30.

Rotello RJ, Hocker MB and Gerschenson LE. 1989. Biochemical evidence for programmed cell death in rabbit uterine epithelium. American Journal of Pathology 68: 435-443

Salamonsen LA and Nancarrow CD. 1994. Cell biology of the oviduct and endometrium. Molecular Biology of the Female Reproductive System. Edited by Findlay JK. Academic Press, Inc. pp 289-328

Salamonsen LA, Nagase H, and Wooley DE. 1995. Matrix metalloproteinases and their tissue inhibitors at the ovine trophoblast-uterine interface. J Reprod Fertil Suppl. 49:29-37

Samuel CA and Perry JS. 1972. The ultrastructure of pig trophoblast rransplanted to an ectopic site in the uterine wall. J Anat. 113: 139-149

Samuel CA. 1971. The development of pig trophoblast in ectopic sites. J Reprod Fertil. 27: 494-495

Sasaki H, Ide N, Sendo F, Takeda Y, Adachi M, Fukai I, and Fujii Y. 2003. Glycosylphosphatidyl inositol-anchored protein (GPI-80) gene expression is correlated with human thymoma stage. Cancer Sci: 94(9): 809-813

Saunders MJ, Edgerton LA, Kagan JM, Stahly TS, and Cromwell GL. 1983. Comparison of intrauterine and subcutaneous sites of estrogen injection for luteal maintenance in swine. J Anim Sci. 57:146-149

Schmidt A, Mavrogianis PA, O'Day-Bowman MB, and Verhage HG. 1997. Species-specific effect of oviductal glycoproteins on hamster sperm binding to hamster oocytes. Mol. Reprod. Dev. 46:201-207

Sendai Y, Komiya H, Suzuki K, Onuma T, Kikuchi M, Hoshi H, and Araki Y. 1995. Molecular cloning and characterization of a mouse oviductspecific glycoprotein. Bio Repro. 53:285–294

Senger PL. 1999. The organization and function of the female reproductive tract. *Pathway to pregnancy and parturition*. Current Conceptions, Inc. pp 8-31

Sharkey AM, Dellow K, Blayney M, Macnamee M, Charnock-Jones S, and Smith SK. 1995. Stage-specific expression of cytokine and receptor messenger ribonucleic acids in human preimplantation embryos. Biol Reprod. 53:974 –981

Sharpe PM and Ferguson MW. 1988. Mesenchymal influences on epithelial differentiation in developing systems. J Cell Sci Suppl. 10: 195-230

Shi SR, Key ME, and Kalra KL. 1991. Antigen retrieval in formalin-fixed, paraffin-embedded tissues: an enhancement method for immunohistochemical staining based on microwave oven heating of tissue sections. J Histochem Cytochem. 39(6):741-748

Simmen RCM, Baumbach GA, and Roberts RM. 1989. Molecular cloning and temporal expression during pregnancy of the messenger ribonucleic acid encoding uteroferrin, a progesterone-induced uterine secretory protein. Mol Endocrinol. 2:253-262

Simmen RCM, Ko Y, Liu XH, Wilde MH, Pope WF, and Simmen FA. 1988. A uterine cell mitogen distinct from epidermal growth factor in porcine uterine luminal fluids characterization and partial purification. Biol Reprod. 38:551-561

Smith WL and DeWitt DL. 1996. Prostaglandin endoperoxide H syntase-1 and -2. Adv Immunol. 62:167-215

Smith WL, Garavito RM, and DeWitt DL. 1996. Prostaglandin endoperoxide H synthases (cyclooxygenases)-1 and -2. J Biol Chem. 271:33157-33160

Southern E, Mir K, and Shchepinov M. 1999. Molecular interactions on microarrays. Nat. Genet. 21:5-9

Southern EM. 1975. Detection of specific sequences among DNA fragments separated by gel electrophoresis. J. Mol. Biol. 98:503-517

Spencer TE and Bazer FW. 1995. Temporal and spatial alterations in uterine estrogen receptor and progesterone receptor gene expression during the estrous cycle and early pregnancy in the ewe. Biol Reprod. 53(6):1527-1543.

Spencer TE and Bazer FW. 2002. Biology of progesterone action during pregnancy recognition and maintenance of pregnancy. Front Biosci. 7:d1879-98

Spencer TE and Bazer FW. 2004. Uterine and placental factors regulating conceptus growth in domestic animals. J. Anim. Sci. 82(E. Suppl.):E4–E13

Spencer TE, Johnson GA, Burghardt RC, and Bazer FW. 2004. Progesterone and placental hormone actions on the uterus: insights from domestic animals. Biol Reprod. 71(1):2-10.

Spencer TE, Wiley AA, and Bartol FF. 1993. Neonatal age and period of estrogen exposure affect porcine uterine growth, morphogenesis, and protein synthesis. Biol Reprod. 48: 741-751

Squires GD, Bazer FW, and Murray FA. 1972. Electrophoretic patterns of porcine uterine protein secretions during the estrous cycle. Biol Reprod. 7:321-325

Stallings-Mann ML, Burke MG, Trout WE, and Roberts RM. 1994. Purification, characterization, and cDNA cloning of a Kunitz-type proteinase inhibitor secreted by the porcine uterus. J Biol Chem. 269(39): 24090-24094

Stallings-Mann ML, Trout WE, and Roberts RM. 1993. Porcine uterine retinol-binding proteins are identical gene products to the serum retinol-binding protein. Biol Reprod. 48:998-1005

Stears RL, Martinsky T, and Schena M. 2003. Trends in microarray analysis. Nat Med. 9:140-145.

Stefanczyk-Krzymowska S, Chlopek J, Grzegorzewski W, and Radomski M. 2005. Local transfer of prostaglandin E2 into the ovary and its retrograde transfer into the uterus in early pregnant sows. Exp Physiol. 90(6):807-814

Stefanczyk-Krzymowska S, Szafranska B, Kaminski TT, and Krzymowski T. 1994. Total content of prostagalndin F(2a) in the endometrium and myometrium from various sections of the porcine uterine horn during the estrous cycle. Prostaglandins. 48(2): 99-108

Stone BA, Seamark RF, Kelly RW, and Deam S. 1986. Production of steroids and release of prostaglandins by spherical pig blastocysts in vitro. Aust J Biol Sci. 39:283-293

Strickland S, Reich E, and Sherman MJ. 1976. Plasminogen activator in early embryogenesis. Enzyme production by trophoblast and parietal endoderm. Cell. 9:231-240

Stroband HWJ, Taverne N, Langenfeld K, and Barends PGM. 1986. The ultrastructure of the uterine epithelium of the pig during the estrous cycle and early pregnancy. Cell and Tissue Research. 246: 81-89

Su ZZ, Madireddi MT, Lin JJ, Young CS, Kitada S, Reed JC, Goldstein NI, and Fisher PB. 1998. The cancer growth suppressor gene mda-7 selectively induces apoptosis in human breast cancer cells and inhibits tumor growth in nude mice. Proc Natl Acad Sci USA. 95: 14400-14405

Tan YF, Li FX, Piao YS, Sun XY, and Wang YL. 2003. Global gene profiling analysis of mouse uterus during the oestrous cycle. Reproduction. 126(2):171-182

Tanaka TS, Jaradat SA, Lim MK, Kargul GJ, Wang X, Grahovac MJ, Pantano S, Sano Y, Piao Y, Nagaraja R, Doi H, Wood WH 3rd, Becker KG, and Ko MS. 2000. Genome-wide expression profiling of mid-gestation placenta and embryo using a 15,000 mouse developmental cDNA microarray. Proc Natl Acad Sci U S A. 97(16):9127-9132

Tarleton BJ, Wiley AA, and Bartol FF. 1999. Endometrial development and adenogenesis in the neonatal pig: effects of estradiol valerate and the antiestrogen ICI 182,780. Biol Reprod. 61: 253-263

Tarleton BJ, Wiley AA, and Bartol FF. 2001. Neonatal estradiol exposure alters uterine morphology and endometrial transcriptional activity in prepubertal gilts. Domestic Animal Endocrinology. 21(2): 111-125

Tarleton BJ, Wiley AA, Spencer TE, Moss AG, and Bartol FF. 1998. Ovary-independent estrogen receptor expression in neonatal porcine endometrium. Biol Reprod. 58: 1009-1019

Tazuke SI and Guidice LC. 1996. Growth factors and cytokines in endometrium, embryonic development, and maternal: embryonic interactions. Semin Reprod Endocrinol. 14:231–243

Tiedemann K and Minuth WW. 1980. The pig yolk sac I: Fine structure of the posthaematopoietic organ. Histochemistry. 68:133-146

Tong AW, Nemunaitis J, Su D, Zhang Y, Cunningham C, Senzer N, Netto G, Rich D, Mhashilkar A, Parker K, Coffee K, Ramesh R, Ekmekcioglu S, Grimm EA, van Wart Hood J, Merritt J, Chada S. 2005. Intratumoral injection of INGN 241, a nonreplicating adenovector expressing the melanoma-differentiation associated gene-7 (mda-7/IL24): biologic outcome in advanced cancer patients. Molec Ther. 11: 160-172

Trubiani O, Pieri C, Rapino M, and Di Primio R. 1999. The c-myc gene regulates the polyamine pathway in DMSO-induced apoptosis. Cell Prolif. 32(2-3): 119-129

Tseng L, Mazella J, Mann WJ, Chumas J. 1982. Estrogen synthesis in normal and malignant human endometrium. J Clin Endocrinol Metab. 55(5): 1029-1031

Tuo W, Harney JP, and Bazer FW. 1996. Developmentally regulated expression of interleukin-1 beta by peri-implantation conceptuses in swine. J Reprod Immunol. 31(3):185-198

Ushizawa K, Herath CB, Kaneyama K, Shiojima S, Hirasawa A, Takahashi T, Imai K, Ochiai K, Tokunaga T, Tsunoda Y, Tsujimoto G, ahdn Hashizume K. 2004. cDNA microarray analysis of bovine embryo gene expression profiles during the pre-implantation period. Reprod Biol Endocrinol.2:77

Vallet JL, Klemcke HG, and Christenson RK. 2002. Interrelationships among conceptus size, uterine protein secretion, fetal erythropoiesis, and uterine capacity. J Anim Sci. 80(3):729-737

van Rens BT and van der Lende T. 2002. Piglet and placental traits at term in relation to the estrogen receptor genotype in gilts. Theriogenology. 57:1651-1667

Vinciotti V, Khanin R, D'Alimonte D, Liu X, Cattini N, Hotchkiss G, Bucca G, de Jesus O, Rasaiyaah J, Smith CP, Kellam P, and Wit E. 2005. An experimental evaluation of a loop versus a reference design for two-channel microarrays. Bioinformatics. 21(4):492-501

Vonnahme KA, Fernando SC, Ross JW, Ashworth MD, Desilva U, Malayer JR, and Geisert RD. 2004. Porcine endometrial expression of kininogen, factor XII, and plasma kallikrein in cyclic and pregnant gilts. Biol Reprod. 70(1): 132-138

Vonnahme KA, Malayer JR, Spivery HO, Ford SP, Clutter A, and Geisert RD. 1999. Detection of kallikrein gene expression and enzymatic activity in porcine endometrium during the estrous cycle and early pregnancy. Biol Reprod. 61(5): 1235-1241

Waclawik A, Rivero-Muller A, Blitek A, Kaczmarek MM, Brokken LJ, Watanabe K, Rahman NA, and Ziecik AJ. 2006. Molecular cloning and spatiotemporal expression of prostaglandin F synthase and microsomal prostaglandin E synthase-1 in porcine endometrium. Endocrinology. 147(1):210-221

Wai PY, Guo L, Gao C, Mi Z, Guo H, and Kuo PC. 2006. Osteopontin inhibits macrophage nitric oxide synthesis to enhance tumor proliferation. Surgery. 140(2): 132-140

Wang M, Tan Z, Zhang R, Kotenko SV, and Liang P. 2002. Interleukin 24 (MDA-7/MOB-5) signals through two heterodimeric receptors, IL-22R1/IL-20R2 and IL-20R1/IL-20R2. J Bil Chem. 277:7341-7247

Wei C, Li J, and Bumgarner RE. 2004. Sample size for detecting differentially expressed genes in microarray experiments. BMC Genomics. 5(1):87

Weisinger G, Gavish M, Mazurika C, and Zinder O. 1999. Transcription of actin, cyclophilin and glyceraldehyde phosphate dehydrogenase genes: tissue- and treatment-specificity. Biochim. Biophys. Acta. 1446: 225-232

Wellstead JR, Bruce NW, and Rahima A. 1989. Effects of indomethacin on spacing of conceptuses within the uterine horn and on fetal and placental growth in the rat. Anat Rec. 225:101-105

White CA and Salamonsen LA. 2005. A guide to issues in microarray analysis: application to endometrial biology. Reproduction. 130(1): 1-13

White FJ, Burghardt RC, Hu J, Joyce MM, Spencer TE, and Hohnson GA. 2006. Secreted phosphoprotein 1 (osteopontin) is expressed by stromal macrophages in cyclic and pregnant endometrium of mice, but is induced by estrogen in luminal epithelium during conceptus attachment for implantation. Reproduction. 132(6): 919-929

White FJ, Ross JW, Joyce MM, Geisert RD, Burghardt RC, and Johnson GA. 2005. Steroid regulation of cell specific secreted phosphoprotein 1 (osteopontin) expression in the pregnant porcine uterus. Bio Reprod. 73(6):1294-1301

Whitworth K, Springer GK, Forrester LJ, Spollen WG, Ries J, Lamberson WR, Bivens N, Murphy CN, Mathialigan N, Green JA, and Prather RS. 2004. Developmental expression of 2489

gene clusters during pig embryogenesis: an expressed sequence tag project. Biol Reprod. 71(4):1230-1243

Whitworth KM, Agca C, Kim JG, Patel RV, Springer GK, Bivens NJ, Forrester LJ, Mathialagan N, Green JA, and Prather RS. 2005. Transcriptional Profiling of Pig Embryogenesis by Using a 15-K Member Unigene Set Specific for Pig Reproductive Tissues and Embryos. Biol Reprod. 72(6): 1437-1451

Wilson ME, Fahrenkrug SC, Smith TPL, Rohrer GA, and Ford SP. 2002. Differential expression of cyclooxygenases-2 around the time of elongation in the pig conceptus. Anim Reprod Sci. 71:229-237

Wilson MJ, Jeyasuria P, Parker KL, and Koopman P. 2005. The transcription factors steroidogenic factor-1 and SOX9 regulate expression of Vanin-1 during mouse testis development. J Biol Chem. 280(7): 5917-5923

Wolff M, Bohlmann MK, Fiedler C, Ursel S, and Strowitzki T. 2004. Osteopontin is up-regulated in human decidual stromal cells. Fertil Steril. 81 (Suppl 1):741-748

Wollenhaupt K, Tomek W, Brussow KP, Tiemann U, Viergutz T, Schneider F, and Nurnberg G. 2002. Effects of ovarian steroids and epidermal growth factor (EGF) on expression and bioactivation of specific regulators of transcription and translation in oviductal tissue in pigs. Reproduction. 123(1):87-96

Wollenhaupt K, Welter H, Brussow KP, and Einspanier R. 2005. Regulation of endometrial fibroblast growth factor 7 (FGF-7) and its receptor FGFR2IIIb in gilts after sex steroid replacements, and during the estrous cycle and early gestation. J Reprod Dev. 51(4): 509-519

Wollenhaupt K, Welter H, Einspanier R, Manabe N, and Brussow KP. 2004. Expression of epidermal growth factor receptor (EGF-R), vascular endothelial growth factor receptor (VEGF-R) and fibroblast growth factor receptor (FGF-R) system in porcine oviduct and endometrium during the time of implantation. J Reprod Dev. 50(3): 269-278

Woo Y, Krueger W, Kaur A, and Churchill G. 2005. Experimental design for three-color and four-color gene expression microarrays. Bioinformatics. 21:Suppl 1. i459-i467

Wooding FBP and Flint APF. 1994. Placentation. *In* "Marshall's Physiology of Reproduction," (G. E. Lamming, Ed.), Vol. III, Part I, pp. 233–460. Chapman & Hall, London.

Xiao CW, Murphy BD, Sirois J, and Goff AK. 1999. Down-regulation of oxytocin-induced cyclooxygenase-2 and prostaglandin F synthase expression by interferon-τ in bovine endometrial cells. Biol Reprod. 60:656-663

Yang YH and Speed T. 2002. Design issues for cDNA microarray experiments. Nat Rev Genet. 3:579-588

Yang YH, Dudoit S, Luu P, Lin DM, Peng V, Ngai J, and Speed TP. 2002. Normalization for cDNA microarray data: a robust composite method addressing single and multiple slide systematic variation. Nucleic Acids Res. 30(4):E15

Young MF, Kerr JM, Termine JD, Weever UM, Wang MG, McBride OW, and Fisher LW. 1990. cDNA cloning, mRNA distribution and heterogeneity, chromosomal location, and RFLP analysis of human osteopontin (OPN). Genomics. 7:491-502

YuenHW, Ziober AF, Gopal P, Nasrallah I, Falls EM, Meneguzzi G, Ang HQ, and Ziober BL. 2005. Suppression of laminin-5 expression leads to increased motility, tumorigenicity, and invasion. Exp. Cell Res. 309(1): 198-210

Zavy MT, Roberts RM, and Bazer FW. 1984. Acid phosphatase and leucine aminopeptidase activity in the uterine flushings of nonpregnant and pregnant gilts. J Reprod Fert. 72:503-507.

Zhang X and Nothnick WB. 2005. The role and regulation of the uterine matrix metalloproteinase system in menstruating and non-menstruating species. Frontiers in Bioscience. 10:353-366

VITA

Jin-Geol Kim was born in Okcheon, Chungbuk in South Korea on April 13, 1973. After graduating from Samyang public elementary school, Okcheon Men middle school to Okcheon high school, he received a Bachelor of Science degree in Animal Science from Chungbuk National University in Cheongju, South Korea in 1999. He then received a Master of Science degree in Animal Science from same University in 2001 and a Master of Science degree under the guidance of Dr. Jonathan Green and Randall Prather in Animal Science from the University of Missouri-Columbia in 2007. His Master program was conducted while serving as the Research Assistant in Animal Science Research Center at the University of Missouri in Columbia. In 2001, he married Sang-Myeong Lee of Okcheon, Chungbuk in South Korea, and they currently reside in Columbia, Missouri.